DOCUMENTATION PAGE

	2. REPORT DATE	3. REPORT TYPE AND DATES COVERED
		THESIS/DISSERTATION

4. TITLE AND SUBTITLE
Rapid Nonconjugate Adaptation of Vertical Voluntary Pursuit Eye Movements

5. FUNDING NUMBERS

6. AUTHOR(S)
Gerald Allan Gleason, Major

7. PERFORMING ORGANIZATION NAME(S) AND ADDRESS(ES)

AFIT Student Attending: University of California

8. PERFORMING ORGANIZATION REPORT NUMBER

AFIT/CI/CIA-91-022D

9. SPONSORING/MONITORING AGENCY NAME(S) AND ADDRESS(ES)

AFIT/CI
Wright-Patterson AFB OH 45433-6583

10. SPONSORING/MONITORING AGENCY REPORT NUMBER

11. SUPPLEMENTARY NOTES

12a. DISTRIBUTION/AVAILABILITY STATEMENT
Approved for Public Release IAW 190-1
Distributed Unlimited
ERNEST A. HAYGOOD, Captain, USAF
Executive Officer

12b. DISTRIBUTION CODE

13. ABSTRACT *(Maximum 200 words)*

14. SUBJECT TERMS

15. NUMBER OF PAGES
239

16. PRICE CODE

17. SECURITY CLASSIFICATION OF REPORT	18. SECURITY CLASSIFICATION OF THIS PAGE	19. SECURITY CLASSIFICATION OF ABSTRACT	20. LIMITATION OF ABSTRACT

Rapid Nonconjugate Adaptation
of Vertical Voluntary Pursuit Eye Movements

By

Gerald Allan Gleason

D.Opt. (Southern California College of Optometry) 1980

DISSERTATION

Submitted in partial satisfaction of the requirements for the degree of
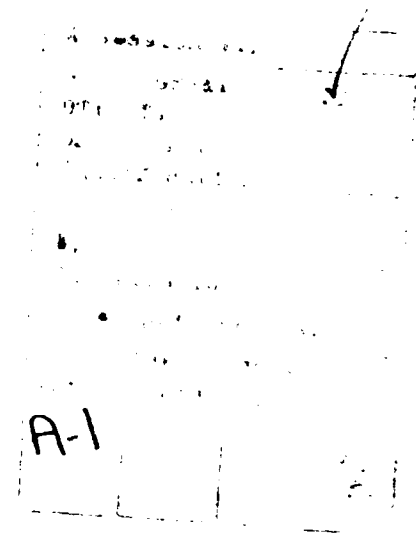
DOCTOR OF PHILOSOPHY

in

PHYSIOLOGICAL OPTICS

in the

GRADUATE DIVISION

of the

UNIVERSITY OF CALIFORNIA at BERKELEY

A-1

Approved:

Chair: ....*Clifton M. Schor*.......... *July 25, 1991*
.... Date *7/25/91*
.....*Edward F. Kelly*..................... *7/25/91*

* * * * * * * * * * * * * * * * * * *

Rapid Nonconjugate Adaptation of Vertical Voluntary Pursuit Eye Movements

Gerald A Gleason

ABSTRACT

The precise yoking of the two eyes during vertical eye movements is normally preserved throughout life. This preservation is due in part to adaptive processes that adjust the relative neural innervations sent to each eye's extraocular muscles (nonconjugate adaptation). This behavioral study investigates adaptive processes that maintain conjugacy along the vertical meridian during three types of ocular motor behavior: voluntary pursuit, saccade, and steady fixation.

Binocular yoking was quantified by binocular recordings of vertical eye position (dual-Purkinje eye tracker) while vertical eye movements were monocularly stimulated. Properties of nonconjugate adaptive processes were inferred from changes in pre- and post-adaptation binocular yoking.

The first study demonstrates that different processes underlie nonconjugate adaptation of vertical pursuits and saccades by selectively altering binocular yoking during either pursuit, or saccade (pulse component) eye movements.

The second and third studies examine the role of gaze-specific phoria adaptation in nonconjugate adaptation of

vertical pursuits and saccades. During the adaptation period, subjects were sequentially exposed to discrete stationary gaze-specific vertical binocular disparities. Nonconjugate changes in vertical pursuit yoking were accounted for by phoria adaptation. However, the pulse component of vertical saccades was not affected by phoria adaptation. These results indicate phoria adaptation shares common processes with nonconjugate adaptation of vertical pursuit, but not with nonconjugate adaptation of vertical saccades.

The fourth study demonstrates other mechanisms, not shared with phoria adaptation, also underlie nonconjugate adaptation of vertical pursuit. Non-phoria mechanisms are gaze-specific and direction (of pursuit) -specific, while phoria mechanisms are only gaze-specific.

The fifth study investigates the vertical spread of phoria adaptation from stimulated gaze positions to neighboring unstimulated gaze positions. If one gaze position is stimulated, phoria adaptation spreads uniformly over all gaze positions. If two gaze positions are differentially stimulated, vertical phoria adaptation behaves as if it were spatially-tuned (modeled by a 9.25 degree Gaussian), and its effectivity (system gain) is limited by a stimulus disparity gradient limit.

These studies demonstrate that preservation of conjugacy relies on multiple adaptive processes.

Clifton M. Schor

2

Dedication

To my Wife,

Vickie

and Sons,

Andy and Nick

Rapid Nonconjugate Adaptation of Vertical

Voluntary Pursuit Eye Movements

Table of Contents

Acknowledgements

CHAPTER 1

INTRODUCTION

Each human eye contains a small retinal area, called the fovea, that is capable of superior visual resolution. Visual resolution decreases rapidly as retinal images are displaced progressively further from the fovea. Hence, we must inspect our environment with only a small area of acute vision.

Four types of voluntary ocular motor behavior have apparently developed in order to maximize use of the fovea. Saccade eye movements allows us to rapidly shift visual fixation from one object to another. Smooth pursuit eye movements allow us to visually track small moving objects. Vergence eye movements allow us to shift visual fixation from one object to another object that is either closer or further away. And finally, steady fixation allows us to maintain visual fixation on a stationary object.

The kinematics of eye movements associated with saccade, pursuit, and vergence eye movements are distinctive (Dodge (1903)), and the areas of the brain associated with each of these eye movements types are, to some extent, anatomically discrete (see Büttner-Ennever (1988) for review. While pursuit and saccade eye movements can be made along any meridian, voluntary vergence eye movements are found only along the horizontal meridian. Little is known about the processes that underlie steady fixation.

Another feature of the human visual system is that, regardless of each eye's orientation, objects whose retinal images fall on the center of each fovea are perceived as aligned. The centers of the two foveas are called corresponding retinal points. Corresponding retinal points are areas of retina in each eye, that when stimulated, give rise to a percept that is in a single direction. Corresponding retinal point pairs are approximately equally and symmetrically distributed about the two foveal centers.

When the two eyes are precisely aimed at an object, the object's retinal images fall on corresponding retinal points, and a single object is perceived. If the eyes are not precisely aimed, the object's retinal images fall on non-corresponding retinal points and the object is simultaneously perceived in two different directions (diplopia).

Theoretically, Panum's area describes the maximum amount of binocular misalignment that can be tolerated before diplopia results (Panum (1858) cited by Tyler (1983)). Panum's area is not a fixed quantity, but increases with retinal eccentricity (Ogle (1950)) and varies with spatiotemporal properties of the visual stimulus (Schor, Wood, and Ogawa (1984)). For the fovea, the extent of Panum's area ranges from 1.5 to 25 arc minutes horizontally and 0.6 to 10 arc minutes vertically (Schor and Tyler (1981)).

In order to prevent diplopia, the human visual system must keep the two eyes precisely aligned during and immediately

after eye movements. To meet this end, both sensory and motor processes are used. For example, during a horizontal saccade, the eyes may diverge as much as 3 degrees (Collewijn et al (1988a) and retinal images are rapidly swept across the retinas, yet during the saccade, diplopia and blur are not perceived. Perception of diplopia and blur are suppressed by a least two processes. During a saccade the visual system becomes less sensitive to luminance (saccadic suppression), and sharp retinal images before and after the saccade suppress perception of blurred images that occur during the saccade (visual masking) (Campbell and Wurtz (1978)).

However, sensory compensation has its limits. The onus lies mainly with the ocular motor system to maintain ocular alignment within small tolerances. Except for vergence eye movements, voluntary eye movements are well-yoked; the two eyes rotate synchronously (Williams and Fender (1977)) and nearly-equally in the same direction (Collewijn et al (1988a,b), Lemij (1990)). Human eye movements are said to be conjugate, because two eyes are constrained to rotate together in this fashion. We can not rotate one eye without affecting the other eye. If one eye is occluded, our eyes remain well-yoked (Collewijn (1988a), Lemij (1990)). Neonates and the congenitally blind exhibit conjugate eye movements (Hering (1868)), indicating conjugacy is an innate trait, rather than a learned coordination, and therefore, is rooted in neural connectivity.

By itself, neural connectivity is inadequate to explain
conjugacy. Developmental changes, such as enlargement of the
orbit, globe, and orbital contents are likely to effect the
two eyes asymmetrically. Senile changes, such as changes in
extraocular muscular morphology (Miller (1975)), orbital fat
(Weale RA (1963)), and normal neuro-muscular attrition that
may occur within the ocular motor system, are also likely to
effect the two eyes asymmetrically. These age-related
asymmetrical changes would disrupt binocular coordination if
conjugacy was solely derived from hard-wired neural
connectivity.

Despite these asymmetrical changes the fidelity of
binocular coordination is maintained during saccades
(Collewijn, et al (1988a,b), Lemij (1990)) and steady
fixation (Hirsch et al (1948), Kephart and Oliver (1952),
Scobee and Bennet (1950)). Presumably, adaptive processes
are responsible for preserving conjugacy by adjusting the
relative amount of neural innervation sent to each eye's
extraocular muscles (nonconjugate adaptation).

Currently, there are no reports of physiological studies
that address nonconjugate adaptation. However, there are
several behavioral studies that demonstrate it is possible to
alter binocular yoking during steady fixation (Ellerbroch and
Fry (1942), Ellerbrock (1948a,b), Henson DB and Dharamshi
(1982a,b), Oohira et al (1991)), saccade (Erkelens et al
(1989), Lemij (1990), Oohira et al (1991)), and pursuit
(Horner et al (1988), Lemij (1990)) eye movements.

4

In these behavioral studies, the relative ocular motor innervation sent to each eye is inferred by monocularly stimulating eye movements (occluding one eye) and then comparing the relative amplitudes of movement manifested by each eye during pursuit and saccade eye movements, or comparing the relative alignment of the two eyes during steady fixation. Nonconjugate adaptation is determined by comparing binocular yoking before and after an adaptation period. Because one eye is occluded during yoking measurements, binocular yoking can not be attributed to (reflexive) fusional eye movements, or to independent processing of sensory and motor control by each eye, and therefore, resulting changes in binocular yoking must be attributed to neural plasticity.

During the adaptation period of these studies, nonconjugate adaptation was stimulated by binocular experience with spectacle-mounted optical magnification before one eye. When spectacle-mounted optical magnification is placed before one eye, unequal eye movements are required to maintain single vision in different gaze positions.

An interesting observation that stems from these studies is that nonconjugate (unequal) binocular eye movements were induced in normal subjects. Therefore, although nonconjugate adaptation may result in conjugate (equal) binocular eye movements in normal environments, the goal of nonconjugate adaptation processes is not to create conjugate (equal)

binocular eye movements. Perhaps, the goal is to reduce
fusional eye movements.

Aside from Lemij (1990) demonstrating that nonconjugate
adaptation of saccade and pursuit does not transfer to
orthogonal meridians, little is known about the processes
that underlie nonconjugate adaptation. For example, it is
not known whether if different eye movement types share a
single nonconjugate adaptation mechanism, or if each eye
movement type possesses its own distinct nonconjugate
adaptation mechanism(s).

In this dissertation, properties of nonconjugate
adaptation along the the _vertical_ meridian during three
voluntary ocular motor behaviors (pursuit, saccade, and
steady fixation) were investigated. Primary emphasis was
placed on pursuit eye movements because with the equipment
used in this study, saccadic eye movements caused a
mechanical artifact that prohibited investigation of intra-
saccadic kinesthetics. The vertical meridian, rather than
the horizontal, was studied for several reasons. First,
vertical phoria adaptation (Henson and Dharamshi (1982)) and
nonconjugate adaptation of vertical saccades (Erkelens et al
(1989)) occurs faster and are more complete. Second,
binocular yoking of vertical saccades is more exact than
yoking for horizontal saccades (Collewijn (1988a,b), Lemij
(1990)). Third, voluntary vergence eye movements may effect
yoking measurements along the horizontal meridian. Fourth,
fluctuations in accommodative posture may cause fluctuations

in horizontal phoria via accomondation-vergence synkinesis (Schor and Kotulak (1986)).

For brevity, future references to pursuit, saccade, and phoria adaptation refer to as such along the vertical meridian only. Furthermore, unless otherwise stated, the pulse (fast) component of saccades will be referred to simply as saccade.

In chapter 2, By demonstrating selective nonconjugate adaptation, pursuit and saccade are shown to have separate adaptation mechanisms. Two experimental paradigms were incorporated in this study. The first paradigm stimulated nonconjugate adaptation of pursuit, with little effect on saccades. The second paradigm stimulated nonconjugate adaptation of vertical saccades, with little effect on pursuit.

In chapter 3, gaze-specific phoria adaptation was shown to share adaptive mechanisms with nonconjugate pursuit adaptation, but not with nonconjugate saccade adaptation. Gaze-specific phoria adaptation was stimulated by multiple stationary gaze-specific binocular disparities. Although, dynamic pursuit eye movements were not stimulated during the adaptation period, the static adapting stimulus was effective in inducing nonconjugate pursuit adaptation. Gaze-specific phoria adaptation accounted for these nonconjugate pursuit changes. Although gaze-specific phoria adaptation had little effect on saccade (pulse), it produced a post-saccadic phoria drift.

In chapter 4, phoria adaptation and nonconjugate adaptation are shown to be gaze-specific. The adapting stimulus was a pursuit stimulus that required equal eye movements in the lower field, and unequal eye movements in the upper field. Gaze-specificity was demonstrated by greater changes in pursuit yoking in the upper field than the lower field. Again, nonconjugate changes in pursuit were accounted for by gaze-specific phoria adaptation, indicating common mechanisms underlie vertical phoria adaptation and nonconjugate pursuit adaptation.

In chapter 5, multiple mechanisms are shown to underlie nonconjugate pursuit adaptation. These mechanisms can be categorized as either phoria or non-phoria. Phoria mechanisms are gaze-specific and are shared with phoria adaptation. Non-phoria mechanisms are direction- (of pursuit) and gaze-specific, and are not shared with phoria mechanisms. Two models of how phoria and non-phoria mechanisms might interact with each other are offered.

In chapter 6, spatial spread of vertical phoria adaptation to unstimulated gaze positions from stimulated gaze positions was investigated. In the first experiment, of this two-experiment study, phoria adaptation was stimulated by a single disparity located at a particular gaze position. The spatial spread of adaptation was mainly idiosyncratic. However, or average, the spread of adaptation was uniform across the orbital field and not spatially-tuned. In the second experiment, phoria adaptation was differentially

stimulated at two discrete gaze positions. In a series of experimental sessions, stimulus disparity amplitude and stimulus separation were systematically varied. A spatial-spread model, similar to a qualitative model originally proposed by Henson and Dharamshi (1982), was inadequate to explain the results. In addition to the spatial-spread model, there is a stimulus disparity gradient-limit which constrains the response of the phoria mechanism.

REFERENCES

Büttner-Ennever JA (Ed.) (1988), Reviews of oculomotor
    research, Vol 2, Neuroanatomy of the oculomotor
    system, Elsevier: Amsterdam

Campbell FW and Wurtz RH (1978), Saccadic omission:
    why we do not see a grey out during a saccadic eye
    movement, Vision Res. 18:1297

Collewijn H, Erkelens CJ, and Steinman RM (1988a),
    Binocular coordination of human horizontal saccadic
    eye movements, J. Physiol. 404:157

Collewijn H, Erkelens CJ, and Steinman RM (1988b),
    Binocular coordination of human vertical saccadic eye
    movements, J. Physiol. 404:183

Dodge Raymond (1903), Five types of eye movements in
    the horizontal meridian plane of the field of regard,
    Am. J. Physiol. 8:307

Ellerbrock V and Fry GA (1942), Effects induced by
    anisometropic corrections, Am. J. Optom. and Arch.
    Am. Acad. Optom. 19:444

Ellerbrock VJ (1948a), Further study of effects
    induced by anisometropic corrections, Am. J. Optom.
    and Arch. Am. Acad. Optom. 25:430

Ellerbrock VJ (1948b), A clinical investigation of
    compensation for vertical prismatic imbalances, Am.
    J. Optom. and Arch. Am. Acad. Optom. 25:309

Erkelens CJ, Steinman RM, And Collewijn H (1989),
    Asymmetrical adaptation of human saccades to
    anisometropic spectacles, Invest. Ophthalmol. Vis.
    Sci. 30:1132

Henson DB and Dharamshi BG (1982a), Oculomotor
    adaptation to induced heterophoria and anisometropia,
    Invest. Ophthalmol. Vis. Sci. 22:234

Henson DB and Dharamshi BG (1982b), Binocular
    oculomotor adaptation to induced incomitant
    deviations, In Functional basis of ocular motility
    disorders, Lennerstrand, Zee, and Keller (Eds.),
    Pergamon Press: Oxford, pages 229 - 231

Hering E (1868), The Theory of Binocular Vision,
    [Translation (1977), Bridgeman B & Stark L (Eds.)]
    Plenum Press: New York

Hirsch MJ, Alpern M, and Shultz HL (1948), The
    variation of phoria with age, Am. J. Optom. and
    Arch. Am. Acad. Optom. 25:535

Horner DG, Gleason G, and Schor CM (1988), The
    recalibration of Hering's law for versional eye
    movements in response to aniseikonia, Invest.
    Ophthalmol. Vis. Sci. 29:136 (abstract 28)

Lemij HG (1990), Asymmetrical adaptation of human
    saccades to anisometropic spectacles, Doctoral
    Dissertation, Erasmus University of Rotterdam

Miller JE (1975), Aging changes in extraocular muscle,
    In Basic Mechanisms of Ocular Motility and their
    Clinical Implications, Lennerstrand G and Bach-y-Rita
    P (Ed.), Wenner-Gren Center International Symposium
    Series, Pergamon: Oxford Vol 24: pages 47-61

Ogle KN (1950), Researches in Binocular Vision, WB
    Saunders: Philadelphia

Oohira H, Zee DS, and Guyton DL (1991), Disconjugate
    adaptation to long-standing, large-amplitude
    spectacle-corrected anisometropia, Invest.
    Ophthalmol. Vis. Sci. 32:1693

Schor C, Wood I, and Ogawa J (1984), Binocular sensory
    fusion is limited by spatial resolution, Vision Res.
    24:661

Schor CM and Kotulak JC (1986), Dynamic interactions
    between accommodation and convergence are velocity
    sensitive, Vision Res. 26:926

Schor CM and Tyler CW (1981), Spatio-temporal
    properties of Panum's fusional area, Vision Res.
    21:683

Scobee RG and Bennet EA (1950), Hyperphoria, a
    statistical study, Arch. Ophthalmol. 43:458

Sethi (nee Dharamshi) B and North RV (1987), Vergence
    adaptive changes with varying magnitudes of prism-
    induced disparities and fusional amplitudes, Am. J.
    Optom. Physiol. Opt. 64:263

Tyler, CW (1983), Sensory Processing of Binocular
    Disparity, In Vergence eye movements: basic &
    clinical aspects, Schor and Ciuffreda (Eds.),
    Butterworths: Boston, pages 199-295

Weale RA (1963), The aging eye, Harper & Row: New
    York

Williams RA and Fender DH (1977), The synchrony of
    binocular saccadic eye movements, Vision Res. 17:303

CHAPTER 2

INDEPENDENT NONCONJUGATE ADAPTATION
OF VERTICAL PURSUIT AND SACCADE

INTRODUCTION

Normally when one eye is occluded, human binocular eye
movements are (within small tolerances) synchronous,
unidirectional, and equal (Collewijn, et al (1988a),
Collewijn et al (1988b), Lemij, (1990)). This well-
coordinated ocular motor behavior is usually described by the
terms "conjugate" and "yoked". Based on gross observations
of conjugate eye movements in neonates, and the congenitally
amaurotic, Ewald Hering (1868) suggested conjugacy resulted
solely from innate ocular motor neural organization.

Although neural connectivity clearly plays an important
role in conjugate eye movements it is also obvious that a
hard-wired neural connectivity model cannot explain the
remarkable stability of well-yoked binocular eye movements
(Collewijn, et al (1988a), Collewijn et al (1988b), Lemij,
(1990)) and heterophorias (Hirsch et al (1948), Kephart and
Oliver (1952), Scobee and Bennet (1950)) occurring over the
course of a normal lifetime. It is unlikely that anatomical
and physiological changes, due to growth, age, and trauma,
are equal and symmetrical between the two eyes. Therefore,
preservation of conjugacy necessitates an ongoing calibration
process which continually monitors and updates the relative

neural innervations sent to the two eyes' extraocular muscles
(nonconjugate adaptation).

Ocular motor plasticity in maintaining conjugate eye
movements has been demonstrated in behavioral studies in
monkey. Cooling of monkey left medial cerebellar nucleus
resulted in increased saccadic dysmetria in both eyes (Vilis
et al (1983)). Induced saccadic dysmetria in both eyes was
either hypometric or hypermetric; however, the amount of
induced dysmetria was unequal and direction-specific. The
right eye consistently made larger and faster rightward
saccades than the left eye; the opposite was true for
leftward saccades. Upward saccades were unaffected. After
cerebellar cooling subsided saccadic dysmetria returned to
normal amounts. These results suggest that the medial
cerebellar nucleus influences the relative size of horizontal
saccades of left and right eyes.

Uni-ocular lesion of two (Snow et al (1985)) or one (Virre
et al (1988)) horizontal extraocular muscle(s) in monkey
initially resulted in nonconjugate saccadic and
vestibuloocular reflex eye movements. If the muscle
compromise was not too great, with binocular experience,
conjugacy was restored within 7 (Virre et al 1988) to 30 days
(Snow et al 1985). Oohira and Zee (1991b) demonstrated
nonconjugate adaptation of saccades in normal monkey over a
seven day period by placing differential amounts of prism
before one eye in the right, central, and left orbital
fields.

Nonconjugate adaptation of saccadic and pursuit eye movements have been induced in humans with optical systems. Anisometropic spectacles (unequal left and right spectacle lens power) create optical images before the left and right eye that are unequal in size. Because spectacles are fixed relative to the head, the two unequal sized images do not move during eye movements. Therefore, unequal binocular eye rotations are necessary to prevent diplopia after shifting fixation from one object to another. Humans with long-time spectacle-corrected anisometropia exhibit nonconjugate (unequal-sized) saccades in an amount that nearly compensates for the unequal magnification before each eye. (Erkelens et al (1989), Lemij (1990), Oohira and Zee (1991a)). These nonconjugate saccades persisted after occluding one eye, indicating that the saccadic inequality resulted from neural re-programming, and was not a direct response to disparate stimuli. Similarly, spectacle-mounted differential magnification induced unequal binocular saccades in normal subjects within a few hours. Differential magnification was produced by either a contact lens-spectacle combination (Erkelens et al (1989), Zee and Levi(1989), Lemij (1990)) or an afocal magnifier (Horner et al (1988)). Also, Horner et al (1988), and Lemij (1990) used optical magnification systems to induce nonconjugate adaptation of pursuit eye movements in normal subjects within a few hours. Nonconjugate adaptation of vertical pursuits and saccades have been induced by differential target motion before each

eye (Schor et al (1990)). Differential target motion was simulated by unequal mirror galvanometer rotation before each eye.

In all the above studies which employed differential optical magnification, subjects were unrestrained and performed normal real-world tasks. Therefore, there was pressure to nonconjugately adapt all classes of eye movements. Hence, these experiments could not distinguish whether a single global mechanism, or several local (eye movement-specific) mechanisms underlay nonconjugate adaptation.

It is possible, for example, that phoria adaptation may underlie nonconjugate adaptation of all conjugate eye movement types (e.g. pursuit and saccade). Since phoria adaptation may vary with headcentric gaze (Ellerbroch (1948a,b), Henson and Dharamshi (1982)), there would be no need to adjust the relative versional innervations sent to extraocular muscles of both eyes. Such a model is neurologically inexpensive and incorporates an already well-established binocular adaptation mechanism. (For brevity, "headcentric gaze" is now referred to as simply "gaze.")

This study examines whether,or not, vertical saccade and pursuit share a common nonconjugate adaptation mechanism. Nonconjugate adaptation of vertical saccades and pursuits were induced by adaptation to nonconjugate target motion which, in different paradigms, emphasized either saccadic or pursuit eye movements. In the following experiments,

16

nonconjugate target motion was simulated by rotating a mirror galvanometer before one eye, 10% faster than another mirror galvanometer before the fellow eye. Therefore, target disparity was scaled to gaze eccentricity (10% gradient disparity). Nonconjugate adaptation was quantified by the difference between pre- and post-adaptation yoking ratios (ΔYR). *Yoking ratio* (YR) *was defined as the ratio of right eye movement* (R) *to left eye movement* (L) *during eye movements stimulated by a monocular-viewed target moving vertically in a fronto-parallel plane.*

$$\Delta YR = YR_{post} - YR_{pre} \hspace{2cm} (1)$$

$$YR = R\ /\ L \hspace{3cm} (2)$$

Eye position recordings used to calculated yoking ratios were obtained under monocular viewing conditions in order to ensure yoking ratio changes were due to neuro-reprogramming, and were not direct responses to vertical disparity. Lemij (1990) demonstrated that yoking of the two eyes improves with binocular viewing, as compared to monocular viewing. Presumably, this improvement was due to fusional vergence. The target, in this study, was restricted to a fronto-parallel plane in order to minimize possible effects induced by accommodation on extraocular muscle tone.

By its very definition, the term yoking ratio implies that the yoking relationship between the two eyes is a scaling

(gain) function. However, evidence in this chapter, in conjunction with with evidence in subsequent chapters, suggests this is not a valid inference; there are gaze-specific mechanisms. Nevertheless, in this study the use of yoking ratio is justified because elicited ocular motor yoking responses were gain-like. The caveat is that these gain-like responses are not descriptive of the basic adaptation mechanism, but rather they occurred as an appropriate response to gain-like disparity stimuli.

The significant result of this study is that vertical pursuit and saccade yoking ratio can be differentially altered. This observation indicates that fast eye movements (saccadic pulse component) possesses an unique nonconjugate adaptation mechanism. Slow eye movements (pursuit) may be underlaid, at least in part, by phoria adaptation. The effects of phoria adaptation are observed in the saccadic late component.

METHODS

Three subjects participated in the study. All had refractive errors less than .5 diopters, stereo thresholds lower than 40", and they did not wear spectacles. Subjects CE and MN were 20 years old, had an overview knowledge of the study, and were paid for their participation. Subject GG, the author, was 37 years old.

Subjects participated in two adaptation paradigms: saccade and pursuit. The adapting stimulus in both paradigms

consisted of nonconjugate (unequal) target motion before the two eyes. In the *saccadic paradigm* each half second the target stepped randomly to one of nine discrete positions along the vertical meridian. In the *pursuit paradigm* the target oscillated smoothly up and down along the vertical meridian at a constant velocity. Respectively, each paradigm emphasized either saccadic or pursuit eye movements. Subjects endured each paradigm under two conditions: during the right eye magnification condition the target motion was 10% greater before the right eye and during the left eye magnification condition the target motion was 10% greater before the left eye. By averaging the results from both conditions, personal biases were de-emphasized. For each subject there was at least a one week interval between sitting for each of the four experimental settings (two paradigms, 2 conditions). A bite bar and head rest were used to minimize head movement during data trials and adaptation periods

Equipment

Binocular vertical eye positions were measured with a SRI dual-Purkinje eye tracker (Crane and Steele (1978)). Voltage analogues, representing independent right and left eye positions, were amplified and then, digitized. Equipment resolution was on the order of a few minutes of arc. Digital resolution exceeded equipment resolution. An EGA graphic monitor displayed vertical binocular eye position and

vergence traces immediately following each trial for on-line inspection by the experimenter. Based on criteria (listed below) the experimenter would accept, or reject, the trial. Accepted trials were saved to hard disk for later off-line analysis. Intra-trial periods, for displaying; inspecting; and saving data trials, were usually less than five seconds.

The SRI dual-Purkinje eye tracker's viewing optics allows a 24-degree diameter field of view. Before the start of each experiment, the subject's eyes were independently spherically-refracted using the SRI's visual stimulators (Crane and Clark (1978)), which are based on the Badal optometer principle (Keating (1988)); thus minimizing target image size changes.

Also before each experiment, the subject's horizontal and vertical phorias were neutralized with an alternate cover test technique. During the phoria neutralization procedure target disparities were controlled by adjusting the orientation of independent vertical- and horizontal-deflecting mirror galvanometers, contained within the SRI's viewing optics, before each eye.

Nonconjugate (unequal) target motion before each eye was induced by unequal rotation of mirror galvanometers before each eye. An AT clone computer was used for data acquisition and storage, on-line data display, and control of left and right vertical-deflecting mirror galvanometers.

Saccade-Induced Lenticular Artifacts of Dual-Purkinje Eye Trackers

By monitoring the relative positions of the first and fourth Purkinje images, the respective images of a point source of light created by reflection off the anterior corneal surface and the posterior surface of the physiological lens, dual-Purkinje eye trackers can distinguish between eye translation and eye rotation. Eye translation is indicated when the two Purkinje images move in concert. Eye rotation is indicated when the two Purkinje images move differentially. Because the physiological lens is not rigidly attached to the rest of the eye, unlike the cornea, the sudden acceleration and de-acceleration of the eye occurring during saccadic eye movement causes translation and rotation of the physiological lens relative to the cornea. This, in turn, causes a relative movement of the first and fourth Purkinje images, which is falsely interpreted as eye rotation. The most obvious artifact is a large overshoot at the end of a saccade followed by a short period of "ringing" (Crane and Steele (1978)). However, two other inter-saccadic artifacts were observed. First, at saccade onset, for a few milliseconds, the saccade appears to go slightly in the wrong direction. Second, the peak saccadic velocity is much faster (greater than 200%) than what is predicted by main sequence charts (Bahill et al (1975)).

The initial misdirection seen in saccadic measurements may be due to relative displacement of the first and fourth Purkinje images caused by the rigidly attached cornea moving before the zonule-suspended physiological lens; the hyper-fast peak velocity measurements may result from the physiological lens rotating faster than the ocular globe due to a "slingshot" effect caused by initial acceleration of the globe and zonule elasticity. Crane and Steele (1978) postulated the large overshoot and ringing artifacts are due to inertial effects on the relative loosely-attached physiological lens after the eye is brought to an abrupt halt at the end of a saccade.

A brief study on two subjects, where first Purkinje output and differential Purkinje output were taken simultaneously, has shown that the end of a vertical saccade, estimated by first Purkinje recordings, is usually within 5 msec of the fourth Purkinje artifact peak. Eye recordings relying exclusively on the first Purkinje image are susceptible to translation artifacts (eye translation is interpreted as eye rotation); however, fourth Purkinje image artifacts do not occur.

In summary, due to mechanical artifacts the SRI dual-Purkinje eye tracker can not accurately measure eye position during and shortly (30 - 45 msec) after a saccade . Therefore, it is necessary to look some time after the end of the real saccadic pulse to get an estimate of the pulse

amplitude. It is possible that during this time the measured pulse amplitude may be effected by post-saccadic drift.

Visual Stimulus

During data trials, the vertical deflecting mirror galvanometers before the two eyes rotated equally causing the SRI's viewing optics' limiting apertures before the two eyes to also move equally. Although, one eye was prevented from seeing the tracking target, each eye could see a aperture in the periphery. Therefore, peripheral fusion of the apertures could reduce the measured nonconjugate adaptation effect. This potential problem was averted by presenting the target in a dark room which made the apertures invisible. The target (fig 1) consisted of a bright uniformly lit background with an opaque cross superimposed on it. Background illumination was dim (.5 cd/m^2), such that the ambient features of the laboratory were barely visible. Verhoeff (1939) and Ellerbrock (1948a)) have pointed out that when one eye is totally occluded, vertical phoria may vary with changes in horizontal vergence posture. In order to control horizontal vergence posture under dissociated conditions, a set of two vertical black lines, that stimulated horizontal fusion, were placed before each eye and were contained within the SRI's viewing optics (fig 1). The horizontal-fusion locks extended vertically over the entire visible field. They appeared superimposed on the target, and were always visible to both eyes.

During data trials, one eye was prevented from seeing the
tracking target by placing a translucent occluder within the
SRI's visual optics distal to the horizontal-fusion locks.
In their position, the horizontal-fusion locks were back-lite
by the bright stimulus target and remained visible to both
eyes. The horizontal-fusion locks always appeared
stationary, even when target motion was simulated by rotation
of vertical-deflecting mirror galvanometers. The target
distance was 160 centimeters.

Procedures

Subject's pupils were dilated, by applying 1 drop of
proparacaine hydrochloride (.5%) and 1 drop of tropicamide
hydrochloride (.5%) in each eye, to prevent vignetting of the
fourth Purkinje image during eccentric gaze positions.
Proparacaine is a short-acting topical anesthetic (Ellis
(1977)). Tropicamide, is an anticholinergic which inhibits
the parasympathetic nervous system (Ellis (1977)). In the
eye, the parasympathetic nervous system innervates the pupil
constrictor muscles and the ciliary muscles. Consequently,
tropicamide causes mydriasis (pupil dilation) and cycloplegia
(inhibits accommodation). In our experiments mydriasis and
cycloplegia began within ten minutes. Cycloplegia appeared
maximum within 20 minutes and lasted less than one hour.
Mydriasis was maximum in 15 to 20 minutes and lasted more
than four hours. Typically pupil diameter exceeded 6
millimeters after dilation.

Each time the subject entered the eye tracker, the two eyes were calibrated separately. During the calibration of each eye, the uninvolved eye was occluded, and the target stepped through nine vertical gaze positions, 2.5 degrees apart, spanning the central twenty degrees along the vertical meridian Three hundred milliseconds of digitized (100 Hz) analogue voltages were taken at each position. Gaze positions (degrees) and digitized analogue voltages were fit to a third-order polynomial. The calibration curve was applied to the calibration data and the results were plotted on an EGA monitor in both graphical and numerical format. The calibration was acceptable if at each calibration step the calculated eye position was within 0.1 degree of the predicted eye position. If the calibration was rejected the procedure was repeated. After a calibration was accepted for each eye, the two sets of four polynomial constants were used to transform data for on-line viewing and later off-line analysis. Calibration files were only applied to trials that directly followed their generation.

A third order polynomial was chosen as the calibration function because the SRI dual Purkinje eye tracker is not linear over the twenty-degree measurement range. There are two sources for this nonlinearity. First, there is a small machine-dependent nonlinearity associated with large angles of eccentric fixation. Second, there is a larger subject-dependent nonlinearity, that is due to irregularities of the human eye's optical surfaces. A third order polynomial

compensated for these nonlinearities, but not for larger
nonlinearities, caused by subject fixation errors or poor
alignment of subject and eye tracker.

The degree of binocular yoking was quantified by recording
binocular eye positions during saccade and pursuit eye
movements while only one eye could view the target. In the
right eye magnification condition (target motion was greater
before the right eye) the right eye was the seeing eye during
data trials and in the left eye magnification condition
(target motion was greater before the left eye) the left eye
was the seeing eye during data trials. If the horizontal-
fusion locks became diplopic, the trial was discarded.

There were two types of data trials: saccade and pursuit.
During saccade data trials (fig 2a-b) the target stepped
vertically from the center position to one of six pseudo-
random positions along the vertical meridian (up or down 3,
6, or 9 degrees). After 1.5 seconds the target stepped back
to the center position. Binocular eye position measurements
were taken during monocular viewing for one second periods at
a sampling rate of 500 Hz, beginning 50 msec before the
target stepped eccentrically. After each trial, vertical
binocular eye position and vergence traces were plotted on an
EGA monitor for inspection by the experimenter. The
experimenter accepted or rejected the trial based on the
following criteria:

1) Eye position traces was steady before saccade onset.

2)   No blink or recording artifacts (e.g. losing the lock
     on the fourth Purkinje image) were present.

3)   At least 100 msec separated the end of the primary
     saccade and the beginning of a secondary (corrective
     saccade).

4)   The latency of the primary saccade was less than 400
     msec.

5)   The primary saccade was in the appropriate direction.

If the trial was rejected, the same target stimulus was
repeated. If the trial was accepted the trial data were
saved to an individual file for later off-line analysis.
Saccades were stimulated every four to five seconds. The
data trial series ended when seventy-two total trials were
saved, twelve trials at each target amplitude. A complete
set of saccade trials, along with calibration, took seven to
eight minutes.

During pursuit data trials the target scrolled smoothly up
and down at a constant 10 degrees/sec creating a triangular
wave pattern (.25 Hz) with a peak-to-peak amplitude of 20
degrees (fig 2c-d). Binocular eye position recordings,
lasting 30 seconds each, were sampled at 100 Hz. After each
trial, vertical binocular eye position and vergence traces
were plotted on an EGA monitor for inspection by the
experimenter. The experimenter rejected the trial if severe
mechanical artifacts were present (e.g. lost lock on the

fourth Purkinje image). Five to seven trials were saved for later off-line analysis. A complete set of pursuit trials, along with calibration, took four minutes.

Adapting Paradigms

During the two-hour adaptation period the subjects binocularly followed the center of the moving target. The subjects were instructed to keep the right and left eye's target fused. The subjects were also told that if they needed to sit away from the eye tracker, then they must close one or both eyes while doing so. During an individual adaptation period small breaks (less than 1 minute) were occasionally taken, but the accumulative time away from the adapting task was less than five minutes. Adaptation paradigms were designed to emphasize either pursuit or saccadic eye movements. Target motion was always 10% greater before one eye.

In the saccade paradigm the target jumped randomly each .5 sec to one of nine equally-spaced positions (2.5 degrees apart) in the central 20 degrees along the vertical meridian. Theoretically, equal amounts of time were spent at each position during the adaptation period; however, small amplitude saccades were stimulated more frequently. Table 1 shows the predicted frequency for each saccade stimulus amplitude. The short, 0.5 sec, inter-saccadic period was designed to emphasize the pulse component of the saccade while minimizing post-saccadic vergence movements. Shorter

inter-saccadic periods were too difficult to track for extended periods of time.

STIMULUS AMPLITUDE (deg)	Probability of Occurrence (%)
2.5	22.2
5.0	19.4
7.5	16.7
10.0	13.9
12.5	11.1
15.0	8.3
17.5	5.6
20.0	2.8

TABLE 1. Probability of saccade stimulus occurrence as a function of stimulus step size.

In the <u>pursuit paradigm</u> the target motion was a 10 degree/sec, 20 degree peak-to-peak triangular wave.

Both adaptation paradigms did not entirely isolate saccadic and pursuit eye movements. In the saccadic paradigm's trials, saccadic latency and duration, together, lasted approximately 250 msec. If these same latency and duration times occurred during the adaptation period then this would leave about 250 msec for fusional vergence eye movements before the next target displacement. In the pursuit paradigm, pursuit eye movements were interspersed with small amplitude (less than 0.5 degree) "catc. up" saccades and larger (0.5 - 1 deg) saccades which occurred when the direction of eye movement changed.

Data Analysis

All calculations were accomplished off-line. Nonconjugate adaptation (Equation 1) of pursuit and saccade eye movements was quantified as the difference between pre- and post-adaptation yoking ratios (YR). At discrete gaze positions, phorias were calculated for saccade and pursuit eye movements. Phoria is defined as the angular difference between right (R) and left (L) eye gaze position when one eye is occluded.

$$\text{Phoria} = R - L \qquad\qquad (3)$$

For each paradigm, each subject's pursuit and saccade yoking ratios and phorias were calculated. Binocular eye and vergence traces from each saccade and pursuit trial were displayed on an EGA monitor. Figure 2 shows examples of conjugate and nonconjugate saccade and pursuit eye movements.

For saccade data, four eye positions were defined: pre-saccadic, pulse, step, and late (fig 2a). A computer algorithm identified the primary saccade onset by a velocity criterion (binocular eye velocity exceeding 60 deg/sec for at least 20 msec). The pre-saccade position was defined as 10 msec before the saccade onset. The pulse-position was identified through interactive means. A computer algorithm identified the lenticular artifact peak amplitude and placed a cursor 40 msec after the peak. Then the experimenter adjusted the placement of the cursor, by eye, to immediately

after the demise of visible artifacts in the eye position traces. The time of pulse-position was between 30 and 45 msec after the artifact peak. The step-position was defined as immediately before the subsequent corrective saccade or 180 msec after the artifact peak, which ever came first. The step-time ranged between 100 and 180 msec and averaged 150 to 160 msec after the peak artifact. The late-position was defined as 10 msec before the end of the one second recording period. The late-time was more than 700 msec after the artifact peak. Usually the late-time was after one or more corrective saccades.

At each of the four defined positions, binocular eye position were averaged over a 10 msec interval. These intervals occurred at the same time for right and left eye data. Phorias were calculated at each position. Saccadic yoking ratios were determined for the pulse, step, and late positions. Pulse amplitudes were calculated for each eye by subtracting pre-saccade position (D_1) from pulse position (D_2).

$$\text{Pulse Amplitude} = D_2 - D_1 \tag{4}$$

Pulse yoking ratios were calculated by the ratio of right eye pulse amplitude (A_R) to left eye pulse amplitude (A_L).

$$\text{Pulse YR} = A_R / A_L \tag{5}$$

Step and late yoking ratios were calculated by a similar method.

Pursuit data were analyzed strictly by computer algorithm. First, a three-bin (30 msec total) smoothing filter was applied to each trial. A sequential bin by bin processing followed. A velocity filter was applied to adjacent bins. Only data bins where the velocity of both eyes were between 5 and 15 deg/sec were considered. For each pursuit trial, Phoria measurements, averaged over 1.5 degree intervals, were calculated for 11 equally spaced (1.5 degrees apart) right eye gaze positions over the central 15 degrees. These phorias are referred to as "dynamic phorias" since their measurements were taken during pursuit movement. These gaze-specific phorias were further divided into three categories based on pursuit direction: upward, downward, and direction-insensitive (upward and downward pooled). An overall pursuit yoking ratio was calculated for each trial by accumulating separate right and left eye adjacent bin differences for bins passing the velocity criteria, and then dividing the final right accumulator by the final left accumulator. Since all data bins represent equal time intervals (10 msec), this method of yoking ratio calculation is equivalent to dividing average right eye velocity by average left eye velocity. Only bins where the right eye gaze position was within the central 13 degrees were included in the overall yoking ratio calculation. This was the region of constant pursuit velocity. In general, the peak-to-peak pursuit response

amplitude was 18 degrees, but beyond 6.5 degree eccentricity
the pursuit velocity slowed down due to subject anticipation
of target direction change. All statistics were calculated
with either StatView II or SuperAnova, both by Abacus
Concepts (Berkeley, California).

RESULTS

NONCONJUGATE SACCADE ADAPTATION

Subjective Observations During Adaptation Periods

Saccade Paradigm

Initially in the saccade adaptation paradigm, all subjects
reported haplopia when the target position was near the
center of the adapting field, and diplopia when the target
was more eccentric; remember, target disparity increased
proportionally with eccentricity. Within - 5 minutes
subjects GG and MN reported an abatement of diplopia when the
target was in the adapting field which produced a right-hyper
disparity (upper field for right eye magnification condition
and lower field for left eye magnification condition). When
this abatement occurred diplopic targets in the opposite
field became more separated, and at times central targets
became slightly diplopic. At fortuitous times when the
target remained in the left-hyper disparity field for several
consecutive target presentations, the left-hyper disparity
field became fused and when the target subsequently moved to
the right-hyper disparity field immediate fusion of the
targets was less likely. On average, subject CE experienced

33

similar amounts of diplopia in upper and lower positions of gaze. However, when the target remained in one hemifield for several target presentations, diplopia was reduced or eliminated in that hemifield and increased in the fellow hemifield.

After sixty minutes of adaptation, none of the subjects reported any reduction in the occurrence of diplopia or in the separation of diplopic targets. After seventy five to ninety minutes, target diplopic separation was reported to decrease. After the two hour adaptation period, diplopia was seen only after the largest saccades and then, diplopic separation was greatly reduced. Judging by the reports of diplopia, all three subjects adapted at approximately the same rate. During the entire adaptation period no subject witnessed diplopic targets moving towards each other in the short, .5 sec, inter-saccadic interval. (The targets appeared either fused or diplopic at the end of the saccade. If the targets were diplopic no reduction of the target's separation was seen.)

Pursuit Paradigm

Initially in the pursuit paradigm, all subjects reported haplopia when the target position was near the center of the adapting field and diplopia when the target was more eccentric. However, within 1 - 2 minutes diplopia ceased in the right hyper field for subjects GG and MN, and to a lesser extent, diplopia decreased in the left-hyper field for subject CE. The early abatement of diplopia in one hemifield

was accompanied by an increase in diplopic separation of targets in the opposite hemifield. After ten to twenty minutes the amount of diplopia started to decrease in the "difficult" hemifield. After forty to sixty minutes diplopia was no longer reported.

Pre-Adaptation Pulse Yoking Ratios

The circles in figures 3a-c (saccade paradigm), and figures 4a-c (pursuit paradigm) represent pre-adaptation pulse yoking ratios from individual saccades plotted against the right eye's pulse amplitude. Similarly, crosses in these figures represent post-adaptation pulse yoking ratios. The top chart in each figure depicts the left eye magnification condition (adaptation to greater target motion before the left eye). With nonconjugate adaptation, the crosses would be lower than the circles. The bottom charts represents the right eye magnification condition. With nonconjugate adaptation, the crosses would be higher than the circles.

Casual inspection of figures 3 and 4 shows that strictly conjugate pre-adaptation saccades, pulse yoking ratio equal to one, were the exception rather than the rule. Furthermore, there are idiosyncratic differences in the yoking ratio versus saccade amplitude pattern. For example, the pre-adaptation saccades of subject GG, figures 3b and 4b, tended to have yoking ratios greater than one (right eye moves more than left eye) for upward saccades and yoking ratios less than one (left eye moves more than right eye) for

35

downward saccades. Also, subject MN consistently showed more variation in pulse yoking ratios than the other two subjects.

Comparison of pre-adaptation data from each subject's four charts revealed a day-to-day within subject variation. For example, in figure 4b (upper chart), GG's pre-adaptation yoking ratios increased with larger amplitude downward saccades and remained relatively invariant for upward saccades of all sizes. However, in the lower chart, GG's pre-adaptation yoking ratios decreased with larger amplitude downward and upward saccades.

Collewijn et al (1988a,b) and Lemij (1990) reported that an occluded eye had slightly smaller pulse amplitudes than the fellow viewing eye. Since the left eye was the viewing eye in the left eye magnification condition and the right eye was the viewing eye in the right eye magnification condition, figures 3 and 4 do not verify higher pre-adaptation yoking ratios (circles) in the lower charts relative to the upper charts.

Figures 5 and 6 depicted averaged pre-adapted yoking ratios grouped by pulse-amplitude (discussed in more detail below). Casual inspection reveals that pulse-amplitude specific yoking ratios are different for downward- and upward- directed saccades. For example, in the bottom chart in figure 5b, downward saccade yoking ratios were relatively independent of pulse amplitude. However, upward saccade yoking ratios increased with with increasing pulse amplitude.

Remember, since all saccades were centrifugal, saccade direction is confounded with gaze position.

Pre-Post Changes in Saccades

Pulse yoking ratio data was grouped into six categories based on the right eye pulse amplitude for the following reasons:

1) Although there were six discrete saccade stimulus amplitudes, the aggregate of saccadic pulse response amplitudes formed a continuum, making matched pre-post comparisons difficult.

2) Variability in pulse yoking ratios was strongly related to saccade amplitude. Grouping data by saccade amplitude effectively factors out related variation from the overall variability, thereby increasing statistical power.

For all subsequent analyses saccade yoking ratios are calculated from data grouped into six categories based on saccade direction (upward versus downward) and amplitude (less than 4 degree, 4 to 7 degrees, greater than 7 degrees). Also, step, and late yoking ratios were grouped based on the right eye's step and late amplitudes. Because most primary saccades were followed by at least one corrective saccade, the right eye's pulse and late amplitude may differ by several degrees; therefore, a single saccade's pulse and late components may contribute to different amplitude categories.

These category criteria were chosen because they resulted in approximately an equal number of saccades in each category.

The circles in figures 5a-c (saccade paradigm), and figures 6a-c (pursuit paradigm) represent grouped pre-adaptation pulse yoking ratios plotted against the right eye's pulse amplitude. Similarly, crosses in these figures represent grouped post-adaptation data. Each error bar represent ± 1 standard deviation of the pulse yoking ratio data around the averaged point. Table 2 shows the average standard deviation for each subject's pre- and post-adaptation grouped data. These averages contain 24 points each. There are six saccade amplitudes for two adaptation conditions (right and left eye magnification) and two adaptation paradigms (saccade and pursuit). The overall pulse yoking ratio variability (average standard deviation) was .022. A within subject paired t-test (table 3) showed no significant difference between pre- and post-adaptation pulse yoking ratio variation. (If the pulse yoking ratio data was not grouped by pulse amplitude then the average pulse yoking ratio standard deviation would increase, depending on the subject, to .026 - .058.)

Subject	Saccade STD Pre-Adapt	Saccade STD Post-Adapt	Paired-t 2-tailed	Probability
C E	.020	.019	- .532	NS
G G	.018	.016	-1.200	NS
M N	.029	.023	- .138	NS

Table 2. Average standard deviation of pre- and post-adaptation pulse yoking ratios for each subject. Within subject paired t-test (df = 23) showed no significant difference between pre- and post-adaptation pulse yoking ratio variation. NS = not significant (p > .05).

In the following sections saccadic yoking ratio changes less than 2.2% are considered unreliable, because the average variability of pulse yoking ratios, expressed as standard deviations, was 2.2% (see above).

.

Nonconjugate adaptation of saccadic pulse

Saccade Paradigm

Following the saccade paradigm (figure 5a-c) pulse yoking ratio changes were always in the expected direction. The pulse yoking ratio decreased for left eye magnification (top charts) and increased for right eye magnification (bottom charts). Within each experimental condition, changes in yoking ratios were approximately equal for the various saccade amplitudes.

For each subject, post-adaptation data from the left eye magnification condition were transformed to make nonconjugate adaptation to left eye magnification resemble nonconjugate adaptation to right eye magnification. This allowed data

39

from the right and transformed left eye conditions to be pooled. Pooling data from the two adapting conditions was used to average over personal biases. The following transformation equation was applied to the post-adaptation data from the left eye magnification condition:

$$YR_{Post}(Transformed) = (2 * YR_{Pre}) - YR_{Post} \qquad (6)$$

For example, if the pre-adaptation yoking ratio was 1.01 and the post-adaptation yoking ratio was .95. This would be a 6% (.06) decrease in the yoking ratio. The transformed yoking ratio would be ((2 * 1.01) - .95 =) 1.07. The transformed yoking ratio would be a 6% increase. Subsequent to transformation, positive pre-post changes in yoking ratio would be expected for all appropriate nonconjugate changes. For all subsequent analyses, each subject's right eye and transformed left eye data are pooled.

Table 3 shows the average change of pulse yoking ratios for each subject via the saccade paradigm. A within subject comparison was done with a paired t-test (df = 11). All subjects had statistically reliable changes in pulse yoking ratios. The overall average change in yoking ratio for the pulse paradigm was reliable (5.7%).

Subject	Mean Change	Paired - t	Probability
C E	.082	8.167	< .0001
G G	.045	10.311	< .0001
M N	.045	8.280	< .0001

Table 3. Average changes in pulse yoking ratio after adapting to saccade paradigm. For each subject data from right and transformed (see text) left eye target motion magnification were pooled. The mean changes in pulse yoking ratios were found to be significant with within subject paired-t test (2-tailed) (df =11) comparisons of pre- and post-adaptation yoking ratios.

Pursuit Paradigm

Following pursuit paradigm adaptation (figs 6a-c) subject CE (fig 6a) showed nonconjugate adaptation for upward saccadic pulse after adapting to left eye magnification and for downward saccade after adapting to right eye magnification. Subject GG (fig 6b) showed little change for both conditions. Subject MN (fig 6c) showed inconsistent nonconjugate changes. For example in the lower chart in figure 6c, yoking ratios decreased for downward saccades and increased for upward saccades. Both subjects CE and MN showed pulse yoking changes that were pulse direction-specific and, to a lesser extent, pulse amplitude-specific.

Table 4 shows the average change of pulse yoking ratios for each subject via the saccade paradigm . A paired t-test (df = 11) was used to make within subject comparisons of pre- and post-adaptation data. Only subject CE had a significant increase in yoking ratio, but less than half of that occurred with the saccade paradigm. It is interesting to note that

during the pursuit paradigm adaptation period subject CE,
made conspicuously larger and more frequent "catch-up"
saccades and larger "turn-around" saccades than the other two
subjects.

The other two subjects showed no net change in yoking
ratio. The overall average change in yoking ratio for the
pulse paradigm was unreliable (.8%).

Subject	Mean Change	Paired - t	Probability
C E	.036	4.420	< .001
G G	-.004	-1.537	NS
M N	-.009	-1.048	NS

Table 4. Average changes in pulse yoking ratio after
adapting to the pursuit paradigm. For each subject data from
right and transformed (see text) left eye target motion
magnification were pooled. Within subject paired-t test (2-
tailed) (df =11) comparisons of pre- and post-adaptation
yoking ratios was significant for subject CE only.. NS = not
significant (p > .05).

Post-saccadic vergence drift

Post-saccadic vergence drift (PSVD) was defined as the
change in phoria between the pulse and step times scaled by
the amplitude of the right eye's saccadic pulse
amplitude (A_R).

$$PSVD = (Phoria_{Pulse} - Phoria_{Step}) / A_R \qquad (7)$$

In general, the pre-adaptation post-saccadic drift of each
eye was upward in direction after both upward and downward
saccades, in agreement with similar findings from Collewijn

(1988b). Figure 7 shows the change in PSVD (post - pre) for the saccade (top chart) and pursuit paradigm (bottom chart) plotted against grouped right pulse amplitude. In general for both paradigms, the step component was effected slightly (< 2%) more than the pulse component; this is denoted by the generally negative change in PSVD. This difference was slightly more prominent after pursuit paradigm adaptation. No saccade amplitude-related trends were noted.

Comparison of Pulse, Step, and Late Yoking ratios

Saccade Paradigm

Table 5 displays the difference between the average change in pulse and step yoking ratio after adaptation to the saccade paradigm. A t-test was used to make within subject pre- and post-adaptation comparisons. The overall difference between pulse and step yoking ratios was unreliable (.7%).

Subject	Pulse - Step	Paired - t	Probability
C E	-.004	-1.09	NS
G G	-.012	-3.90	< .01
M N	-.005	-1.29	NS

Table 5. Average differences between pulse and step yoking ratio changes after adapting to saccade paradigm. Within subject paired-t test (2-tailed) (df =11) comparisons of pulse and step yoking ratio changes were made. NS = not significant (p > .05).

Table 6 displays the difference between the average change in pulse and step yoking ratio after adaptation to the pursuit paradigm. A within subject t-test was used to make

pre- and post-adaptation comparisons. The overall difference

between pulse and late yoking ratios was unreliable (1.1%).

Subject	Pulse - Step	Paired - t	Probability
C E	-.004	-1.32	NS
G G	-.016	-6.78	< .001
M N	-.013	-6.31	< .001

Table 6. Average differences between pulse and step yoking
ratio changes after adapting to pursuit paradigm. Within
subject paired-t test (2-tailed) (df =11) comparisons of
pulse and step yoking ratio changes were made. NS = not
significant (p > .05).

Table 7 displays the difference between the average change

in pulse and late yoking ratio after adaptation to the

saccade paradigm. A t-test was used to make within subject

pre- and post-adaptation comparisons. The overall difference

between pulse and late yoking ratios was unreliable (1.2%).

Subject	Pulse - Late	Paired - t	Probability
C E	.017	3.300	< .01
G G	.008	1.358	NS
M N	.010	1.329	NS

Table 7. Average differences between pulse and late yoking
ratio changes after adapting to saccade paradigm. Within
subject paired-t test (2-tailed) (df =11) comparisons of
pulse and step yoking ratio changes were made. NS = not
significant (p > .05).

Table 8 displays the difference between the average change

in pulse and late yoking ratio after adaptation to the

pursuit paradigm. A t-test was used to make within subject

44

pre- and post-adaptation comparisons. The overall difference

between pulse and late yoking ratios was reliable (2.9%).

Subject	Pulse - Late	Paired - t	Probability
C E	-.018	-4.32	< .01
G G	-.034	-5.55	< .001
M N	-.034	-4.74	< .001

Table 8. Average differences between pulse and late yoking ratio changes after adapting to pursuit paradigm. Within subject paired-t test (2-tailed) (df =11) comparisons of pulse and step yoking ratio changes were made.

Summary - Saccades

In both adapting paradigms, the change in pulse yoking

ratio was consistently, but unreliably, smaller than then the

step yoking ratio. In the saccade paradigm the pulse yoking

ratio was consistently, but unreliably, larger than the late

yoking ratio. In the pursuit paradigm the pulse yoking ratio

was reliably smaller than the late yoking ratio. After

adaptation to the saccade paradigm, the saccadic pulse yoking

ratios changed equally for saccades of different amplitudes.

However, pulse yoking ratio changes were direction-specific

after adaptation to the pursuit paradigm.

NONCONJUGATE PURSUIT ADAPTATION

Pre-Adaptation Pursuit Yoking Ratios

Similar to saccades, strictly conjugate pursuits do not

exist. Figures 8 and 9 display the average overall yoking

ratio of pre- and post-adaptation to the pursuit and saccade

paradigm. The open circles represent pre-adaptation pursuit yoking ratios and the crosses represent post-adaptation yoking ratios. The symbols on the right and left sides of the charts represent the left and right eye magnification conditions. Small idiosyncratic noncomitancies were noted in all pre-adaptation data trials. Furthermore, there was daily variation. On a given day the pursuit yoking ratio variation between trials was very small. Table 9 shows the average standard deviation of pre- and post-adaptation yoking ratios. Component standard deviations were determined from trials conducted on a single day. Similar to saccades there was no significant difference between the standard deviations of pre- and post-adaptation yoking ratios. The average standard deviation of pursuit yoking ratio on a given day was 1%.

Subject	Pursuit STD Pre-Adapt	Pursuit STD Post-Adapt	Paired-t 2-tailed	Prob- ability
C E	.010	.011	.322	NS
G G	.007	.009	.940	NS
M N	.012	.012	.163	NS

Table 9. Average standard deviation of pre- and post-adaptation pursuit yoking ratios for each subject. Within subject paired t-test (df = 3) showed no significant difference between pre- and post-adaptation pursuit yoking ratio variation. NS = not significant (p > .05).

In the following sections, pursuit yoking ratio changes less than 1% are considered unreliable, because the average inter-trial pursuit yoking variability, expressed as standard deviations, was 1% (see above)

Pre-Post Changes in Pursuits

All subsequent pursuit analyses are preceded by within subject pooling of right and transformed (equation 6) left eye magnification data.

Pursuit Paradigm

Table 10 shows the average change of pursuit yoking ratios for each subject via the pursuit paradigm. A paired t-test was used to make within subject pre- and post-adaptation comparisons. All subjects had large increases in pursuit yoking ratio which where reliably different. The overall average change in pursuit yoking ratio was 7.8%.

Subject (df)	Mean Change	Paired - t	Probability
C E (13)	.083	17.43	< .0001
G G (10)	.061	11.19	< .0001
M N (10)	.090	.090	< .0001

Table 10. Average changes in pursuit yoking ratio after adapting to the pursuit paradigm. For each subject data from right and transformed (see text) left eye magnification were pooled. Within subject paired-t test (2-tailed) comparisons of pre- and post-adaptation

Saccade Paradigm

Table 11 shows the average change of pursuit yoking ratios for each subject via the saccade paradigm. A within subject comparison was done with a paired t-test. Only subject CE had a large increase in yoking ratio. Subject GG had a small, (1.8%) increase in pursuit yoking ratio, but because of small inter-trial variability, this was a reliable

47

difference. The changes in subject MN's pursuit yoking

ratios were not significant. The overall average pursuit

yoking ratio change was 3.1%. Subject CE accounted for 80%

of the pursuit yoking ratio change.

Subject (df)	Mean Change	Paired - t	Probability
C E (12)	.072	10.700	< .0001
G G (9)	.018	5.250	< .001
M N (12)	.001	.044	NS

Table 11. Average changes in pursuit yoking ratio after
adapting to the saccade paradigm. For each subject data from
right and transformed (see text) left eye magnification were
pooled. Within subject paired-t test (2-tailed) comparisons
of pre- and post-adaptation. NS = not significant (p > .05).

The two charts in Figure 10 depict pre- and post-

adaptation changes in phoria plotted against right eye gaze

position. Because eye position measurements were made during

pursuit eye movements, these phorias are referred to as

dynamic phorias. The top and bottom charts represent

adaptation to right eye magnification within the pursuit and

the saccade paradigm for one subject. These charts

illustrate a consistent finding: dynamic phorias do not show

pursuit direction selectivity. That is, the direction of

pursuit travel (upward versus downward) did not influence

dynamic phorias. Furthermore, the pursuit paradigm always

induced gradient-like changes in the dynamic phoria pattern

(top chart in figure 10), and the saccade paradigm always

resulted in irregular gaze-dependent changes in the dynamic

phoria pattern (bottom chart in figure 10 was the most

48

extreme example of irregular changes in the dynamic phoria
pattern).

The bottom chart in figure 10 shows an unique result in
that the gaze-specific phoria change was not only
significant, but paradoxical. The gaze-specific phoria
changes were opposite to that of the disparity stimulus.
However, this subject (MN) gave an almost identical result
for the left eye magnification condition. Therefore, after
pooling of right and transformed left eye magnification
condition data, the pooled yoking ratio change was not
reliable. This is why table 12 only shows a pursuit yoking
ratio change of .1% for subject MN in the saccade paradigm.
The similar results from the two adapting conditions suggests
that, for this subject, the changes in pre-post pursuit
yoking ratios were due to idiosyncratic bias rather than
nonconjugate adaptation. These paradoxical results may have
resulted from fatigue, or perhaps, the mechanisms which
normally calibrate pursuit yoking were confused by the
saccade paradigm's adapting stimulus, causing these
mechanisms to lose their normal calibration.

Summary - Pursuits

Adaptation to the pursuit paradigm resulted in reliable
large changes in pursuit yoking ratios in all subjects.
However, adaptation to the saccade paradigm resulted in small
(< 2%) changes in pursuit yoking ratios in two subjects and
large changes in one subject, CE. The pursuit paradigm

induced gradient-like changes in the dynamic phoria pattern.

These gradient-like dynamic phoria changes indicate that the

pursuit yoking ratio change was uniform over all measured

gaze positions. In contrast, after adapting to the saccade

paradigm, a consistent finding was that the changes in

dynamic phoria patterns varied irregularly across different

gaze positions. This suggests gaze-specific changes in

pursuit yoking ratio. Dynamic phorias were not direction-

specific; that is, the dynamic phoria did not vary with the

direction of pursuit travel (up versus down).

FINAL SUMMARY

Figure 11 represents yoking ratio changes for pursuit eye

movements and individual saccadic components (pulse, step,

and late) as single global-averaged values. Figures 12a-c

are similar, but each applies to only one subject. Casual

inspection of each individual's charts (fig 12a-c) reveal the

same pursuit and saccadic yoking ratio change patterns as

those found in the global chart (fig 11).

In the saccade paradigm (fig 11 circles), the greatest

change in yoking ratio occurred in the saccadic pulse and

step components. The smallest change occurred in pursuit.

The saccadic late component changed by an intermediate

amount. Subject CE accounted for most of the increase in

pursuit yoking ratio. Subjects GG and MN each had less than

a 2% yoking ratio change in pursuit eye movements.

In the pursuit paradigm (fig 11 squares), the greatest change in yoking ratio occurred with pursuit eye movements. The saccadic components changed much less than the pursuit. Within saccades, the pulse component changed the least and the late component changed the most. Again, subject CE accounted for most of the change in the saccadic pulse yoking ratio change. Subjects GG and MN each demonstrated less than a 1% yoking ratio change in saccadic pulse and step components.

Table 12 reduces saccadic pulse and pursuit yoking ratio changes, from all subjects and adaptation conditions, to single global-averages. Overall significance of saccadic pulse and pursuit yoking ratio changes was tested with a three-way within ANOVA (Tables 13 - 16). In the pursuit paradigm, the pursuit yoking ratio change was significant ($p = .010$), but the saccadic pulse change was not. In the saccade paradigm, the pursuit yoking ratio change was *not* significant, but the saccadic pulse change was significant ($p < .05$).

PARADIGM:	Saccadic Pulse Yoking Ratio Change	Pursuit Yoking Ratio Change
Saccade	5.7% (p<.05)	3.1% (NS)
Pursuit	0.8% (NS)	7.8% (p=.01)

TABLE 12. Global-averaged saccadic pulse and pursuit yoking ratio changes. Averages includes data from all subjects and adaptation conditions. Parentheses contain statistical significance (3-way within ANOVA). See text for details.

Pursuit Paradigm: Pursuit Yoking Ratio Change

Source	df	Sum of Squares	F-Value	P-Value
Subject	2	.001		
ADAPT	1	.106	85.569	.0115
ADAPT * Subject	2	.002		
EYE MAG	1	.013	.450	.5713
EYE MAG * Subject	2	.058		
TRIALS	5	.002	1.276	.3464
TRIALS * Subject	10	.004		
ADAPT * EYE MAG	1	3.018E-4	.210	.6917
ADAPT * EYE MAG * Subject	2	.003		
ADAPT * TRIALS	5	4.722E-4	1.115	.4112
ADAPT * TRIALS * Subject	10	.001		
EYE MAG * TRIALS	5	.004	2.322	.1204
EYE MAG * TRIALS * Subject	10	.003		
ADAPT * EYE MAG * TRIALS	5	.001	1.251	.3557
ADAPT * EYE MAG * TRIALS * Subject	10	.002		

Dependent: PURSUIT YOKING RATIO

Table 13. Summary Table (three-way within ANOVA) for testing significance of pre- and post-adaptation changes in pursuit yoking ratios in the pursuit paradigm. Independent variables were ADAPT (pre and post), EYE MAG (Adapting Condition - Target motion magnification before right or left eye), and TRIALS (individual pursuit data trials). There were three subjects (CE, GG, MN).

Saccade Paradigm: Pursuit Yoking Ratio Change

Source	df	Sum of Squares	F-Value	P-Value
Subject	2	.018		
ADAPT	1	.019	1.736	.3183
ADAPT * Subject	2	.021		
EYE MAG	1	.001	.992	.4242
EYE MAG * Subject	2	.001		
TRIALS	5	.001	1.872	.1865
TRIALS * Subject	10	.002		
ADAPT * EYE MAG	1	3.441E-4	.047	.8484
ADAPT * EYE MAG * Subject	2	.015		
ADAPT * TRIALS	5	2.590E-4	.531	.7490
ADAPT * TRIALS * Subject	10	.001		
EYE MAG * TRIALS	5	.001	.567	.7240
EYE MAG * TRIALS * Subject	10	.002		
ADAPT * EYE MAG * TRIALS	5	3.713E-4	1.349	.3206
ADAPT * EYE MAG * TRIALS * Subject	10	.001		

Dependent: PURSUIT YOKING RATIO

Table 14. Summary Table (three-way within ANOVA) for testing significance of pre- and post-adaptation changes in pursuit yoking ratios in the saccade paradigm. Independent variables were ADAPT (pre and post), EYE MAG (Adapting Condition - Target motion magnification before right or left eye), and TRIALS (individual pursuit data trials). There were three subjects (CE, GG, MN).

Pursuit Paradigm: Pulse Yoking Ratio Change

Source	df	Sum of Squares	F-Value	P-Value
Subject	2	.008		
ADAPT	1	.001	.262	.6598
ADAPT * Subject	2	.007		
EYE MAG	1	4.201E-5	.002	.9692
EYE MAG * Subject	2	.044		
TRIALS	5	.044	2.402	.1117
TRIALS * Subject	10	.037		
ADAPT * EYE MAG	1	6.806E-7	.001	.9789
ADAPT * EYE MAG * Subject	2	.002		
ADAPT * TRIALS	5	.001	5.044	.0145
ADAPT * TRIALS * Subject	10	.001		
EYE MAG * TRIALS	5	.009	1.575	.2526
EYE MAG * TRIALS * Subject	10	.012		
ADAPT * EYE MAG * TRIALS	5	3.497E-4	.108	.9879
ADAPT * EYE MAG * TRIALS * Subject	10	.006		

Dependent: PULSE YOKING RATIO

Table 15. Summary Table (three-way within ANOVA) for
testing significance of pre- and post-adaptation changes in
saccadic pulse yoking ratios in the pursuit paradigm.
Independent variables were ADAPT (pre and post), EYE MAG
(Adapting Condition - Target motion magnification before
right or left eye), and TRIALS (six categories based on pulse
amplitude of the right eye). There were three subjects (CE,
GG, MN).

Saccade Paradigm: Pulse Yoking Ratio Change

Source	df	Sum of Squares	F-Value	P-Value
Subject	2	.008		
ADAPT	1	.058	20.165	.0462
ADAPT * Subject	2	.006		
EYE MAG	1	.002	.571	.5289
EYE MAG * Subject	2	.008		
TRIALS	5	.030	1.300	.3377
TRIALS * Subject	10	.046		
ADAPT * EYE MAG	1	.002	1.183	.3903
ADAPT * EYE MAG * Subject	2	.003		
ADAPT * TRIALS	5	.001	1.745	.2121
ADAPT * TRIALS * Subject	10	.001		
EYE MAG * TRIALS	5	.003	.394	.8422
EYE MAG * TRIALS * Subject	10	.016		
ADAPT * EYE MAG * TRIALS	5	3.633E-4	.269	.9201
ADAPT * EYE MAG * TRIALS * Subject	10	.003		

Dependent: PULSE YOKING RATIO

Table 16. Summary Table (three-way within ANOVA) for testing significance of pre- and post-adaptation changes in saccadic pulse yoking ratios in the saccade paradigm. Independent variables were ADAPT (pre and post), EYE MAG (Adapting Condition - Target motion magnification before right or left eye), and TRIALS (six categories based on pulse amplitude of the right eye). There were three subjects (CE, GG, MN).

DISCUSSION

Independent Nonconjugate Adaptation

This study confirms several previous studies (cited above) that it is possible, within a few hours to alter the two eyes' yoked relationship during pursuit and saccade eye movements. This study extends those finding's by providing evidence that, at least in part, different mechanisms subserve nonconjugate adaptation of vertical pursuit and saccade eye movements. In two of three subjects, pursuit or saccade eye movements could be nonconjugately adapted with little (<2%) or no transfer to the other eye movement type.

With the third subject (CE) the pursuit paradigm was 44% as effective as the saccade paradigm in inducing pulse yoking ratio changes (3.6% vs 8.2%). Perhaps, this small crossover of adaptation was influenced by CE's relative greater frequency and size of "catch-up" saccades during pursuit eye movements. However, both adaptation paradigms induced a large increase in CE's pursuit yoking ratio (8.3% and 7.2% for the pursuit and saccade paradigms, respectively). These results could be explained if CE possessed a robust phoria adaptation ability that responded effectively to both adaptation paradigms, and this robust phoria adaptation underlaid nonconjugate pursuit adaptation. Phoria adaptation can be gaze-specific (Ellerbroch (1948a,b), Henson and Dharamshi (1982)). The effects of phoria adaptation are most likely to be seen in the saccadic late component. The fact that CF's saccadic late yoking ratio changes were twice that of the

other two subjects (5% vs 2.5% and 6.5% vs 3% for pursuit and saccade paradigms, respectively) supports the idea that nonconjugate pursuit adaptation induced by the saccade paradigm in subject CE where underlaid by gaze-specific phoria adaptation. Unfortunately, since static phorias (phorias measured during attempted steady fixation) were not measured, gaze-specific comparisons with dynamic phorias (phorias measured during pursuit eye movements) could not be made. Therefore, this issue remains unresolved.

The concept of independent pursuit and saccade nonconjugate adaptation mechanisms is further supported by differences in the time course of adaptation, indicated by subjective reports of diplopia, and by differences in gaze-specificity. Diplopia subsided within 40 to 60 minutes into the pursuit paradigm adaptation period; in contrast, at the end of the two hour saccade paradigm adaptation period diplopia was still present for saccades responding to target displacement greater than seventeen degrees. Unfortunately, diplopic separation is not a precise indicator of relative eye position because the appreciation of diplopia has sensory, as well as motor, components. Kertesz (1983) demonstrated that after a two degree vertical step in disparity, haplopia was reported while up to a half degree in vergence error remained. Furthermore, Fender and Julesz (1967) have shown that, under certain conditions, once sensory fusion is established it is possible to retain fusion even though a fixation disparity of 65 arc-minutes was

gradually introduced. These two studies reduce the credibility of using subjective reports of haplopia to gauge ocular motor responses.

The pursuit paradigm caused a gradient-like change in (pursuit) dynamic phorias. The saccade paradigm caused an approximately uniform change in saccadic pulse yoking ratios for all saccade amplitudes. Gradient-like phoria changes and uniform shifts in yoking ratios would be expected from gain-based mechanisms. However, these gain-like responses are not descriptive of the basic nonconjugate adaptation mechanisms, but rather they occurred as appropriate responses to gain-like disparity stimuli. In a gain-based nonconjugate mechanism, a scalar would control the relative ocular motor innervations sent to each eye. In this scheme nonconjugate adaptation would consist of adjusting the size of the scalar. Because one parameter controls all, nonconjugate change would spread equally to all gaze positions. In this study, the inappropriate stimuli revealed that pursuit and saccade nonconjugate adaptation mechanisms are gaze-specific and therefore, not gain-based. The pursuit paradigm induced pulse direction-specific changes in pulse yoking ratios, and the saccade paradigm induced gaze-specific dynamic phoria changes.

Four inferences can be drawn from these observations. First, each adapting paradigm provoked gain-like changes in one eye movement type, and not the other. This response specificity provides additional evidence for the presence of

independent pursuit and saccade nonconjugate adaptation mechanisms. _Second_, each eye movement type responded well to one type of adaptation paradigm and ineffectively to the other. This indicates that pursuit and saccade nonconjugate adaptation mechanisms are driven by different stimuli and that the appropriate stimulus for one may be inappropriate to the other, leading to irregular and sometimes paradoxical results. _Third_, pursuit and saccade nonconjugate adaptation are not gain-controlled; that is, a single scalar parameter is inadequate to describe the modification of the two eyes' yoked relationship. In this study, the gain-like responses to appropriate stimuli were simply the correct responses to gradient-disparity stimuli. In contrast, inappropriate stimuli revealed the gaze-specific nature of saccade and pursuit nonconjugate adaptation. _Fourth_, direction-specific pulse yoking changes may indicate separate nonconjugate mechanisms underlie upward- and downward-directed saccades. However, whether direction-specific pulse yoking changes actually occurred is not clear because, in this study, saccade direction was confounded with field position.

Variability of Yoking Ratios

Pursuit yoking variability, expressed as inter-trial standard deviation, was very small (1%). During each 2 hour adaptation period, assuming the subjects attended to the task for all but five minutes, the subjects would have either tracked a target 69,000 degrees in the pursuit paradigm, or

would have made almost 14,000 saccades in the saccade paradigm. However, pursuit yoking variability was not reliably altered following adaptation period. Therefore, nonconjugate adaptation, and concentrated periods of voluntary eye movements, does not reliably add noise (variability) to pursuit yoking.

(Saccadic) pulse yoking variability, expressed as inter-trial standard deviations, was strongly dependent on pulse amplitude and -direction. Across subjects, these variances were largely idiosyncratic, and do a lesser extent, diurnal. After pulse-amplitude variability was factored out, remaining yoking variation was small (2%) and fairly consistent for all saccade sizes. Yoking variability related to pulse-amplitude and pulse-direction may arise in areas, within the vertical saccade system, related to planning saccadic size and direction, such as the superior colliculi. The deep layers of the superior colliculus retinotopically code saccadic direction and size (review - Sparks and Hartwich-Young (1989)). Pure vertical saccades involve both superior colliculi (Kömpf et al (1979).

Pulse yoking ratio variability did not reliably change after adaptation; this indicates that nonconjugate mechanisms are not major sources of noise in the pulse yoking process.

It is not known whether the main source of noise in pursuit and saccade yoking was introduced in a multiplicative, or additive process. The same is not known about innervations associated with nonconjugate pursuit

adaptation. Therefore, it is not possible to draw conclusions about the relative placement of nonconjugate mechanisms, within the pursuit or saccade system, relative to the main yoking noise source.

Phoria Adaptation

Phoria is the vergence error while monocularly viewing a fixed target. When a prism is placed before one eye the measured phoria, with prism in place, will initially change by an amount equal to the prism. However, within a few minutes the measured phoria, with the prism still in place, will revert back to the pre-prism value; this induced phoria change, known as phoria (or prism) adaptation, results from a change in open-loop (monocular viewing) vergence posture.

The two lenses in anisometropic spectacles have different refractive powers, and in turn, create two images of different sizes. Because spectacles are fixed relative to the head, the spectacle images do not move with eye movement. Therefore, when gaze is shifted to bi-fixate an object the eyes are required to move unequally. Anisometropic spectacles create a disparity stimulus that is scaled to gaze position (gradient disparity).

Long-time anisometropic spectacle wearers typically exhibit phorias through the spectacles, measured at different gaze positions, that are less than what is predicted by the spectacle's differential magnification (Ellerbroch (1948a),

Erkelens (1989), Lemij (1990)). This indicates that phoria adaptation has gaze position-specific qualities.

Henson and Dharamshi (1982) postulated phoria adaptation occurs over limited adaptation fields. In Henson and Dharamshi's model, maximum phoria adaptation occurs at the (headcentric) gaze position used during adaptation. From this position of maximum adaptation, there is a graded spread of adaptation to neighboring gaze positions such that the half-height of adaptation was twenty degrees from the adapting gaze position. Sethi (nee Dharamshi) and Henson (1984) noted that phoria adaptation to prism was faster than phoria adaptation to gradient disparity. They postulated phoria adapted slower to gradient disparities because overlapping adaptation fields, each adapting to a different gaze-specific disparity, interfered with each other.

In this study, except for subject CE in the saccade paradigm, the first subjective change noted in the adaptation period was a loss of diplopia in one "easy" hemifield accompanied by an increase in diplopic separation in the opposite "difficult" hemifield. The "easy" hemifield was idiosyncratic and related to the direction of stimulus disparity. For example, the hemifield with a right hyper disparity stimulus (the upper field for the right eye magnification condition and the lower field for the left eye magnification condition) was always the "easy" hemifield for subjects GG and MN. This change occurred within a few minutes in both adaptation paradigms. During the pursuit

paradigm adaptation period there was a gradual ebbing of diplopic separation in the "difficult" hemifield. The most eccentric gaze position (largest disparity) in the "difficult" hemifield was the last position to be fused.

These observations are not consistent with Henson and Dharamshi's proposed series of overlapping (headcentric) gaze-specific adaptation fields. First, it is unlikely that all adapting fields would have the same phoria bias, thus generating an initial rapid broadly-tuned phoria shift. Second, because the adapting fields have a graded spread, the most extreme position in the "difficult" hemifield would not be expected to be the last position fused since it is furthermost from the dominant adapting fields.

These observations are more easier reconciled by a global and a local phoria adaptation mechanisms. The global phoria mechanism has a rapid onset and generalizes over all headcentric gaze positions. The local phoria adaptation mechanism has a slower onset, and consists of limited gaze-specific phoria adaptation fields with graded spread, similar to Henson and Dharamshi's model.

REFERENCES

Bahill AB, Ciuffreda KJ, Kenyon R, and Stark L (1977), Dynamic and static violations of Hering's Law of equal innervation, Am. J. Optom. Physiol. Opt. 53:786

Bahill AT, Clark ML, and Stark L (1975), The main sequence, a tool for studying human eye movements, Math. Biosci. 24(3/4):191

Bridgeman B & Stark L (1868), The Theory of Binocular Vision, Hering E [Translation (1977), Bridgeman B & Stark L (Eds.)] Plenum Press: New York

Collewijn H, Erkelens CJ, and Steinman RM (1988a), Binocular coordination of human horizontal saccadic eye movements, J. Physiol. 404:157

Collewijn H, Erkelens CJ, and Steinman RM (1988b), Binocular coordination of human vertical saccadic eye movements, J. Physiol. 404:183

Crane H and Clark M (1978), Three dimensional visual stimulus deflector, Applied Optics 17:706

Crane H and Steele C (1978), Accurate three dimensional eye tracker, Applied Optics 17:691

Ellerbrock V and Fry GA (1942), Effects induced by anisometropic corrections, Am. J. Optom. and Arch. Am. Acad. Optom. 19:444

Ellerbrock VJ (1948a), Further study of effects induced by anisometropic corrections, Am. J. Optom. and Arch. Am. Acad. Optom. 25:430

Ellerbrock VJ (1948b), A clinical investigation of compensation for vertical prismatic imbalances, Am. J. Optom. and Arch. Am. Acad. Optom. 25:309

Ellis PP (1977), Ocular therapeutics and pharmacology, 5th Edition, Mosby Company:Saint Louis

Erkelens CJ, Steinman RM, And Collewijn H (1989), Asymmetrical adaptation of human saccades to anisometropic spectacles, Invest. Ophthalmol. Vis. Sci. 30:1132

Fender DH and Julesz B (1967), Extension of Panum's fusional area in binocularly stabilized vision, J. Opt. Soc. Am. 57:819

Henson DB and Dharamshi BG (1982), Oculomotor adaptation to induced heterophoria and anisometropia, Invest. Ophthalmol. Vis. Sci. 22:234

Hering E (1868), The Theory of Binocular Vision, [Translation (1977), Bridgeman B & Stark L (Eds.)] Plenum Press: New York

Hirsch MJ, Alpern M, and Shultz HL (1948), The variation of phoria with age, Am. J. Optom. and Arch. Am. Acad. Optom. 25:535

Horner DG, Gleason G, and Schor CM (1988), The recalibration of Hering's law for versional eye movements in response to aniseikonia, Invest. Ophthalmol. Vis. Sci. 29:136 (abstract 28)

Keating M (1988), Geometric, physical, and visual optics, Butterworths: Boston

Kephart NC and Oliver JE (1952), A study of the relationship between lateral phoria and age, Am. J. Optom Arch Am Acad Optom 8:423

Kertesz AE (1983), Vertical and cyclofusional disparity vergence, In Vergence eye movements: basic and clinical aspects, Schor and Ciuffreda (Eds.), Butterworths: Boston, Chapt 9, page 317

Kömpf D, Pasik T, Pasik P, and Bender MB (1979), Downward gaze in monkeys. Stimulation and lesion studies, Brain 102:527

Lemij HG (1990), Asymmetrical adaptation of human saccades to anisometropic spectacles, Doctoral Dissertation, Erasmus University of Rotterdam

Oohira A, Zee DS, and Guyton DL (1991a), Disconjugate adaptation to long-standing, large-amplitude spectacle-corrected anisometropia, Invest. Ophthalmol. Vis. Sci. 32:1693

Oohira A and Zee DS (1991b), Disconjugate ocular motor adaptation in rhesus monkey, (In Press)

Schor CM (1979), The relationship between fusional vergence eye movements and fixation disparity, Vision Res. 19:1359

Schor CM, Gleason J, and Horner D (1990), Selective nonconjugate binocular adaptation of vertical saccades and pursuits, Vision Res. 30:1827

Scobee RG and Bennet EA (1950), Hyperphoria, a
    statistical study, Arch. Ophthalmol. 43:458

Sethi (nee Dharamshi) B and Henson DB (1984), Adaptive
    changes with prolonged effect of comitant and
    noncomitant vergence disparities, Am. J. Optom.
    Physiol. Opt. 61:506

Snow R, Hore J, and Villis T (1985), Adaptation of
    saccadic and vestibuloocular systems after
    extraocular muscle tenectomy, Invest. Ophthalmol.
    Vis. Sci. 26:924

Sparks DL and Hartwich-Young R (1989), In Reviews of
    oculomotor research, Vol 3, The neurobiology of
    saccadic eye movements, Büttner-Ennever JA (Ed.),
    Elsevier: Amsterdam Chapt 5, page 213

Verhoeff FH (1939), Hyperphoria tests based on a new
    principle, Arch. Ophthalmol. 22:743

Vilis T, Snow R, and Hore J (1983), Cerebellar
    saccadic dysmetria is not equal in the two eyes,
    Exp. Brain Res. 51:343

Virre E, Cadera W, and Villis T (1988), Monocular
    adaptation of the saccadic system and Vestibuloocular
    reflex, Invest. Ophthalmol. Vis. Sci. 29:1339

Zee DS and Levi L (1989), Neurological aspects of
    vergence eye movements, Rev Neurol (Paris) 145:613
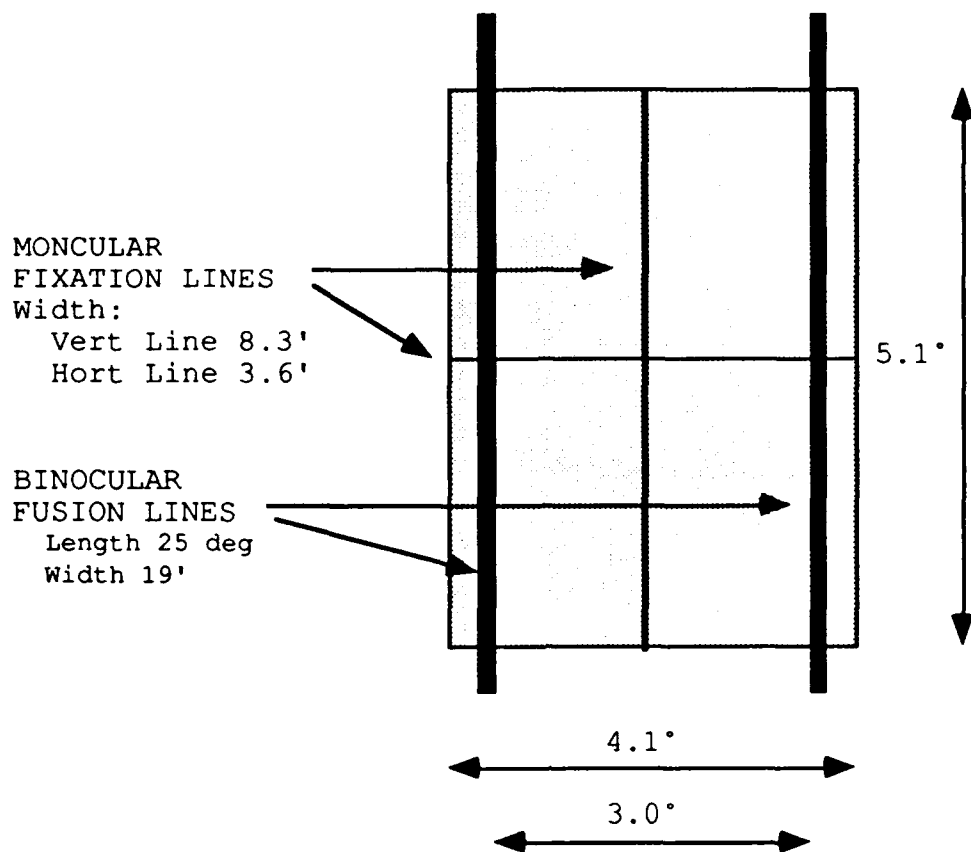
FIG 1 The monocular tracking target consisted of a high contrast horizontal and vertical line superimposed on a bright uniformly illuminated background. Subjects were instructed to fixate the intersection of the vertical and horizontal lines throughout the session. Two sets of two parallel, vertical lines were placed in the right and left eye channels of the SRI's visual optics to provide a horizontal binocular fusion lock while the vertical vergence loop remained open.
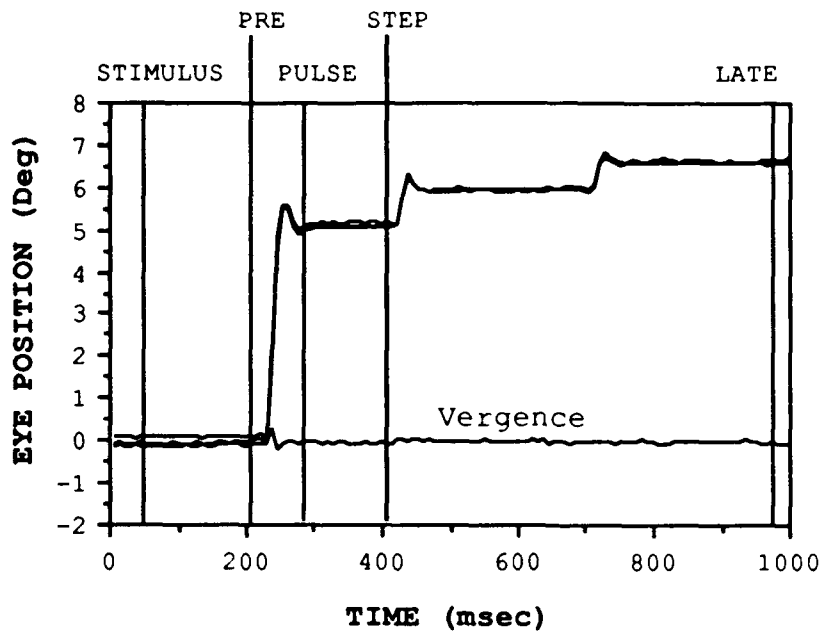
FIG 2a. Binocular vertical saccadic eye movement recordings depict a conjugate saccade; there is very little change in vergence during the pulse (fast phase) component. The vergence trace is the difference between right and left eye traces. The label "STIMULUS" above the graph represents the time at target was displaced. The remaining four labels represent saccade bench marks (see text pages 18 and 19) used in data analyses.
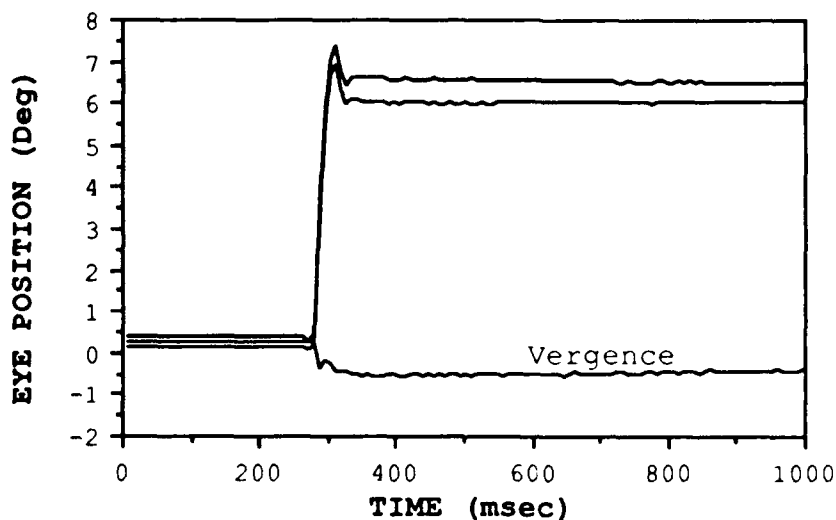
FIG 2b. Binocular vertical saccadic eye movement recordings depict a nonconjugate saccade; most of the vergence change occurs during the pulse component. The vergence trace is the difference between right and left eye position traces. Note prominent lenticular artifact at the end of saccade fast phase.

68
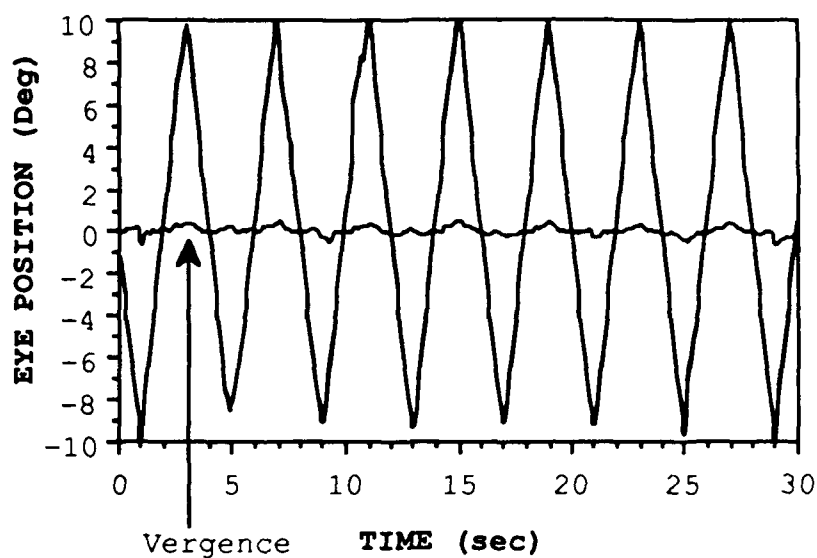
FIG 2c. Binocular vertical pursuit eye movement recordings depict a conjugate pursuit. The vergence line flucuates relatively little. The vergence trace is the difference between right and left eye position traces.
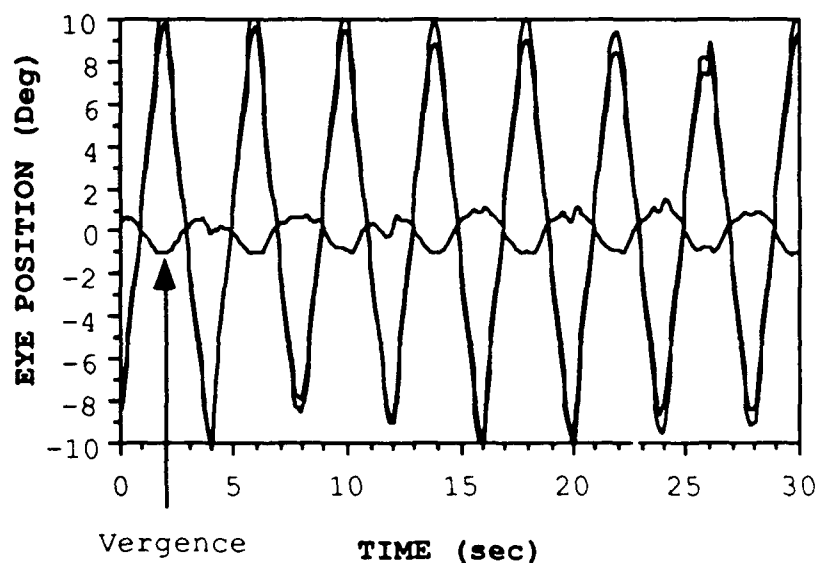
FIG 2d. Binocular vertical pursuit eve movement recordings depict a nonconjugate pursuit. The left eye is moving 8% faster than the right eye. The vergence trace is the difference between right and left eye position traces.

FIG 3a-c. <u>Saccade Paradigm.</u> Pre- and post-adaptation saccadic pulse yoking ratios (R/L) are plotted against right eye pulse amplitude (- = downward saccade; + = upward saccade). The top chart in each figure shows data from the left eye magnification condition and the bottom chart shows data from the right eye magnification condition. Circles depict pre-adaptation pulse yoking ratios and crosses depict post-adaptation pulse yoking ratios. Nonconjugate adaptation would result in crosses lower than circles in the top charts and crosses higher than circles in the bottom charts. Figures 3a, 3b, 3b represent data from subjects: CE. GG, and MN, respectively.
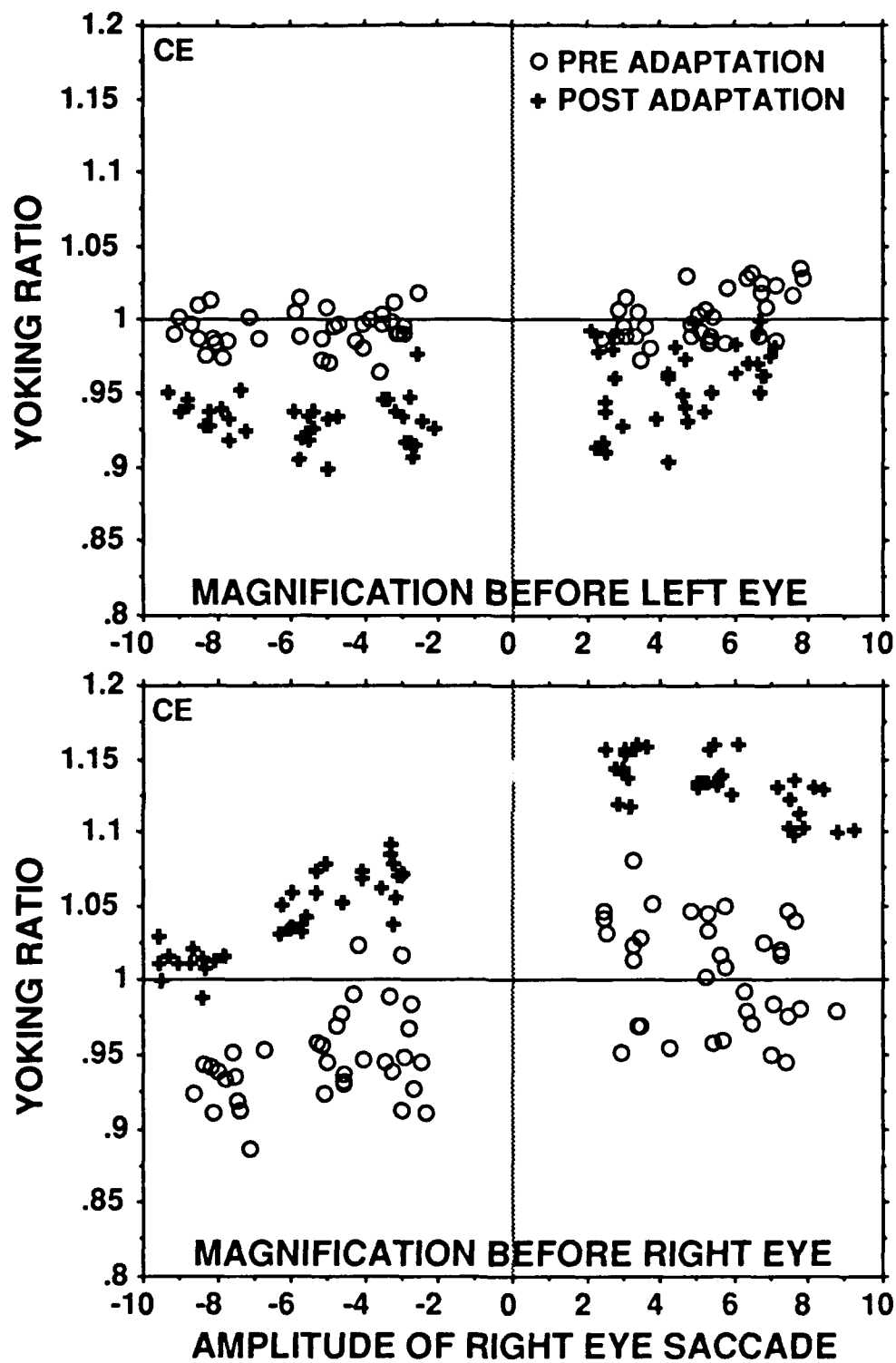
FIG 3a. Saccade Paradigm - Subject CE.
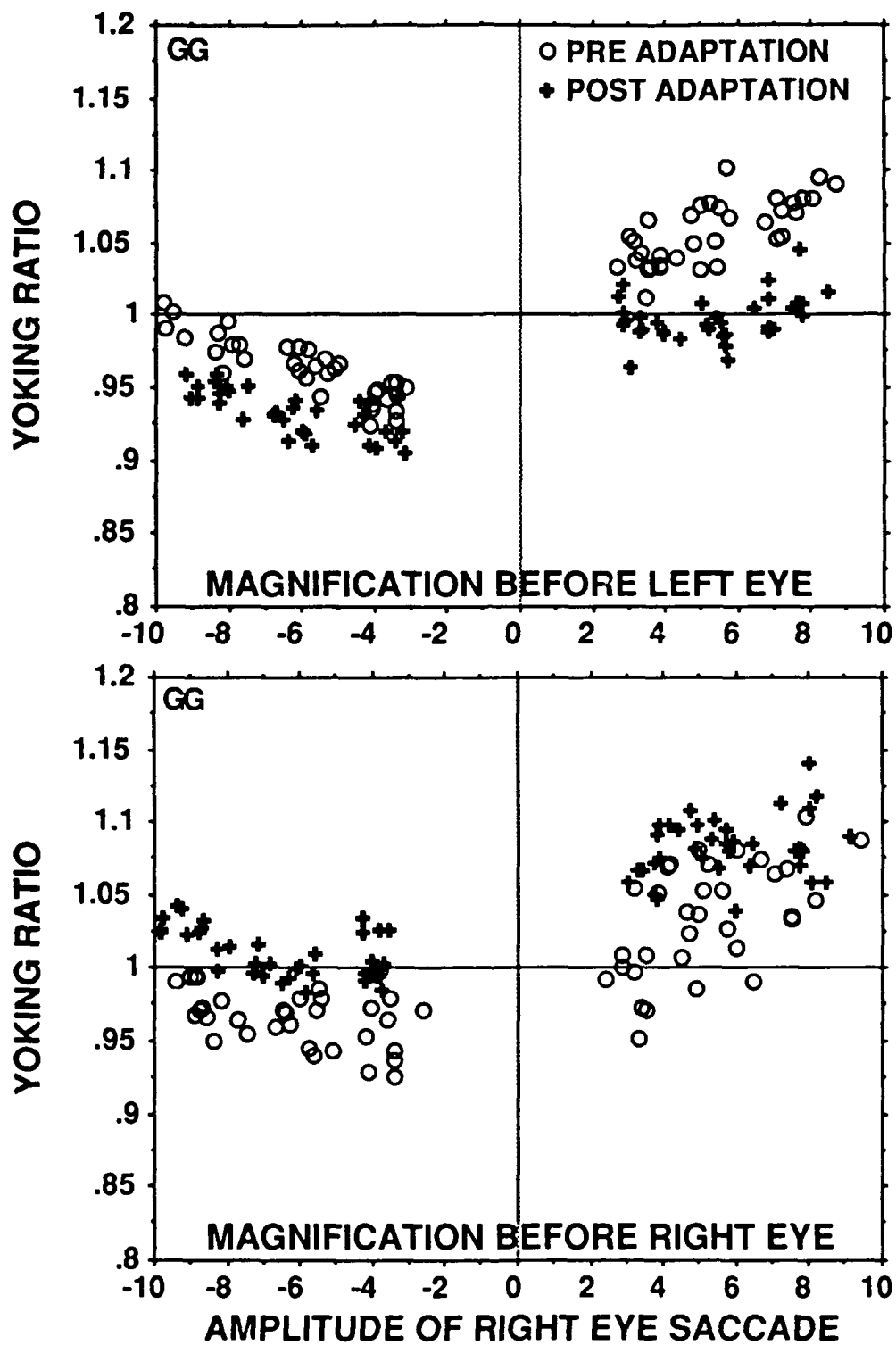
FIG 3b Saccade Paradigm – Subject GG.
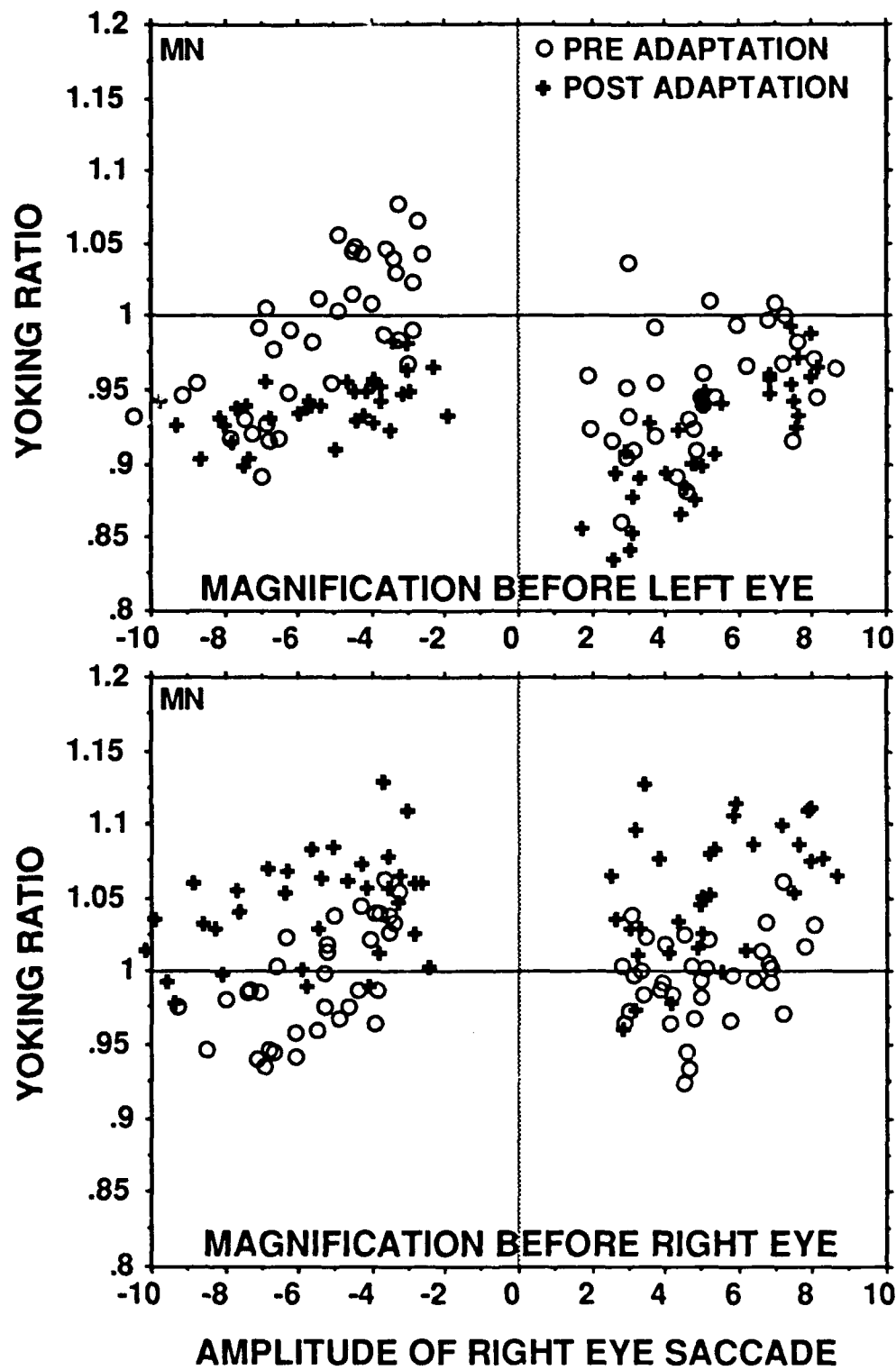
FIG 3c Saccade Paradigm – Subject MN.

FIG 4a-c. <u>Pursuit Paradigm.</u> Pre- and post-adaptation saccadic pulse yoking ratios (R/L) are plotted against right eye pulse amplitude (- = downward saccade; + = upward saccade). The top chart in each figure shows data from the left eye magnification condition and the bottom chart shows data from the right eye magnification condition. Circles depict pre-adaptation pulse yoking ratios and crosses depict post-adaptation pulse yoking ratios. Nonconjugate adaptation would result in crosses lower than circles in the top charts and crosses higher than circles in the bottom charts. Figures 3a, 3b, 3b represent data from subjects: CE. GG, and MN, respectively.
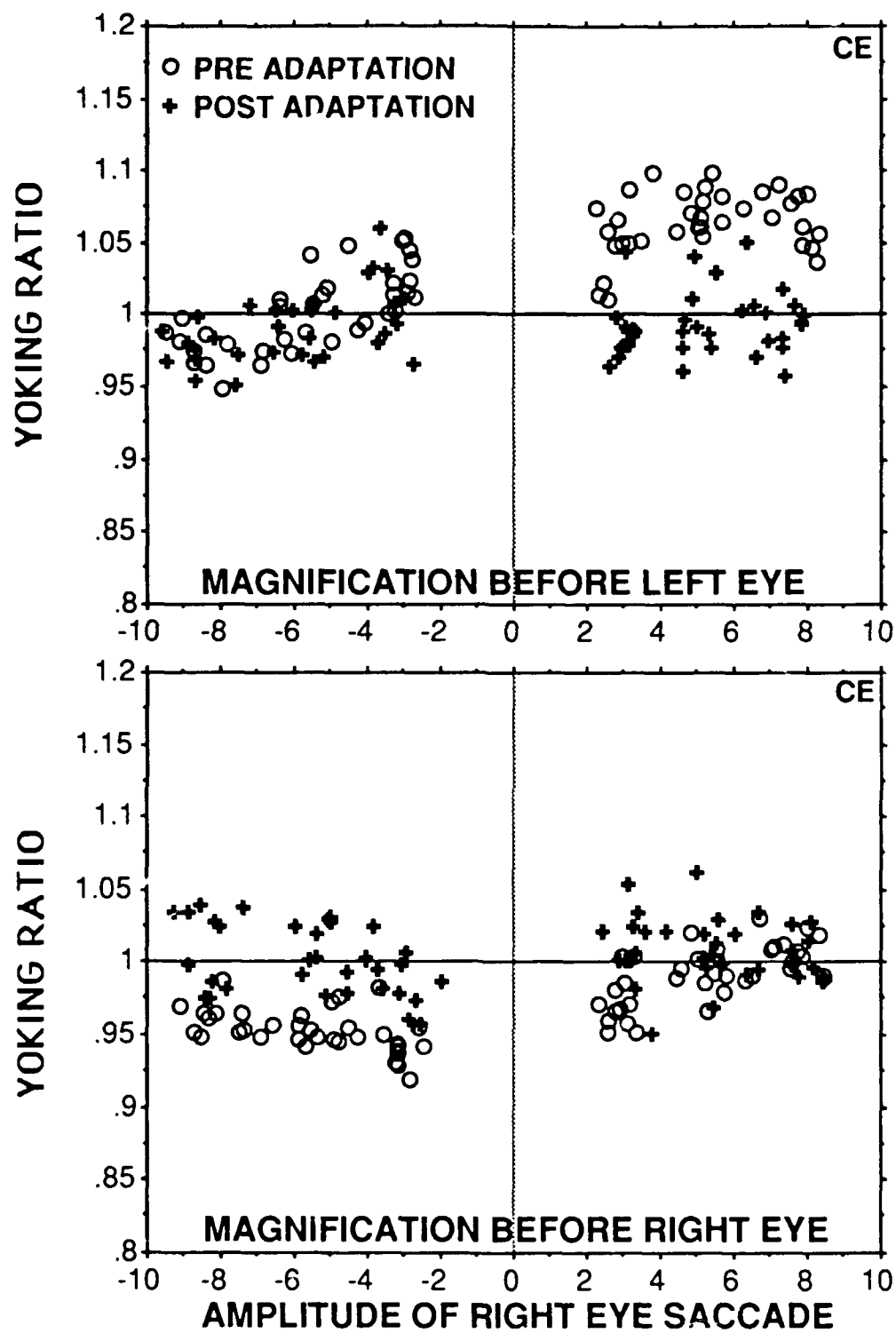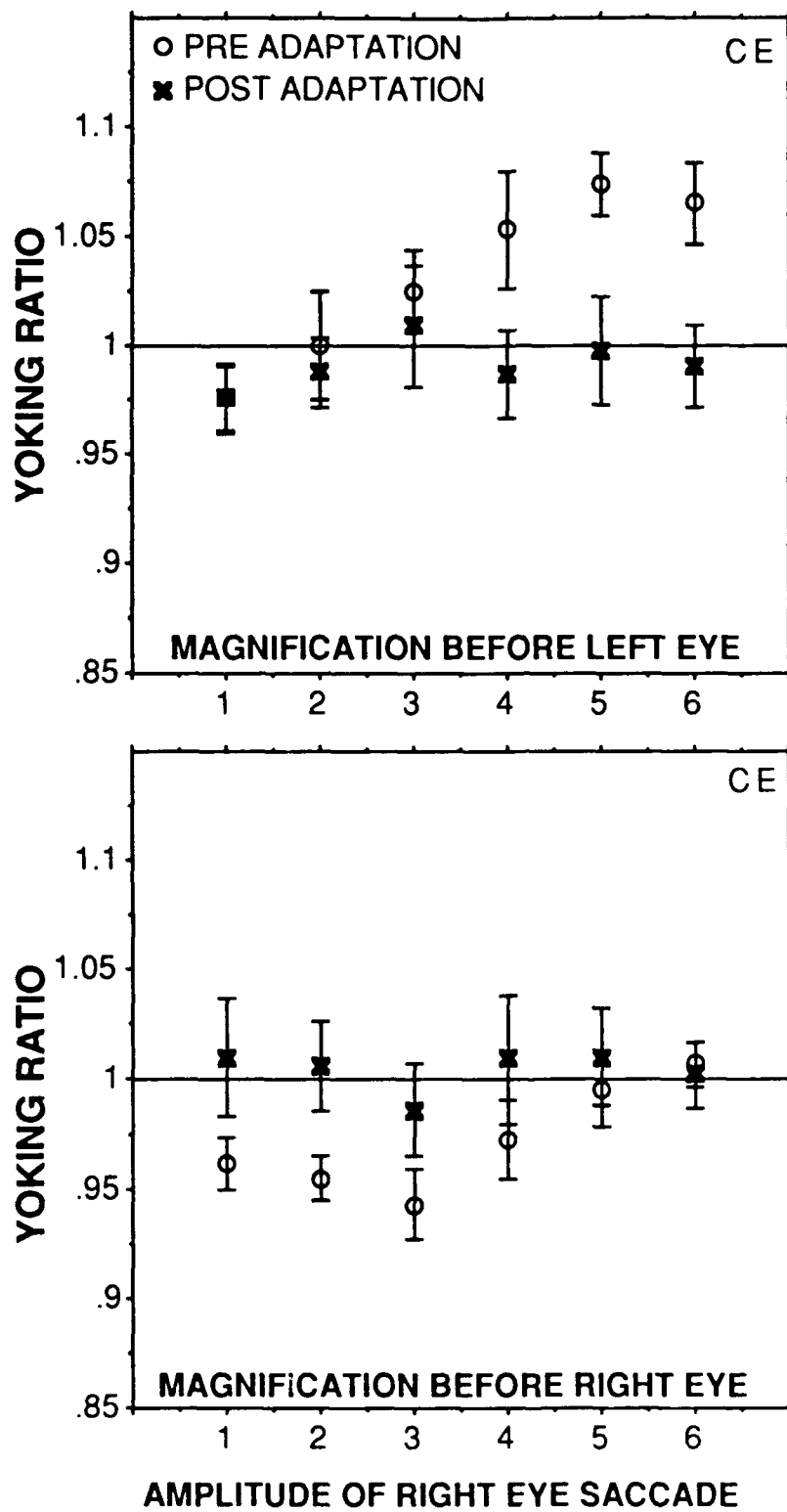
FIG 4a Pursuit Paradigm - Subject CE.
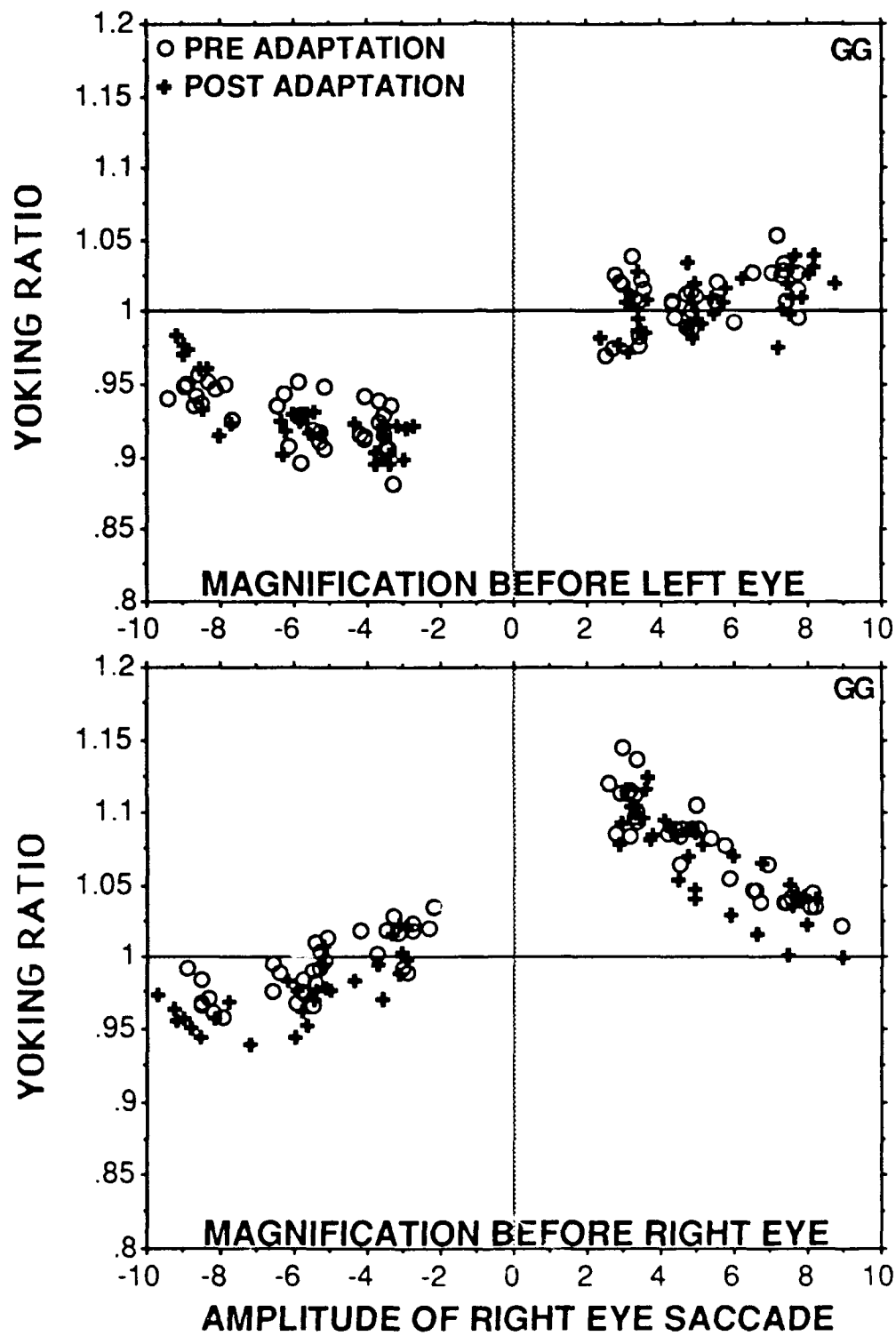
FIG 4b Pursuit Paradigm - Subject GG.
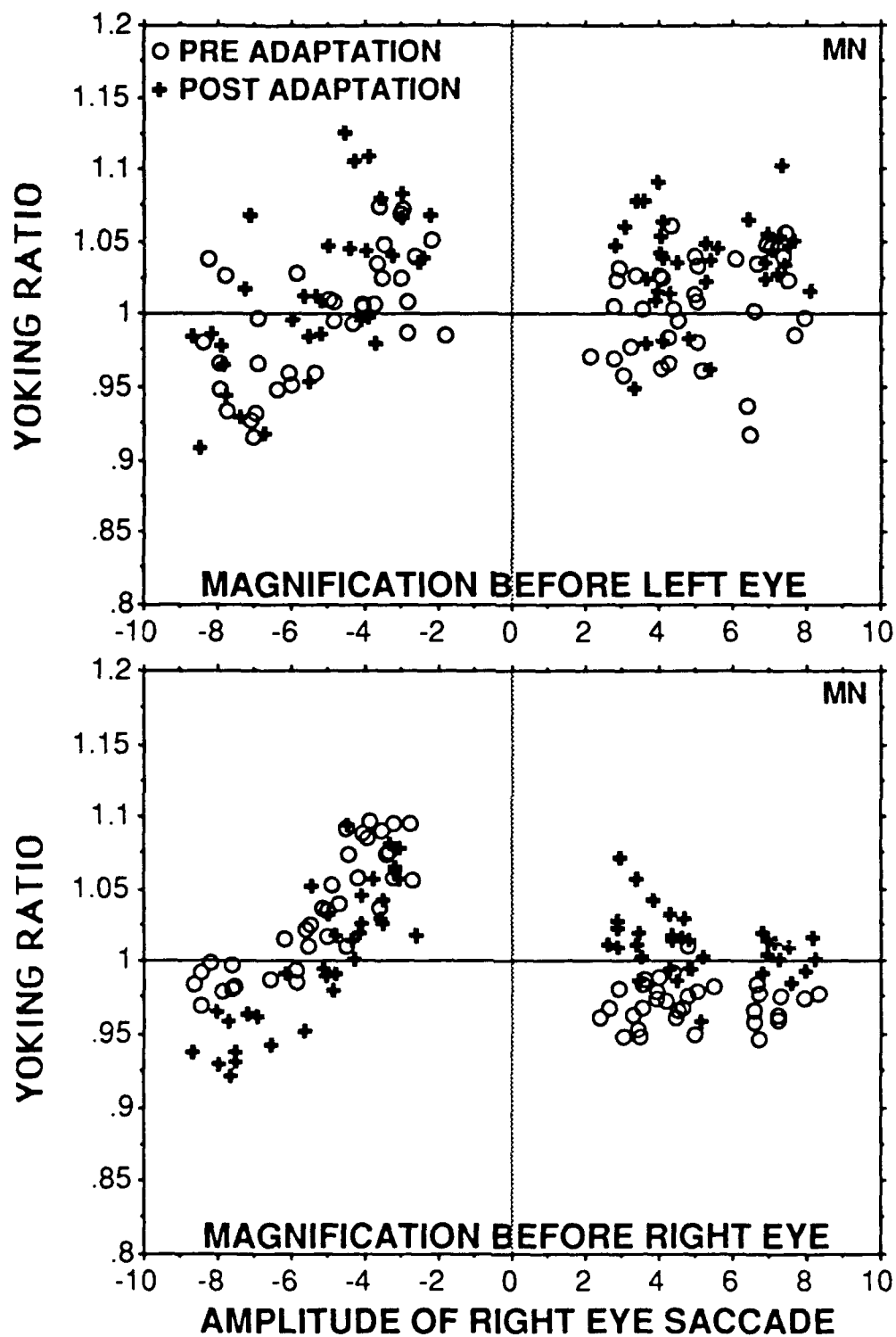
FIG 4c Pursuit Paradigm - Subject MN

FIG 5a-c. Saccade Paradigm. Each subject's saccadic pulse yoking ratios (R/L) are plotted against right eye pulse amplitude (- = downward saccade; + = upward saccade). Top chart shows data from left eye magnification condition and bottom chart shows data from right eye magnification condition. Circles depict pre-adaptation pulse yoking ratios and crosses depict post-adaptation pulse yoking ratios. Nonconjugate adaptation would result in crosses lower than circles in the top chart and crosses higher than circles in the bottom chart. The following table relates each chart's category number with the right eye's pulse amplitude.

Category Number	1	2	3	4	5	6
Saccade Component Direction and Amplitude	Down > 7 deg.	Down 4-7 deg.	Down < 4 deg.	Up < 4 deg.	Up 4-7 deg.	Up > 7 deg.

FIG 5a. Saccade Paradigm - Subject CE.
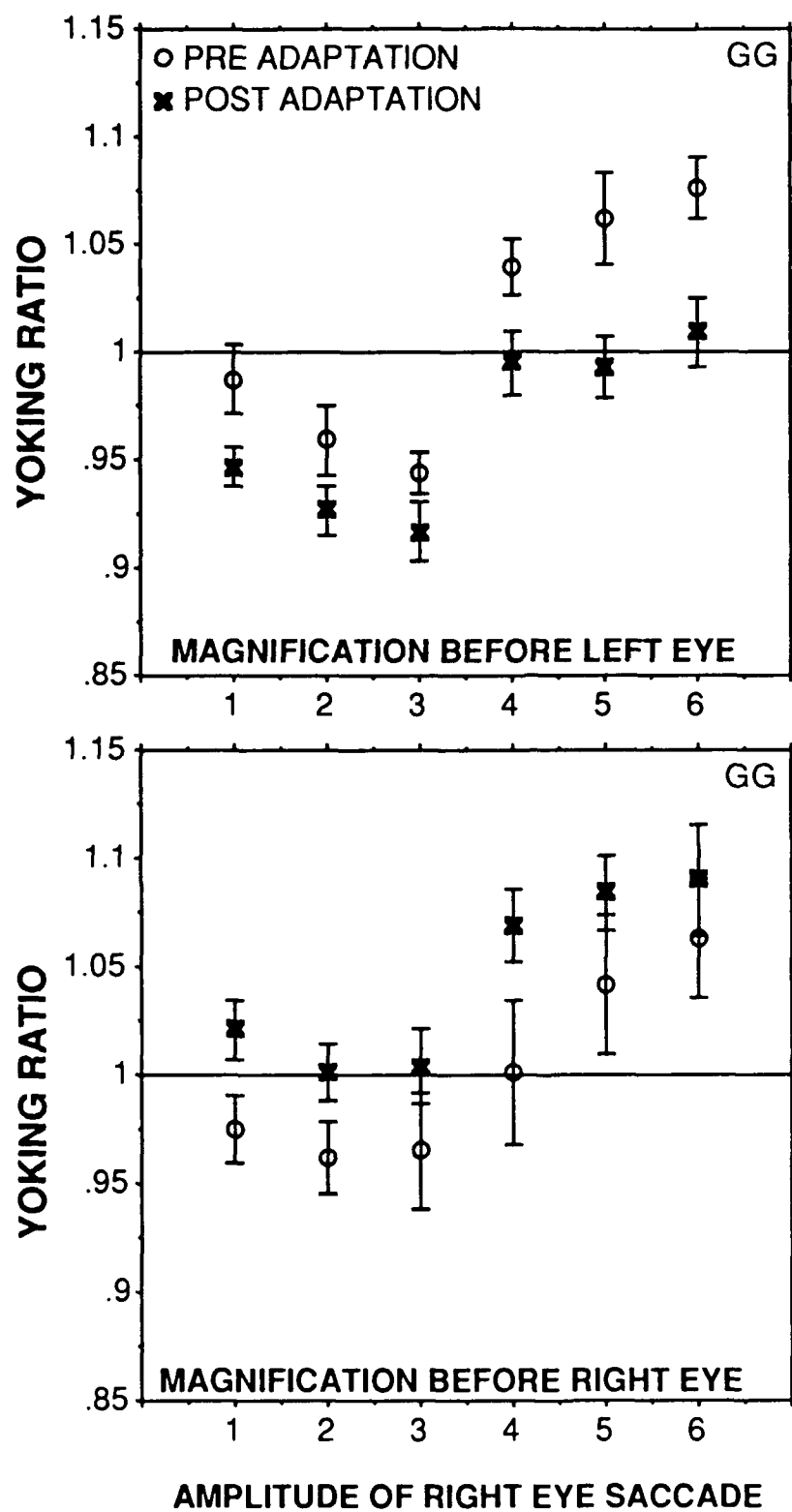
FIG 5b. Saccade Paradigm – Subject GG.
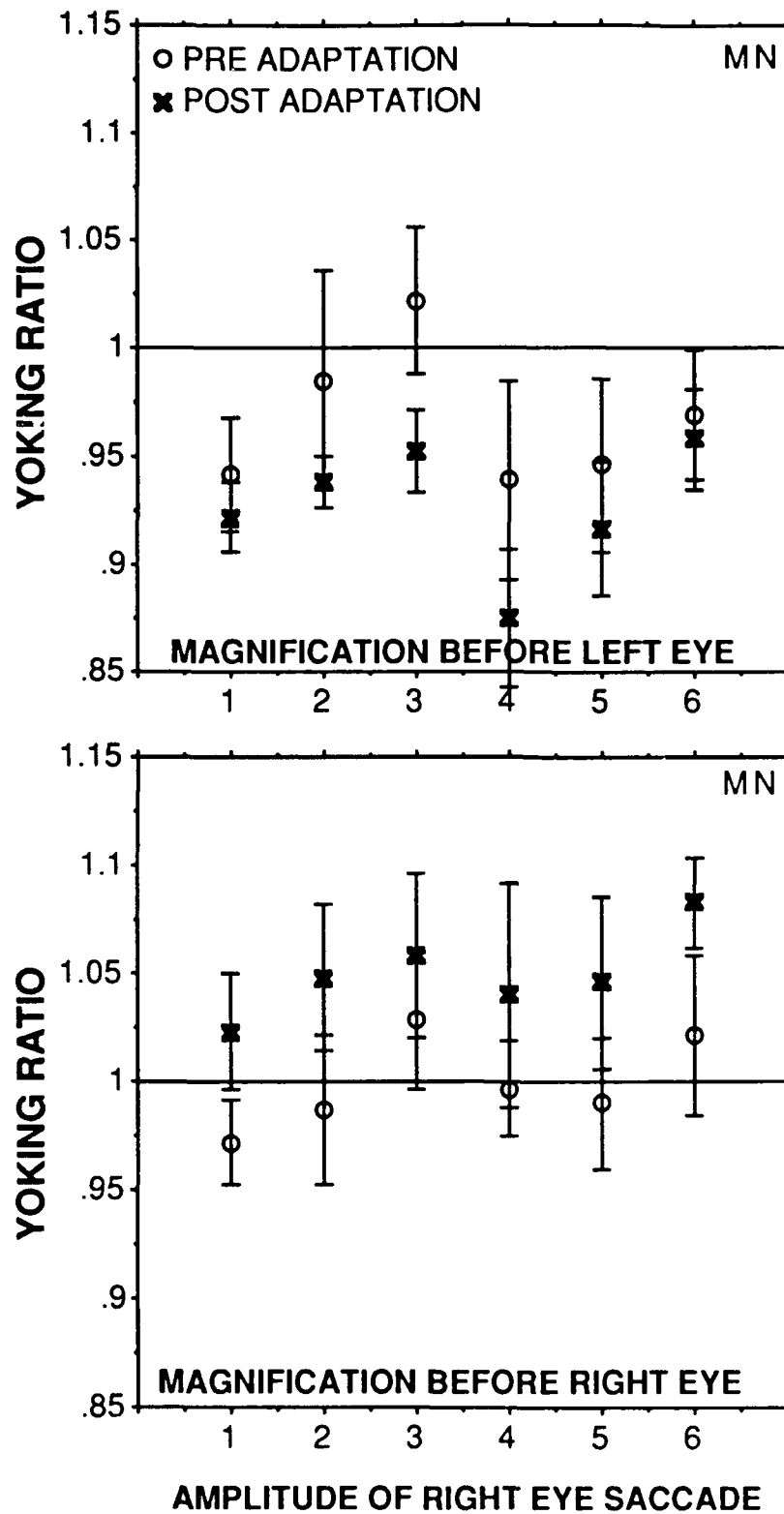
FIG 5c. Saccade Paradigm - Subject MN.

FIG 6a-c. _Pursuit Paradigm._ Each subject's saccadic pulse yoking ratios (R/L) are plotted against right eye pulse amplitude (- = downward saccade; + = upward saccade). Top chart shows data from left eye magnification condition and bottom chart shows data from right eye magnification condition. Circles depict pre-adaptation pulse yoking ratios and crosses depict post-adaptation pulse yoking ratios. Nonconjugate adaptation would result in crosses lower than circles in the top chart and crosses higher than circles in the bottom chart. The following table relates each chart's category number with the right eye's pulse amplitude.

Category Number	1	2	3	4	5	6
Saccade Component Direction and Amplitude	Down > 7 deg.	Down 4-7 deg.	Down < 4 deg.	Up < 4°	Up 4-7 deg.	Up > 7 deg.

FIG 6a. Pursuit Paradigm - Subject CE.
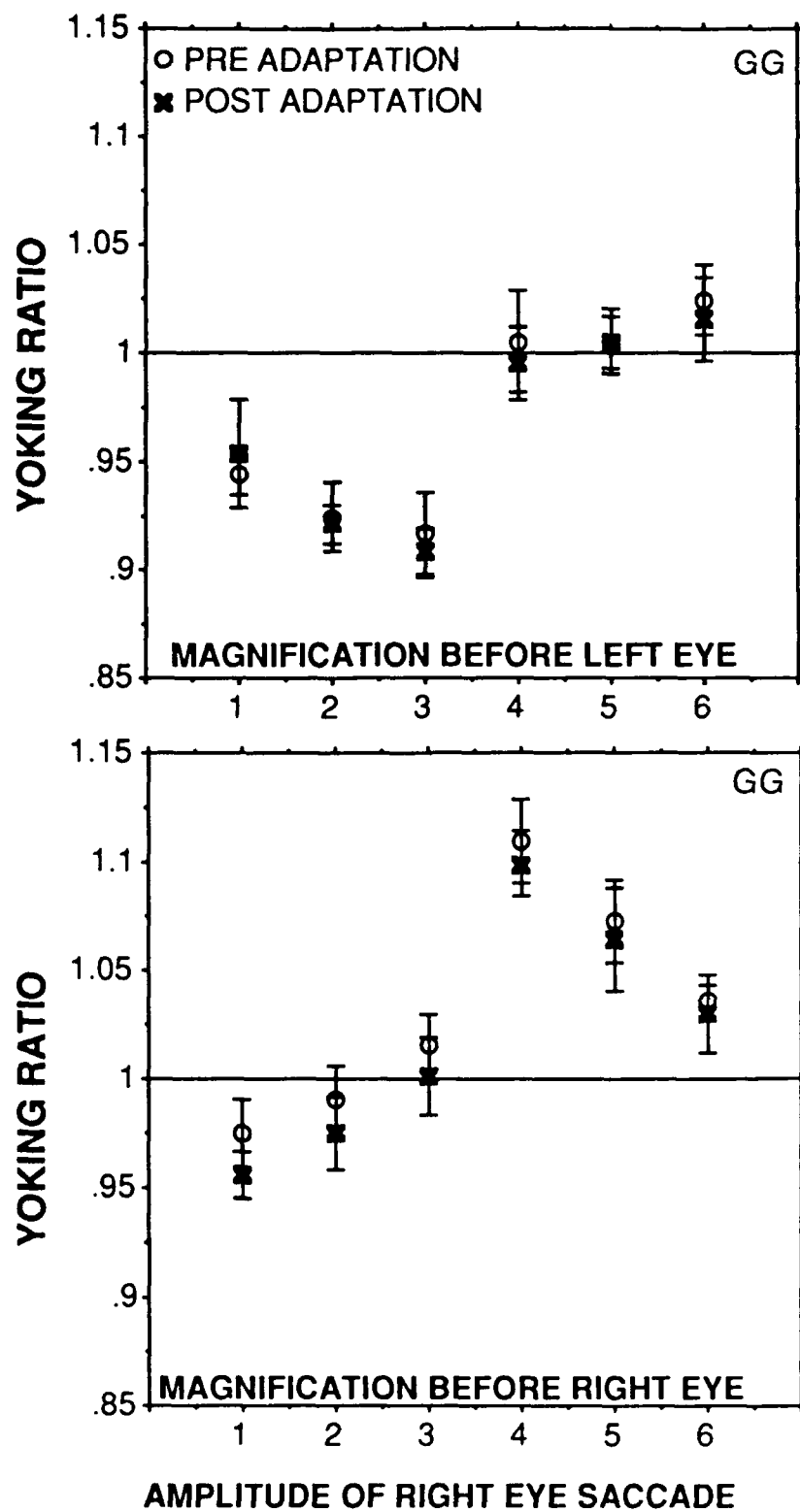
FIG 6b. Pursuit Paradigm - Subject GG.
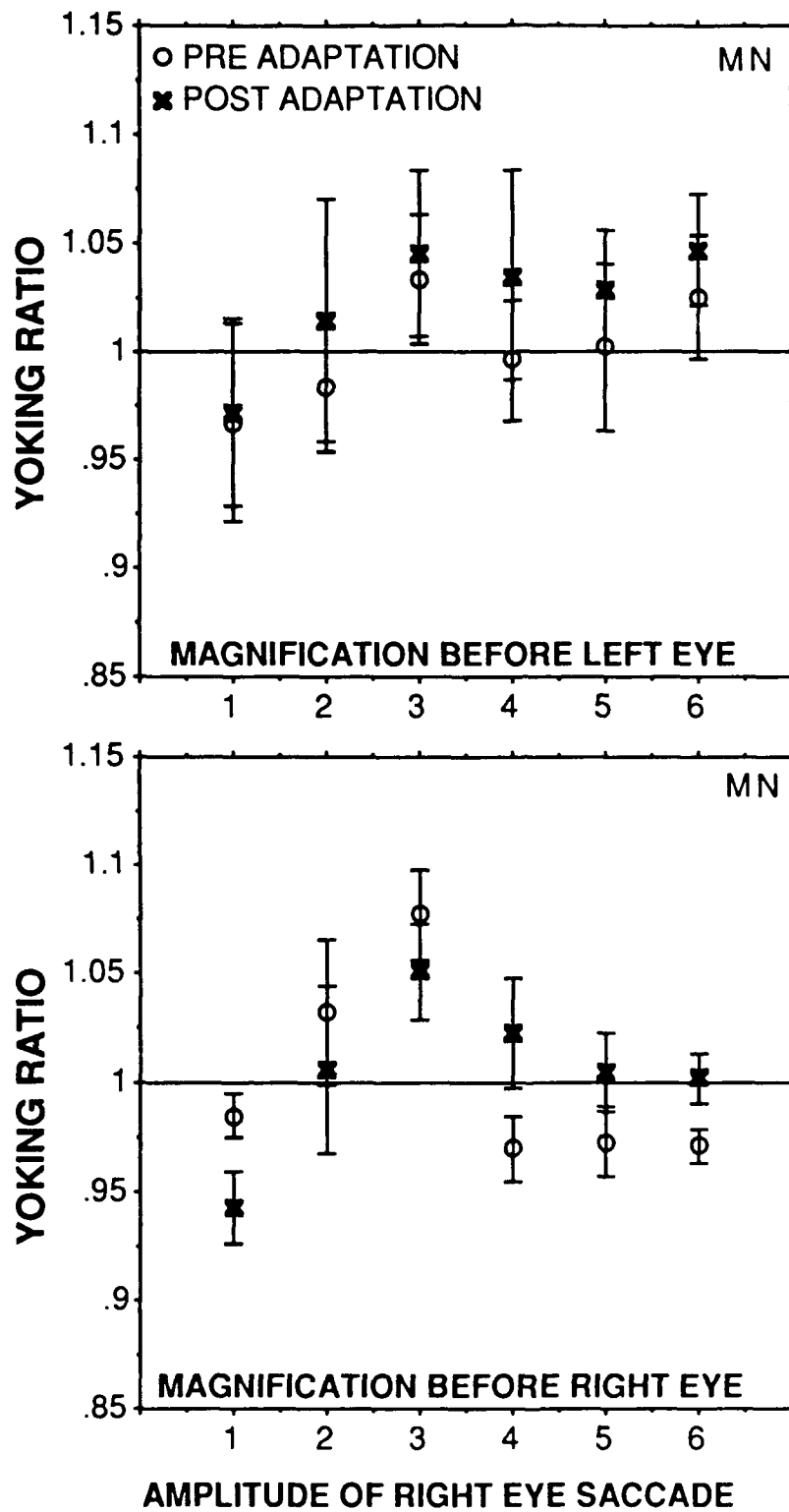
FIG 6c. Pursuit Paradigm - Subject MN
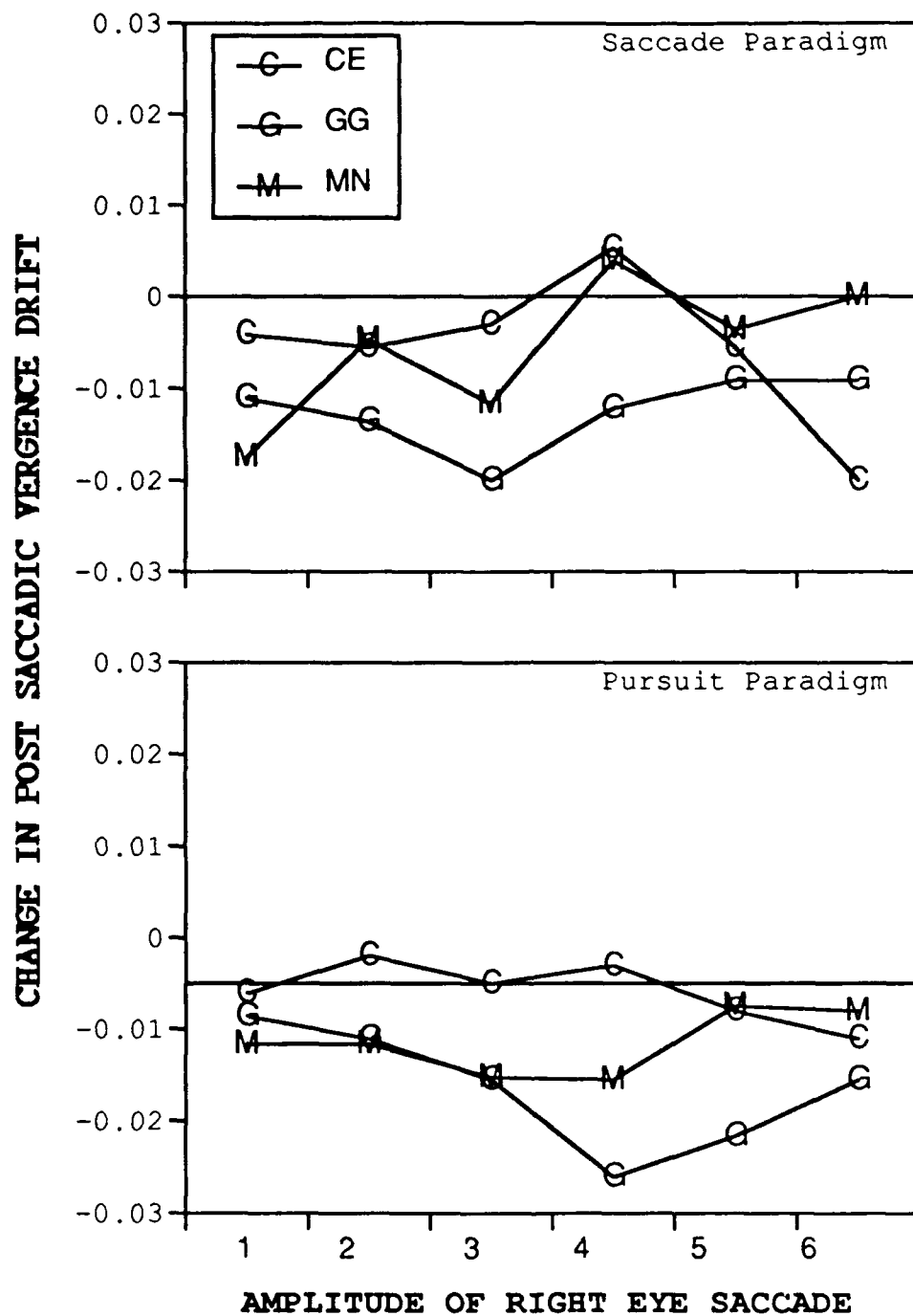
FIG 7. The change in pre- post-adaptation post saccadic vergence drift (PSVD) is plotted relative to right eye pulse amplitude. A negative PSVD change portrays greater adaptive change in the step phoria than the pulse phoria. Data from the saccade and pursuit paradigms are represented, respectively, in the top and bottom charts.

FIG 8. <u>Pursuit Paradigm.</u> Each subject's individual pre-
(circles) and post- (crosses) adaptation <u>pursuit yoking ratio</u>
averages are plotted separately on different charts. Yoking
ratio averages are separated by adapting conditions. In the
left eye magnification condition, target motion was greater
before the left eye in the adaptation period. In the right
eye magnification condition, target motion was greater before
the right eye in the adaptation period. With nonconjugate
adaptation the crosses are expected to be below the circles
on the left side of the charts and above the circles on the
right side of the charts. Each point is the average of 5 - 7
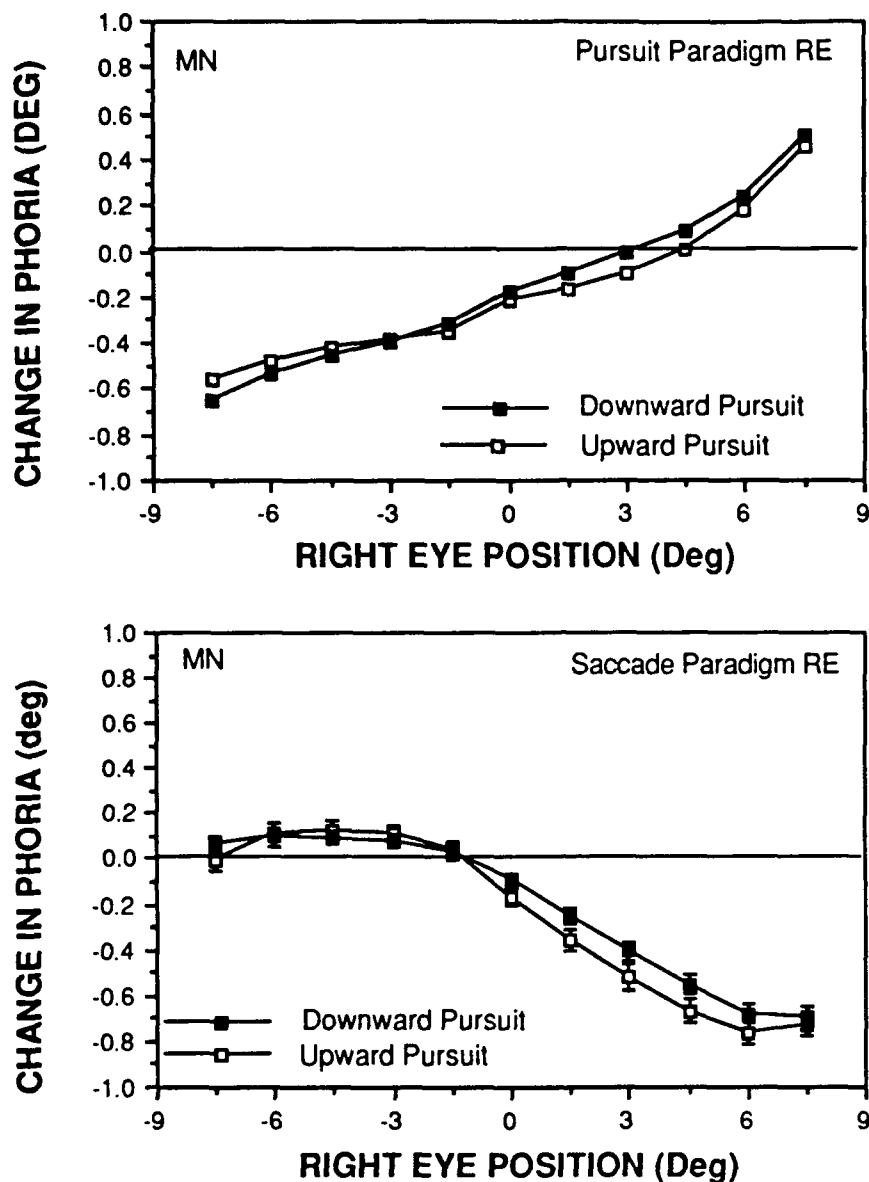trials; the error bars represent ± 1 standard deviation.

FIG 8. Saccade Paradigm. Each subject's individual pre- (circles) and post- (crosses) adaptation pursuit yoking ratio averages are plotted separately on different charts. Yoking ratio averages are separated by adapting conditions. In the left eye magnification condition, target motion was greater before the left eye in the adaptation period. In the right eye magnification condition, target motion was greater before the right eye in the adaptation period. With nonconjugate adaptation the crosses are expected to be below the circles on the left side of the charts and above the circles on the right side of the charts. Each point is the average of 5 - 7 trials; the error bars represent ± 1 standard deviation.

FIG 10. Pre- and post-adaptation changes in dynamic phorias
are plotted relative to right eye vertical gaze position (+ =
upper field of gaze). A change towards right hyper-phoria is
represented as a positive change. Phoria measurements are
called "dynamic" because they are measured during pursuit eye
movement. Open squares refer to upward pursuit tracking and
filled squares relate to downward. Each point presents
phoria averaged from 5 - 7 trials. The both charts are from
subject MN under the right eye magnification condition;
however the top chart represent adaptation to the pursuit
paradigm and the bottom chart represents the saccade
paradigm.
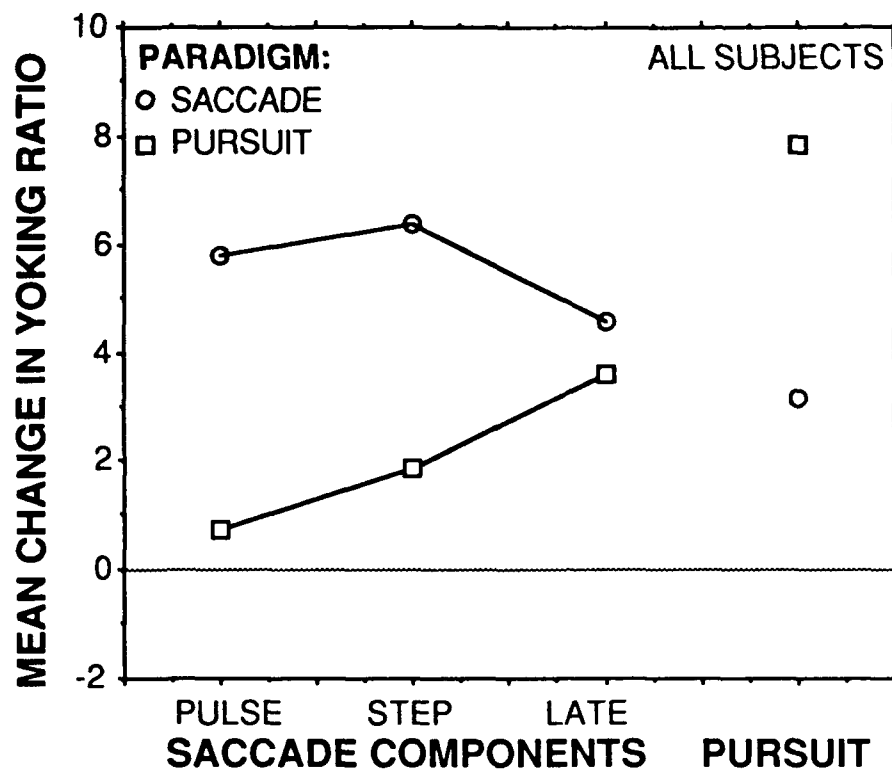
FIG 11. The global-average per centage (%) change in saccadic and pursuit yoking ratios are plotted for saccade and pursuit paradigms. Data from all subjects and experimental conditions are included.
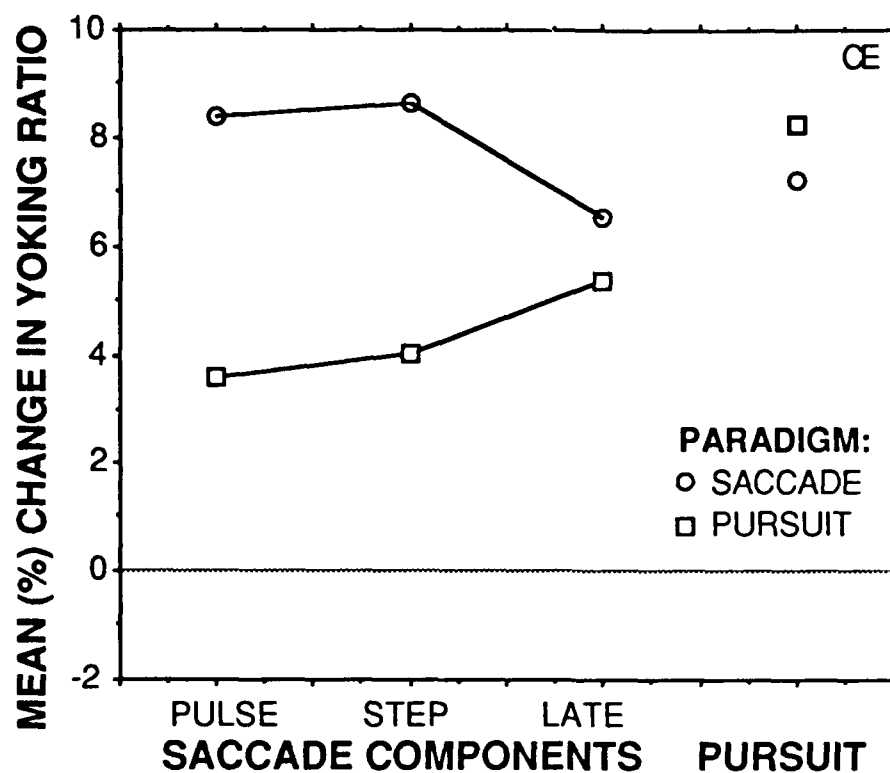
FIG 12a. Subject CE's average per centage change in saccadic and pursuit yoking ratios are plotted for saccade and pursuit paradigms. Data from all experimental conditions are included.
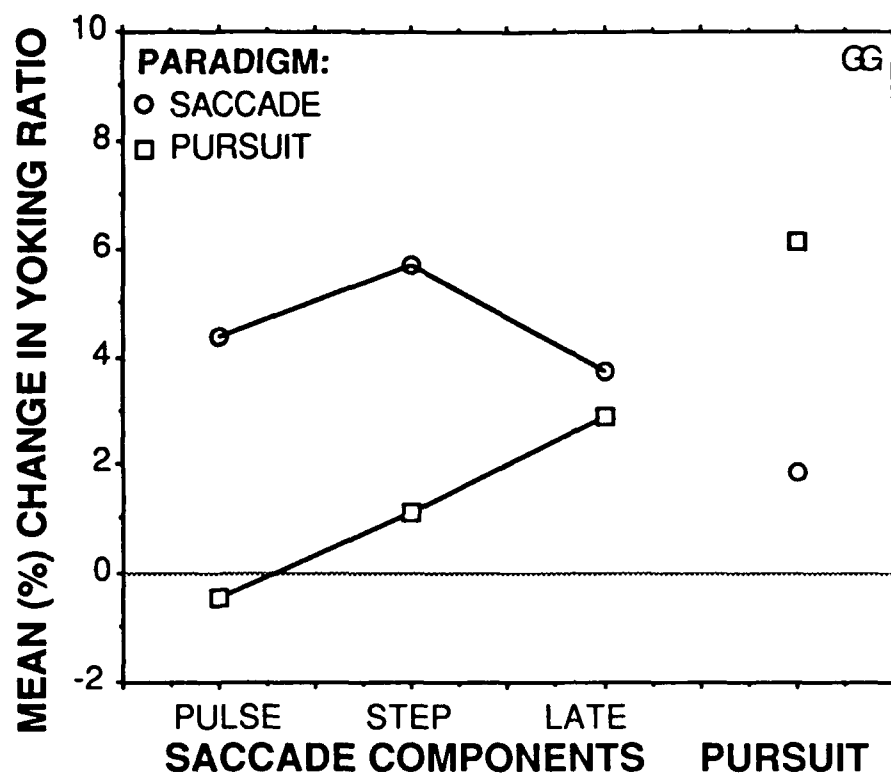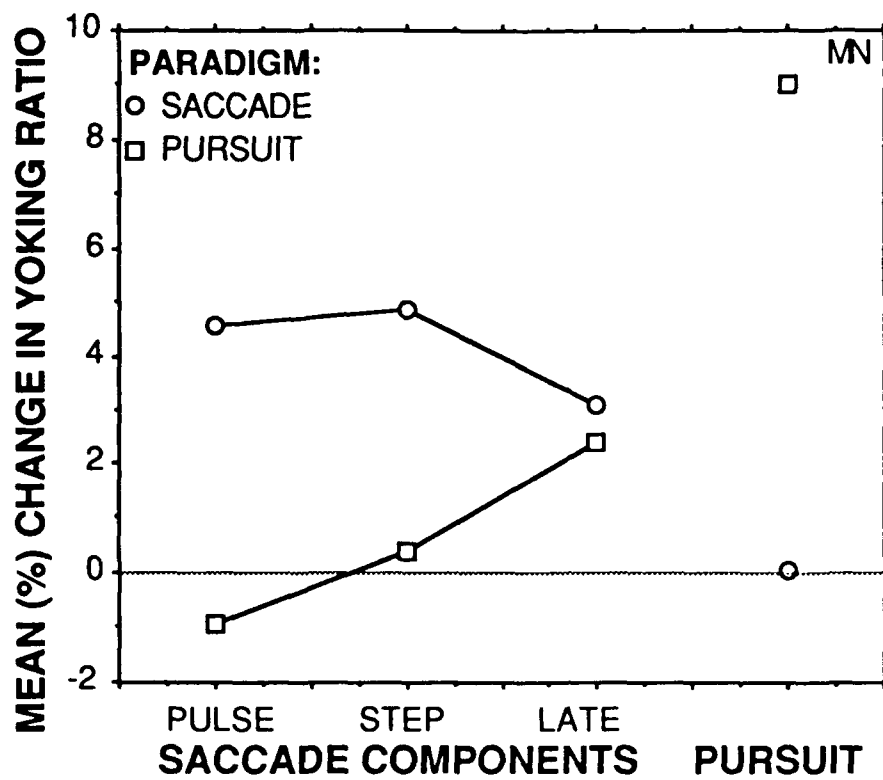
FIG 12b Subject GG's average per centage change in saccadic and pursuit yoking ratios are plotted for saccade and pursuit paradigms. Data from all experimental conditions are included.

FIG 12c. Subject MN's average per centage change in saccadic and pursuit yoking ratios are plotted for saccade and pursuit paradigms. Data from all experimental conditions are included.

CHAPTER 3

IS NONCONJUGATE ADAPTATION OF VERTICAL PURSUIT EYE MOVEMENTS INFLUENCED BY PHORIA ADAPTATION?

INTRODUCTION

Pursuit eye movements allow individuals to maintain foveal
alignment with small moving objects, and are said to be
yoked, or conjugate, because an occluded eye moves in close
concert with its fellow, visually-following eye. The close
precision of pursuit yoking is due, in part, to an adaptive
process. Studies of nonconjugate pursuit adaptation,
stimulated by either differential spectacle-mounted
magnification before each eye (Horner et al (1988), Lemij
(1990)) or by differential target motion before each eye
(Schor et al (1990)), demonstrate that within a few hours,
changes in pursuit yoking (nonconjugate adaptation) can be
induced in normal subjects.

The term "steady-fixation" describes ocular motor behavior
when a subject attempts to visually fixate a small stationary
object for an extended period of time. If one of the
subject's eyes is occluded during steady fixation of a
distant object, the occluded eye's visual axis will stay
within a few degrees of the now monocularly-viewed object.
Phoria is the vergence error during monocular occlusion.
Phoria remains relatively constant over a normal lifetime

(Hirsch et al (1948), Kephart and Oliver (1952), Scobee and Bennet (1950)) due to an adaptive process (Schor 1983)

Phoria is measured by occluding one eye while the fellow eye is fixating a small distant stationary object. When the eye is unoccluded it will rotate to visually fixate the object. Phoria is equal to the angular rotation of the previously occluded eye. When a prism is placed before an eye, initially phoria will change by an amount equal to the prism. However, within a few minutes with the prism still in place, the phoria will revert back to the pre-prism value. This adjustment in the two eyes' relative open-loop alignment is known as phoria (or prism) adaptation. Studies indicate phoria adaptation may vary with headcentric gaze (Ellerbroch and Fry (1942), Ellerbroch (1948a), Allen(1974), Henson and Dharamshi (1982), Sethi and Henson (1984), Oohira and Zee (1991). For brevity, all future references to "headcentric gaze" are referred to as simply "gaze."

The lenses contained in anisometropic spectacles have unequal optical powers and therefore, create optical images that are unequal in size. Because these lenses are fixed relative to the head, their differentially magnified images do not move with eye rotation. Therefore, unequal eye movements are required to compensate for spectacle-induced differential magnification when gaze is shifted from one small object to another.

Anisometropic spectacles create a differential prismatic effect that varies proportional to gaze position (gradient

97

disparity). Therefore, when a subject first wears anisometropic spectacles, the induced phoria will also vary proportional to gaze position (anisophoria). However, long-time anisometropic spectacle wearers have little gaze-specific phoria variation (Ellerbroch and Fry (1942), Ellerbroch (1948a), Allen(1974)). This implies that gaze-specific phoria adaptation compensates for spectacle induced anisophoria (Friedenwald (1936)).

Gaze-specific phoria adaptation occurs after performing normal daily activities for 4 hours (Henson and Dharamshi (1982)) or 2 - 3 days (Sethi and Henson (1984)) with differential optical magnification (contact lens-spectacle combination) before the eyes. Gaze-specific phoria adaptation has also been demonstrated in rhesus monkey after placing, before one eye, different amounts of prism in the left, central, and right fields of gaze (Oohira and Zee (1991b).

The role of gaze-specific phoria adaptation in nonconjugate pursuit adaptation is not known. For example, open-loop vergence posture during monocularly stimulated pursuit eye movements may be determined by innervations that originate entirely from within the pursuit eye movement system. That is, innervations that determine open-loop vergence posture during steady fixation (phoria) are disregarded during pursuit eye movements (Separate Mechanisms Hypothesis). A second possibility is that nonconjugate pursuit adaptation is due entirely to gaze-specific phoria

adaptation. That is, innervations that determine gaze-specific phoria add linearly to unchanged pursuit innervations (Phoria Addition Hypothesis), thereby, resulting in unequal binocular pursuit eye movements. A third possibility is a combination of the above; phoria adaptation underlies nonconjugate pursuit adaptation, however, separate nonconjugate pursuit mechanisms also exist.

The effect of phoria adaptation on nonconjugate pursuit adaptation was studied by comparing gaze-specific static phorias (measured during steady fixation) and dynamic phorias (measured during pursuit eye movements). If the Separate Mechanisms Hypothesis is correct then changes in gaze-specific static phorias would not generalize over to dynamic phorias. If the Phoria Addition Hypothesis is correct then gaze-specific dynamic phoria changes would mimic static phoria changes.

Gaze-specific static and dynamic phorias, before and after phoria adaptation, were alike. This indicates nonconjugate pursuit adaptation induced by gaze-specific fixation disparities was largely due to gaze-specific phoria adaptation. Despite large changes in static phoria, the saccadic pulse was effected insignificantly. This indicates gaze-specific phoria adaptation and nonconjugate saccadic pulse adaptation are underlaid by different mechanisms.

METHODS

Subjects

Three subjects participated in this study. Subjects GG and BL were habitually uncorrected myopes with refractive errors less than .5 diopters. Subject DP, a two-diopter isotropic myope, normally wore contact lenses. All subjects had stereopsis thresholds of at least 30" arc. Subject GG, the author, was 37 years old. Subjects BL and DP were 46 and 24 years old, respectively; each had an overview knowledge of the study.

Equipment

Binocular vertical eye positions were measured with a SRI dual-Purkinje eye tracker (Crane and Steele (1978)). Voltage analogues, representing independent right and left eye positions, were amplified and then, digitized. Equipment resolution was on the order of a few minutes of arc. Digital resolution exceeded equipment resolution. An EGA graphic monitor displayed vertical binocular eye position and vergence traces immediately following each trial for on-line inspection by the experimenter. If the trial was devoid of mechanical artifacts (e.g. losing the lock on the fourth Purkinje image) the trial was saved to a hard disk for later off-line analysis.

Target motion was simulated by rotation of vertical-deflecting mirror galvanometers (Crane and Clark (1978)).

Nonconjugate (unequal) target motion before each eye was induced by independent control of mirror galvanometers before each eye. The SRI dual-Purkinje eye tracker's viewing optics allows a 24 degree diameter field of view.

An AT clone computer was used for data acquisition and storage, on-line data display, and control of left and right vertical-deflecting mirror galvanometers. A bite bar and head rest were used to minimize head movement during data trials and adaptation periods

Visual Stimulus

The target (fig 1) consisted of a bright uniformly lit background with a opaque cross and three concentric squares superimposed on it. Background illumination was dim (.5 cd/m^2), such that the ambient features of the laboratory were barely visible. During trials, the vertical deflecting mirror galvanometers rotated equally (unlike during the adaptation period) causing the limiting apertures to move equally. Peripheral fusion of the limiting apertures could reduce the measured nonconjugate adaptation effect. The dim background illumination minimized the visibility of the limiting apertures of the SRI's viewing optics. Target distance was 160 centimeters.

Because horizontal vergence posture may effect vertical phoria measurements (Verhoeff (1939), Ellerbrock (1948a)), horizontal vergence posture was controlled, while leaving vertical vergence posture open-loop, by placing a set of two

vertically-oriented lines within the SRI's viewing optics before each eye (fig 1). These horizontal-fusion locks extended over the entire vertical extent of the visible field and always appeared stationary.

During trials, the left eye was prevented from seeing the vertical-scrolling target by placing a translucent occluder distal to the horizontal-fusion locks. The horizontal-fusion locks were backlighted by the bright stimulus target and thus, remained visible to both eyes.

Procedures

Pre-Experiment Procedures

Before the start of each experiment, the eye tracker viewing optics were adjusted so that, for each eye, the images of the target and horizontal-fusion locks were set conjugate with optical infinity. This was accomplished by looking through the eye tracker's viewing optics with a 6X telescope (pre-focused for optical infinity), and then adjusting the SRI's visual stimulators (Crane and Clark (1978)) so that the target appeared clear. The 6X telescope reduces accommodative and depth of focus errors by a factor of 36. The light vergence entering an afocal telescope is magnified by the square of the telescope's magnification at the telescope's exit pupil (Keating (1988)). For subject DP, a 2 diopter myope, -2.00 D lenses was placed before each eye, within the SRI viewing optics, conjugate with the normal spectacle plane; then, using the telescope, the images of the horizontal-fusion lines were placed conjugate with the target

images. The SRI's visual stimulators (Crane and Clark (1978)), are based on the Badal optometer principle (Keating (1988)). Thus, changes in target image size are minimized as SRI's visual optics are adjusted.

Subject's horizontal and vertical phorias were neutralized before each experiment. Polarize filters were used to visually dissociate two lines placed in the horizontal and two lines placed in the vertical meridian. Each eye saw one vertical and one horizontal line. Vertical and horizontal phorias were neutralized with a vernier alignment task combined with an unilateral cover test, during which the left eye was intermittently unoccluded. During the phoria neutralization procedure, target disparities were controlled by adjusting the orientation of independent vertical- and horizontal-deflecting mirror galvanometers, contained within the SRI's viewing optics, before each eye.

Subject's pupils were dilated with 1 drop of .5% tropicamide hydrochloride (Ellis (1977)) in each eye to prevent vignetting of the fourth Purkinje image during eccentric gaze positions. Typically, dilated pupil diameter exceeded 6 millimeters for at least four hours.

Calibration

Each eye was calibrated separately each time a subject entered the eye tracker for data trials. During calibration, the uninvolved eye was occluded. Three hundred milliseconds of digitized (100 Hz) analogue voltages were taken at nine

positions, 2.5 degrees apart, spanning the central twenty degrees along the vertical meridian. Gaze positions (degrees) and dijitized analogue voltages were fit to a third order polynomial. The calibration curve was then applied to the calibration data and the results were plotted on an EGA monitor in both graphical and numerical format. The calibration was acceptable if at each calibration step the calculated eye position was within .1 degree of the predicted eye position. If the calibration was rejected the procedure was repeated. After a calibration was accepted for each eye the two sets of four polynomial constants were stored to a file to transform data during later off-line analysis. Calibration files were only applied to trials that directly followed their generation.

Data Trials (Quantifying prism induced aftereffects)

Before and after a one hour adaptation period (discussed below), binocular eye recordings were taken during three types of ocular motor tasks: pursuit, steady fixation, and saccades. All data trials were performed with the left eye occluded (monocular-viewing). Therefore, pre- and post-adaptation changes in ocular motor yoking behavior are attributed to neural re-programming, rather than fusional vergence.

After each trial, vertical binocular eye position and vergence traces were plotted on an EGA monitor for inspection by the experimenter. The experimenter repeated the trial if

severe mechanical artifacts were present (e.g. lost lock on the fourth Purkinje image). Otherwise, the trial was saved to a hard disk. If the horizontal-fusion lines became diplopic then the trial was repeated.

During pursuit trials the target scrolled smoothly up and down at a constant 5 °/sec, creating a triangular wave pattern with a peak-to-peak amplitude of 20 degrees. (fig 2). Two trials of binocular recordings were sampled at 100 Hz for twenty seconds.

Static phoria trials immediately followed pursuit trials, and therefore, shared the same calibration. In each of two static phoria trials, the target stepped to one of nine positions along the vertical meridian in a twenty-one step sequence that is graphically depicted in figure 3. While the subject fixated the stationary target at each stimulus position, the experimenter monitored voltages, related to each eye's gaze position, on an oscilloscope and pressed a key when both voltage traces where steady to sample binocular eye positions at 100 Hz for 300 msec. The target then stepped to the next position. The period between target steps was 1.5 to 3 seconds long. A calibration, two pursuit trials, and two static phoria trials took approximately 4.5 minutes.

During saccade trials, the target stepped pseudo-randomly from the center position to one of six positions along the vertical meridian (up or down 2.7, 5.3, or 8 degrees). After 1.5 seconds the target stepped back to the center position.

Recordings of binocular eye position were taken for one second periods at a sampling rate of 500 Hz, beginning 50 msec before the target stepped eccentrically. After each trial, vertical binocular eye position and vergence traces were plotted on an EGA monitor for inspection by the experimenter. The experimenter would accept, or reject, the trial based on the following criteria:

1) Viewing eye position trace was steady before saccade onset.

2) No blink or recording artifacts (e.g. losing the lock on the fourth Purkinje image) were present.

3) The latency of the primary saccade was less than 400 msec.

4) The primary saccade was in the appropriate direction.

Rejected trials were immediately repeated. Accepted trials were saved as individual files for later off-line analysis. Saccades were stimulated every four to five seconds. The saccade trial series ended when seventy-two total trials were saved, twelve trials at each target amplitude. A complete set of saccade trials, along with calibration, took seven to eight minutes.

Saccade trials were accomplished at a different time than pursuit and static phoria trials. Therefore, saccade trials had a separate calibration file. After completion of pre-

adaptation static phoria trials, saccade trials were
conducted five minutes later. After completion of post-
adaptation static phoria trials, the subject watched the
adapting stimulus for ten more minutes before saccade trials
were performed.

Adapting Stimulus

Phoria adaptation was induced by repeated random exposure
to nine gaze-specific vertical fixation disparities. The
amplitude of each fixation disparity was scaled to target
eccentricity (10% gradient disparity). The term, fixation
disparity, is used here to indicate a prismatic disparate
stimulus that is only visible when the eyes are fixating a
stationary target.

Pursuit eye movements are stimulated by retinal image
motion (Rashbass (1961), Pola and Wyatt (1980)), retinal
image position error (Robinson (1965), Pola and Wyatt (1980,
1985)), and perceived target motion (for review see Howard
(1982), pages 247-252). In this study, the stimulus for
conjugate pursuit eye movements was minimized during the
adaptation period by presenting stationary, disparate targets
for binocular-viewing. Furthermore, the left eye was occluded
for 0.5 sec, beginning immediately before stepping the target
to new gaze positions. Because the disparity stimulus was
not present during, and shortly after, the gaze-shifting
saccade, the effect of gaze-specific phoria adaptation on
saccadic pulse was also studied.

During the one hour adaptation period, every 10.5 seconds the target randomly stepped to one of nine positions along the vertical meridian. The nine positions extended over the central twenty degrees and were spaced 2.5 degrees apart. The left eye's target movement was scaled to the right eye's. For subjects GG and DP the left target moved 10% more than the right target. This created a 10% gradient disparity. For example, when the target was 10 degrees up, the target disparity was 1 degree right-hypo; when the target was 5 degrees down, the target disparity was .5 degree right-hyper. The disparity stimulus is depicted in figure 4. For subject BL, the left target moved 10% less than the right target.

The subjects binocularly viewed the disparate target at a gaze position for ten seconds. Then, the left eye's target was blanked (by extreme rotation of the left vertical-deflecting mirror galvanometer), followed by the right eye's target stepping to a new position. Five hundred milliseconds later, the left eye's target would be be presented at its new position. Then, the cycle would repeat.

The subjects were instructed to maintain fixation on the center of the target's cross and, using moderate effort, to keep the targets fused. The subjects were also instructed to close one or both eyes if they sat away from the eye tracker. During an individual's adaptation period, accumulative time away from the task was less than 1 minute.

Data Analysis

Pursuit data were analyzed strictly by computer algorithm. First, a three-bin (30 msec) smoothing filter was applied to each trial. A sequential bin by bin processing followed. A velocity filter was applied to adjacent bins. Only data bins where the velocity of both eyes were between 2.5 and 10 deg/sec were considered. For each pursuit trial, phoria measurements, averaged over 0.5 degree intervals, were calculated for 29 equally spaced (1.5 degrees apart) right eye gaze positions over the central fifteen degrees. Phoria was calculated as the difference between right (R) and left (L) eye positions.

$$Phoria = R - L \qquad (1)$$

Only the central fourteen degrees were considered in phoria calculations because this was the range of constant pursuit velocity. These phorias are referred to as dynamic phorias since their measurements were taken during pursuit eye movement. These gaze-specific dynamic phoria values were further divided into three categories based on pursuit direction: upward, downward, and direction insensitive (pooled upward and downward).

Pursuit yoking ratio was defined as the ratio of right eye movement (ΔR) to left eye movement (ΔL) during pursuit eye movement during a given time interval.

Yoking Ratio = (ΔR) / (ΔL)   (2)

For each trial, an overall pursuit yoking ratio was
calculated over the central 13 degrees by accumulating
separate right and left eye adjacent bin differences for bins
passing the velocity criteria; and then dividing each trial's
final right accumulator result by the left. Since all data
bins represent equal time intervals (10 msec), this method of
yoking ratio calculation is equivalent to dividing average
right eye velocity by average left eye velocity. Phorias and
yoking ratios from both trials were averaged.

Static phoria data were analyzed strictly by computer
algorithm and separated by right eye gaze position. These
gaze-specific static phoria values were further divided into
three categories based on the direction of the intervening
gaze-shifting saccades: upward, downward, and direction
insensitive. Phorias from both trials were averaged.

Saccade data were analyzed interactively because of the
lenticular artifact associated with dual-Purkinje eye
trackers (see chapter 2 methods) A brief study on two
subjects indicated the actual end of the saccadic pulse was
usually within 5 msec of the artifact peak.

In each saccade trial, three eye positions were defined:
pre-saccade, pulse, and late (fig 5). The primary saccade
onset was located by a computer algorithm that identified
binocular eye velocity exceeding 60 deg/sec for at least 20
msec. The pre-saccade position was defined as 10 msec before

the saccade onset. The pulse-position was identified through interactive means. A computer algorithm identified the peak amplitude of the lenticular artifact, and placed a cursor 40 msec after the peak. Then, the experimenter adjusted the placement of a cursor, by eye, to immediately after the demise of visible artifact in the eye position traces. The time of pulse-position ranged between 30 and 45 msec after the artifact peak. The late-position was defined as 10 msec before the end of the 1-second recording period. The late-time was usually 700 to 750 msec after the artifact peak. Usually the late-time was preceded by one or more corrective saccades.

At each of the three defined positions, binocular eye position were averaged over a 10 msec interval. These intervals occurred at the same time for right and left eye data. Saccadic yoking ratios were determined for the pulse and late positions. Pulse amplitudes were calculated for each eye by subtracting pre-saccade position (D_1) from pulse position (D_2).

$$\text{Pulse Amplitude} = D_2 - D_1 \qquad\qquad (3)$$

Then, pulse yoking ratios were calculated as the ratio of right eye pulse amplitude (A_R) to left eye pulse amplitude (A_L).

$$\text{Pulse YR} = A_R / A_L \qquad\qquad (4)$$

Late yoking ratios were calculated by a similar method.

Pulse and late yoking ratios were grouped into one of six categories based on the amplitude and direction of the right eye pulse (or late) amplitude. The categories were: upward or downward less than 3 degrees, 3 - 5.5 degrees, and greater then 5.5 degrees. These criteria resulted in approximately equal numbers of saccades in each category. Using the average pre- and post-adaptation yoking ratios in each category, an overall average yoking ratio change, and standard deviation, were calculated.

RESULTS

Subjective Observations During Adaptation Period

Within a few minutes from the start of the adaptation period, all subjects reported fusion became much easier in one hemifield, while in the opposite hemifield diplopic separation increased. Similar observations were reported in chapter 2. In this study, diplopia faded in the right-hyper disparity field for subject GG, and in the left-hyper disparity field for subjects DP and BL. In chapter 2, the "easy" field was related to an idiosyncratic preference towards a particular hyper-disparity. At fortuitous times, when the target remained in the difficult field for several consecutive presentations, the extreme gaze positions in the "difficult" field became fused; however, when the target returned to the "easy" field, the target was difficult to

fuse initially, but within a few random presentations it, again, became easy and the difficult field, again, became "difficult". With time, the duration of diplopia, after gaze shifts, diminished. After 45 minutes of adaptation, all subjects noticed brief diplopia only after large changes in field position (> 15 degrees). At the end of 60 minutes, subjects GG and BL rarely appreciated diplopia, while subject DP was briefly diplopic only after large fixation changes.

Gaze-Specific Phoria Adaptation Influences Nonconjugate Adaptation of Vertical Pursuit

Although the adapting stimulus did not stimulate pursuit eye movements, it was highly effective in inducing nonconjugate pursuit adaptation in all three subjects. The average change in pursuit yoking ratio was 8.2% (.082). Table 1 lists the pre- and post-adaptation yoking ratios for each subject. Full adaptation would have resulted in a yoking ratio change of -10% (-0.1) for subjects DP and GG; and a change of +10% (+0.1) for subject BL.

Subjects	Pre-Adapt Yoking Ratio	Post-Adapt Yoking Ratio	Yoking Ratio Change
BL	1.009	1.103	.094
DP	1.028	.956	-.072
GG	1.017	.938	-.081

Table 1. Pre- and Post-adaptation pursuit yoking ratios, and their differences are listed for each subject. Pursuit yoking ratio is the ratio of right eye to left eye movement during pursuit eye movement. Full adaptation would result in a yoking ratio change of -.1 for subjects GG and DP, and +.1 for subject BL.

Figures 6a-c depicts each subject's gaze-specific pre- and post-adaptation static and dynamic phorias. For all three subjects, gaze-specific static and dynamic phorias are nearly superimposed for both the pre- and post-adaptation condition. This close match of gaze-specific static and dynamic phorias provides clear evidence that, within the experimental conditions, nonconjugate changes in smooth pursuit were almost entirely due to gaze-specific phoria adaptation, thus supporting the Phoria Addition Hypothesis.

Directional-Specificity of Nonconjugate Pursuit Adaptation

For each subject, gaze-specific static phorias were separated based on the direction of the intervening gaze-shifting saccade. Comparison of pre- and post-adaptation gaze-specific static phorias demonstrated little difference, usually less than 0.1 degree, between upward- and downward-directed gaze-specific static phorias (table 2). Similarly, pursuit direction had little effect on pre-adapt gaze-

specific dynamic phorias; for all subjects, differences were
less than 0.1 degree (table 2).

SUBJECT	DYNAMIC		STATIC	
	Pre-Adapt	Post-Adapt	Pre-Adapt	Post-Adapt
BL	0.03 (0.01)	0.00 (0.08)	0.04 (0.05)	0.15 (0.10)
DP	0.00 (0.04)	0.20 (0.06)	0.00 (0.07)	-0.08 (0.07)
GG	-0.08 (0.02)	0.36 (0.09)	-0.05 (0.10)	-0.07 (0.08)

Table 2. For each subject and adaptation condition, the
average difference (and standard deviation) between dynamic
phorias, at 29 gaze positions, during either upward or
downward pursuit eye movement, or between static phorias, at
9 gaze positions, depending on whether intervening gaze-
shifting saccades were upward or downward. Because the post-
adapt phorias for subjects BL and GG where measured at
different gaze positions than their pre-adapt phorias, an
interpolation technique was used to estimate post-adapt gaze-
specific phorias at the same gaze positions used for pre-
adapt gaze-specific phorias. Positive values represent
upward-directed phorias being more right-hyper than downward-
directed phorias.

In contrast, subject GG, and to a lesser extent subject

DP, demonstrated a uniform separation of upward and downward

gaze-specific dynamic phorias without a concurring

directional-separation of static phorias. On average, these

subjects' upward pursuit phorias were 0.36 degree and .20

degree more right hyper than their downward pursuit phorias.

The two charts in figure 7 plots subject GG's upward and

downward-directed gaze-specific static and dynamic phorias

averaged from all trials. The top chart represents pre-

adaptation trials; the average directional-specific

separation of both static and dynamic phorias were less than
0.1 degree (table 2). The bottom chart represents post-
adaptation trials; the average directional-specific
separation was 0.07 degree for static phorias, and 0.36
degree for dynamic phorias.

The top chart of figure 8 shows one cycle of pursuit eye
movement by subject GG before the adaptation period.
Likewise, the bottom chart in figure B shows one cycle of
post-adapt pursuit eye traces. In both charts, the thick
line represents dynamic phoria. Two observations can be
made. First, nonconjugate pursuit adaptation is indicated by
the change from relative righ -hypo phoria in lower gaze
positions before adaptation to relative right-hyper phoria in
lower gaze positions after adaptation. Second, nonconjugate
pursuit adaptation has direction-specific components. A
horizontal line, representing a given gaze position near the
center of the field, was added to both charts to improve
clarity. In the top chart, at the two places the horizontal
line intersects the eye traces, the phoria trace has the same
value. This indicates pre-adaptation phoria was dependent
only on gaze position. In the lower chart, the horizontal
line intersects the eye traces at two places. The phoria
trace has different values at these points of identical gaze
direction, which indicates that post-adapt phoria was
dependent on both pursuit direction and gaze position.

The direction-specific changes observed in dynamic phorias
were not due to the left, occluded eye lagging temporally

behind the right, seeing eye. Subject GG's results could be
duplicated if his left eye lagged behind his right eye by a
constant 72 msec (or for subject DP, 40 msec). However, this
was not the case since during the pursuit trials his two eyes
always reversed direction synchronously.

Direction-specific changes observed in dynamic phorias,
without concurrent changes in static phorias, indicate other
mechanisms, in addition to phoria mechanisms, contribute to
nonconjugate adaptation of vertical pursuit.

One caveat must be mentioned. In general, gaze-specific
static phorias were independent of the direction of
intervening gaze-shifting saccades. However, the static
phoria measurement procedure reached the extreme positions
(up or down 10 degrees) by one of two ways (fig 3). The
first way was by a 10 degrees saccade from the center of the
field; the second way was by a sequence of 2.5 degrees
saccades starting at the opposite extreme gaze position. The
method of approach produced phoria differences, up to .25
degree, at these extreme gaze positions.

(Lack of) Nonconjugate Adaptation of Saccadic Pulse and Gaze-
Specific Phoria Adaptation

Overall pulse yoking ratio variability, expressed as
standard deviation, was 0.022, 0.026, 0.038 for subjects BL;
GG; and DP, respectively. Because yoking ratios were
strongly dependent on saccade amplitude and direction,
saccade yoking ratio data were averaged into one of six

categories based on the right eye saccade amplitude and direction (see Chapter 2 methods). After grouping, pulse yoking ratio variability, expressed as standard deviation, was 0.013, 0.018, 0.022 for subjects BL; GG; and DP, respectively.

For each subject, averaged values of pulse yoking ratio were used to calculate pre- and post-adaptation changes within each category. Overall average yoking ratio change and standard deviation are shown in Table 3 and Figure 9 shows these changes graphically.

SUBJECT	Pulse Yoking Ratio CHANGE (STD)	Late Yoking Ratio CHANGE (STD)
BL	0.008 (.007)	0.055 (0.013)
DP	-0.013 (.013)	0.056 (0.017)
GG	-0.013 (.013)	0.056 (0.012)

Table 3. Average change in pulse and late yoking ratios. Pre- and post-adaptation yoking ratios were grouped into one of six categories based on right eye saccade amplitude (see methods). Mean change and standard deviations were calculated from pre- and post-adaptation comparisons of categorized data. Full adaptation would be represented by a mean yoking ratio change of +0.1 for subject BL, and -0.1 for subjects DP and GG.

Although pursuit yoking ratios were vigorously altered in all subjects by the adapting paradigm (average = 8.2%), saccadic pulse yoking ratios were minimally effected in all subjects (average = 1.1%). Late yoking ratios were moderately altered in all subjects (average = 5.6%).

Before adaptation, post-saccadic phoria drift (PSPD) was minimal in all three subjects. After adaptation, all

subjects (monocularly-viewing) showed a slow, linear PSPD in
the appropriate direction, based on the disparity stimulus,
that was present at the end of the eye tracker's lenticular
artifact ($\approx$ 35 msec after the pulse), and was usually still
ongoing at the end of the one second recording window. For
example, subject GG showed a PSPD that increased left-hyper
phoria in the upper field and increased right-hyper phoria in
the lower field. Induced PSPD increased with saccade
amplitude. The top chart in figure 10, depicts a pre-
adaptation upward saccade by subject GG; note very little
PSPD. The bottom chart in figure 10 depicts a post-
adaptation upward saccade by subject GG; note the left-hyper
PSPD. This appropriate PSPD is reflected in Table 3 and
figure 9 by moderate changes in late yoking ratios. These
observations suggests, at least for small amplitude saccades
(< 8 degrees), gaze-specific phoria adaptation does not
effect nonconjugate pulse adaptation, and that the
innervations that determine phoria continue long (> 1 sec)
after the completion of the vertical saccadic pulse.

CONCLUSIONS

Phoria Adaptation and Nonconjugate Pursuit Adaptation

Comparisons of gaze-specific dynamic and static phorias
were remarkably similar, indicating that vertical phoria and
nonconjugate pursuit adaptation shared a common mechanism(s).
These results suggest that the gaze-specific innervations
that determine open-loop vertical vergence posture during

steady fixation remain active during vertical pursuit eye
movements. Phoria-determining innervations appear to add
linearly to innervations that drive relatively slow pursuit
eye movements.

Direction Specificity of Nonconjugate Pursuit Adaptation

In two subjects, post-adaptation dynamic phorias were
dependent on gaze-position and direction of pursuit travel.
However, static phorias where not effected by the direction
of small-amplitude saccades. This discrepancy indicates that
separate directional-specific adaptive mechanisms contained
within the pursuit system also underlie nonconjugate
adaptation of vertical pursuit. Directional-specific
nonconjugate adaptation mechanisms are addressed in chapter
5.

Gaze-specific Phoria Adaptation and Saccadic Pulse
Nonconjugate Adaptation

Although the adapting stimulus was highly effective in
inducing gaze-specific phoria changes and nonconjugate
pursuit changes (8.2%), it was ineffective in producing
nonconjugate saccadic pulse changes (1.1%). This indicates
different mechanisms subserve phoria adaptation and
nonconjugate saccadic pulse adaptation .

In the saccade paradigm in chapter 2, two hours of viewing
binocularly a disparate target (10% gradient disparity), that
randomly stepped each 0.5 second to a new gaze position,

induced moderate changes in the pulse yoking ratio (5.7%).
The differences between this study and the saccade paradigm
are too great to decipher the adequate stimulus for
nonconjugate saccadic pulse adaptation. In this study, the
subjects were exposed to less than 350 target displacements
and were monocular during, and 200 - 300 msec after, gaze-
shifting saccades. In the saccade paradigm, the subjects
were exposed to 14,000 target displacements and were always
viewing binocularly. The failure to nonconjugately adapt
saccadic pulse in this study maybe due either to the low
number of stimulated saccades, or to the absence of disparity
processing during, or immediately following, saccades.

Effect of Exposure Interval

This adaptation paradigm is very similar to the one used
by Schor et al (1990). The major difference between these
two studies is the exposure time of the disparate targets at
each gaze position (2 versus 10 seconds). In the Schor et al
(1990) study, static phoria measurements were not taken.
However, the overall change in pursuit and saccade yoking
ratios was 2.6% and 1.1%, as compared to 8.2% and 1.1%
reported in this study. Assuming the small nonconjugate
pursuit yoking changes reported by Schor et al resulted from
gaze-specific phoria adaptation, their meager gaze-specific
phoria adaptation probably resulted from an inadequate
exposure period, two seconds, to each fixation disparity.
Perlmutter and Kertesz (1978) reported the fusional motor

response to a 0.9 degree step change in vertical disparity takes approximately eight seconds to complete, in contrast to less than one second needed for fusional motor responses to a similar horizontal disparity. Because phoria adaptation is thought to be dependent on motor fusion output (Schor (1979)), a two second exposure period appears to be insufficient time for slow vertical fusional movements to stimulate gaze-specific phoria adaptation.

In both this study and Schor et al (1990), the yoking of the two eyes during the saccadic pulse were relatively unaffected. There was an overall pulse yoking ratio change of 1.1% in both studies. However, in the current study large changes in gaze-specific phoria adaptation were induced without concurrent changes in pulse yoking ratio. This suggests nonconjugate pulse adaptation and gaze-specific phoria adaptation are underlaid by separate mechanisms.

This study demonstrated that discreet gaze-specific fixation disparities are adequate to induce gaze-specific phoria and nonconjugate pursuit adaptation, and that to achieve these adaptations, disparity feedback during pursuit or saccade eye movements is not necessary. Because the adapting target randomly jumped to different gaze positions (each with a discreet disparity), static phoria adaptation was shown to be truly gaze-specific, rather than due to memory of a sequence of regularly positioned and varied disparities.

REFERENCES

Allen DC   (1974),   Vertical prism adaptation in
    anisometropes,   Am. J. Optom. Physiol. Opt. 51:252

Crane H and Clark M   (1978),   Three dimensional visual
    stimulus deflector,   Applied Optics 17:706

Crane H and Steele C   (1978),   Accurate three
    dimensional eye tracker,   Applied Optics 17:691

Ellerbrock V and Fry GA   (1942),   Effects induced by
    anisometropic corrections,   Am. J. Optom. and Arch.
    Am. Acad. Optom. 19:444

Ellerbrock VJ   (1948a),   Further study of effects
    induced by anisometropic corrections,   Am. J. Optom.
    and Arch. Am. Acad. Optom. 25:430

Ellis PP   (1977),   Ocular therapeutics and pharmacology,
    5th Edition, Mosby Company:Saint Louis

Friedenwald, J   (1936),   Diagnosis and treatment of
    anisophoria,   Arch. Ophthalmol. 15:283

Henson DB and Dharamshi BG   (1982),   Oculomotor
    adaptation to induced heterophoria and anisometropia,
    Invest. Ophthalmol. Vis. Sci. 22:234

Horner DG, Gleason G, and Schor CM   (1988),   The
    recalibration of Hering's law for versional eye
    movements in response to aniseikonia,   Invest.
    Ophthalmol. Vis. Sci. 29:136 (abstract 28)

Howard IP   (1982),   Human Visual Orientation,   Wiley:
    New York

Keating M   (1988),   Geometric, physical, and visual
    optics,   Butterworths: Boston

Lemij HG   (1990),   Asymmetrical adaptation of human
    saccades to anisometropic spectacles,   Doctoral
    Dissertation, Erasmus University of Rotterdam

Oohira A and Zee DS   (1991),   Disconjugate ocular motor
    adaptation in rhesus monkey,   (In Press)

Perlmutter AL and Kertesz AE   (1978),   Measurement of
    human vertical fusional response,   Vision Res. 18:219

Pola J and Wyatt HJ (1980), Target position and
    velocity: the stimuli for pursuit eye movements,
    Vision Res. 20:523

Pola J and Wyatt HJ (1985), Active and passive smooth
    eye movements: effects of stimulus size and location,
    Vision Res. 25:1063

Rashbass C (1961), The relationship between saccadic
    and smooth tracking eye movements., J. Physiol.
    159:326

Robinson, DA (1965), The mechanics of human smooth
    pursuit eye movements., J. Physiol. 180:569

Schor CM (1979), The relationship between fusional
    vergence eye movements and fixation disparity,
    Vision Res. 19:1359

Schor CM, Gleason J, and Horner D (1990), Selective
    nonconjugate binocular adaptation of vertical
    saccades and pursuits, Vision Res. 30:1827

Sethi (nee Dharamshi) B and Henson DB (1984), Adaptive
    changes with prolonged effect of comitant and
    noncomitant vergence disparities, Am. J. Optom.
    Physiol. Opt. 61:506

FIG 1. The tracking target, scaled 33% here, was superimposed on a 25 x 19 cm bright background. The horizontal-fusion locks were contained within the right and left eye channels of the SRI visual optics. The horizontal fusion locks extended the entire height of the visible field (24 degrees), and were always visible to both eyes. During trials, while the left eye was prevented from seeing the tracking target, the horizontal fusion locks controlled horizontal vergence posture, but left vertical vergence posture open-loop. Viewing distance was 160 cm.
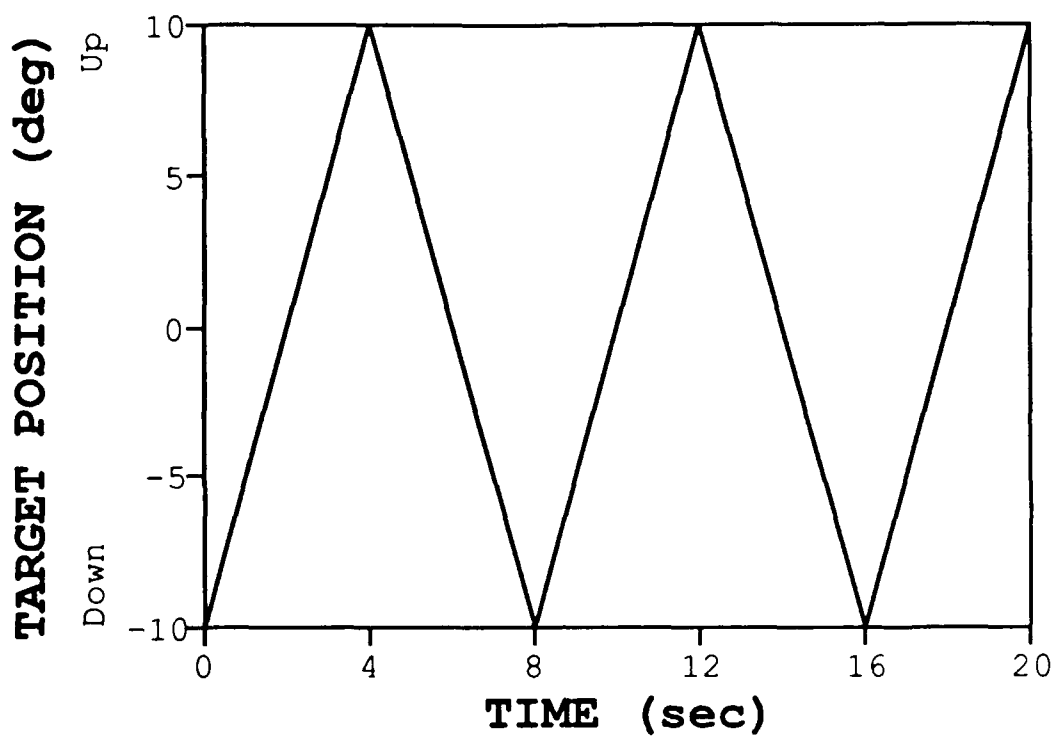
FIG 2. Target motion during twenty second pursuit trials consisted of a vertically-directed triangular-wave with a constant velocity of 5 deg/sec.
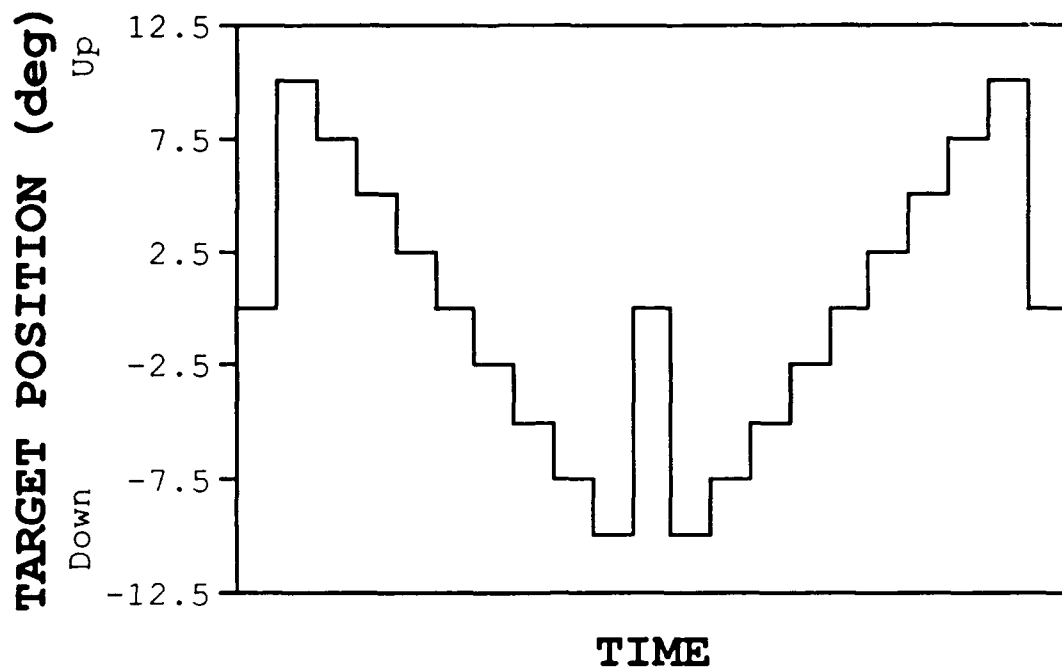
FIG 3. Schematic depicts sequence of target positions used during static phoria trials. The time intervals between target steps were determined by the experimenter (see text for details), and were not equally spaced as shown in this figure.
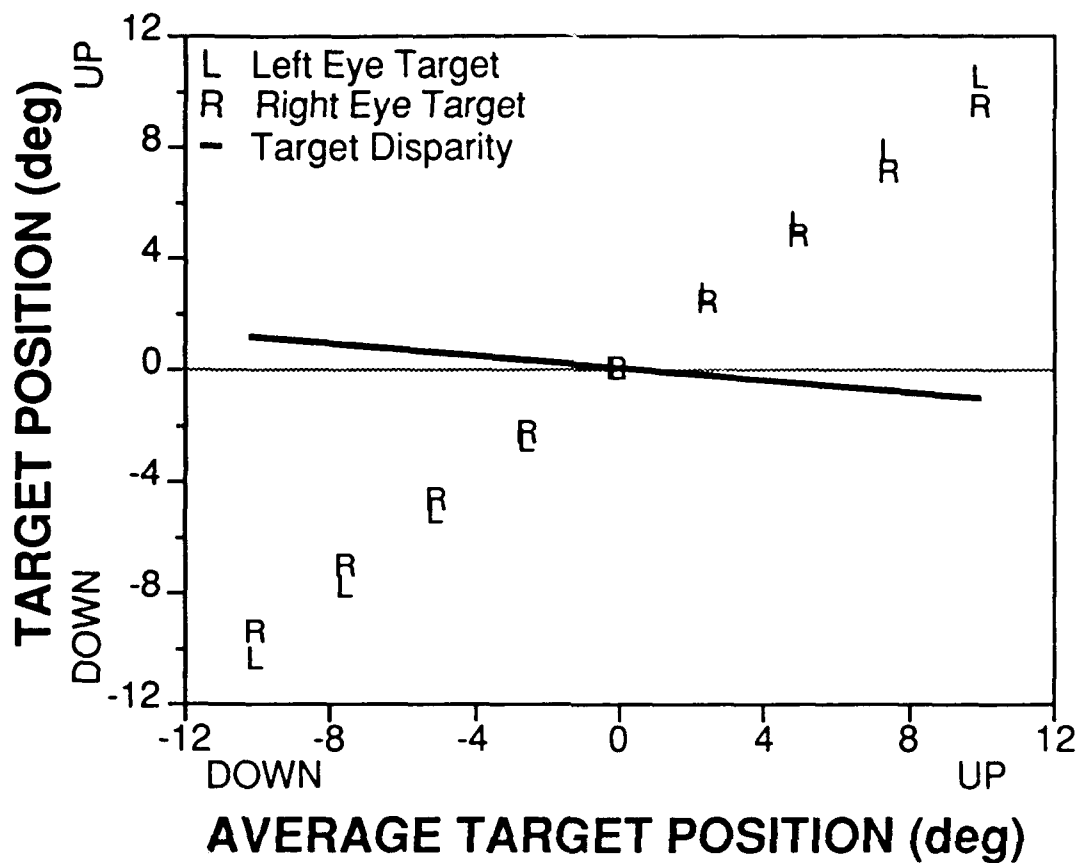
FIG 4. Schematic depicts left (L) and right (R) target positions for each of the nine gaze positions stimulated during the adaptation period for subjects GG and DP. Target disparity (thick line) is equal to the vertical separation of the left and right target at each gaze position (R - L). Target disparity was scaled to 10% of gaze eccentricity (10% gradient disparity).
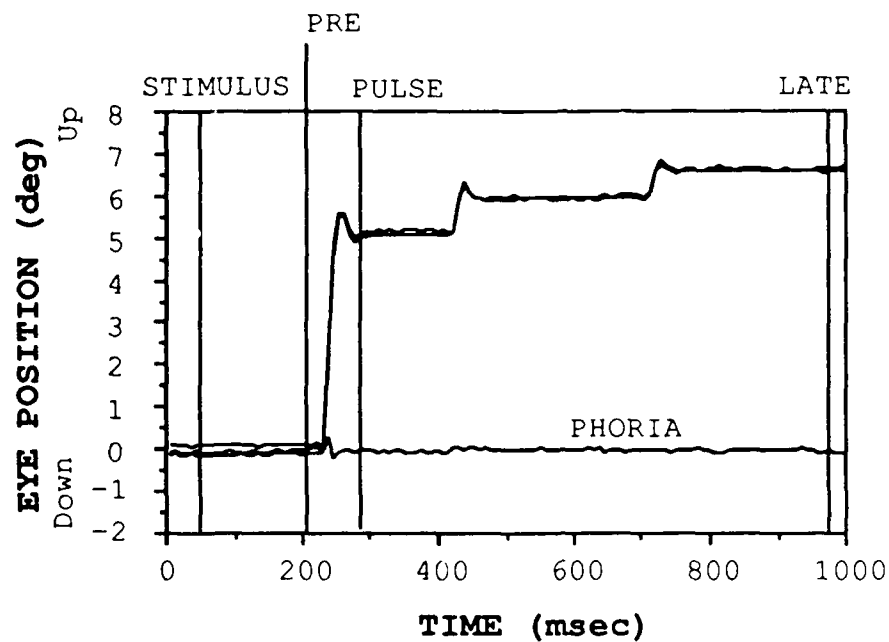
FIG 5. Binocular eye traces of an upward-directed saccade are depicted along with phoria trace (R-L). Pre-saccade, pulse, and late time-components used in data analyses are marked by vertical lines (see text for details).
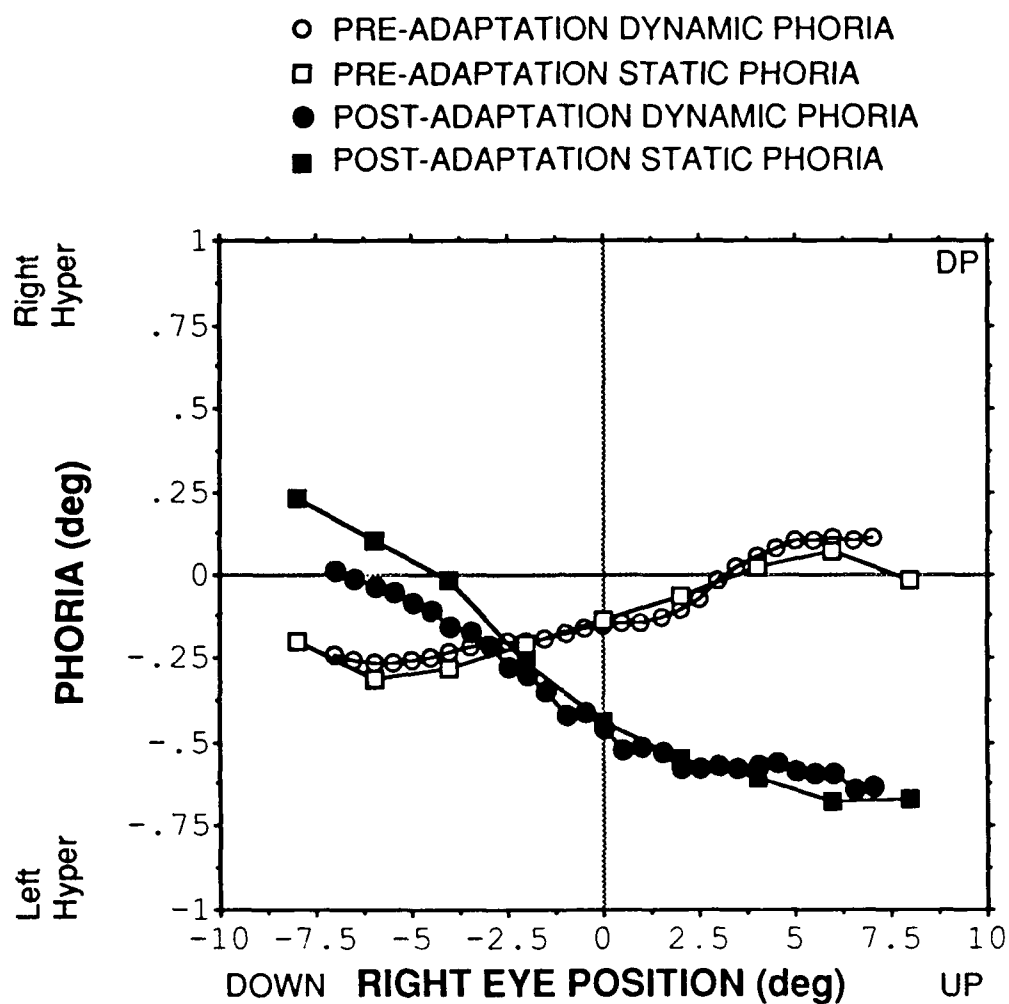
Fig 6a. Subject DP's pre- and post-adaptation dynamic and static phorias are plotted relative to right eye gaze position
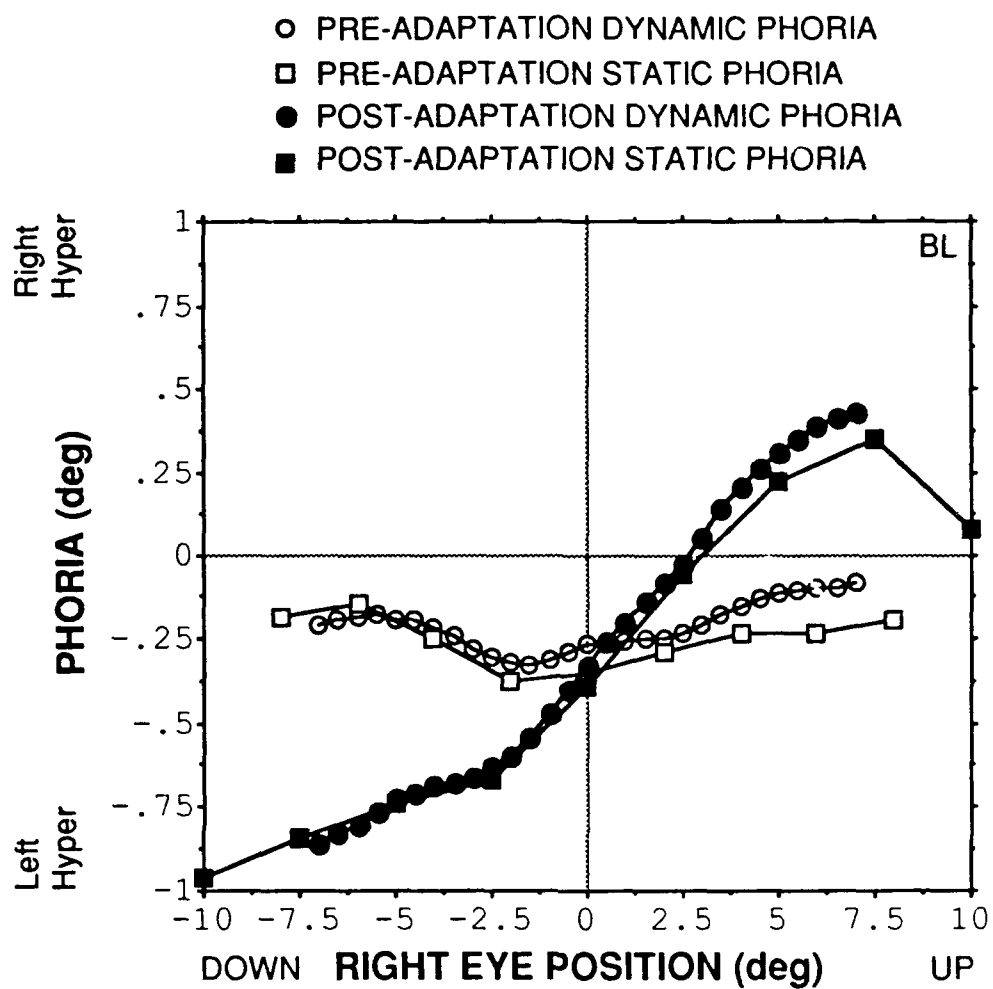
Fig 6b. Subject BL's pre- and post-adaptation dynamic and static phorias are plotted relative to right eye gaze position
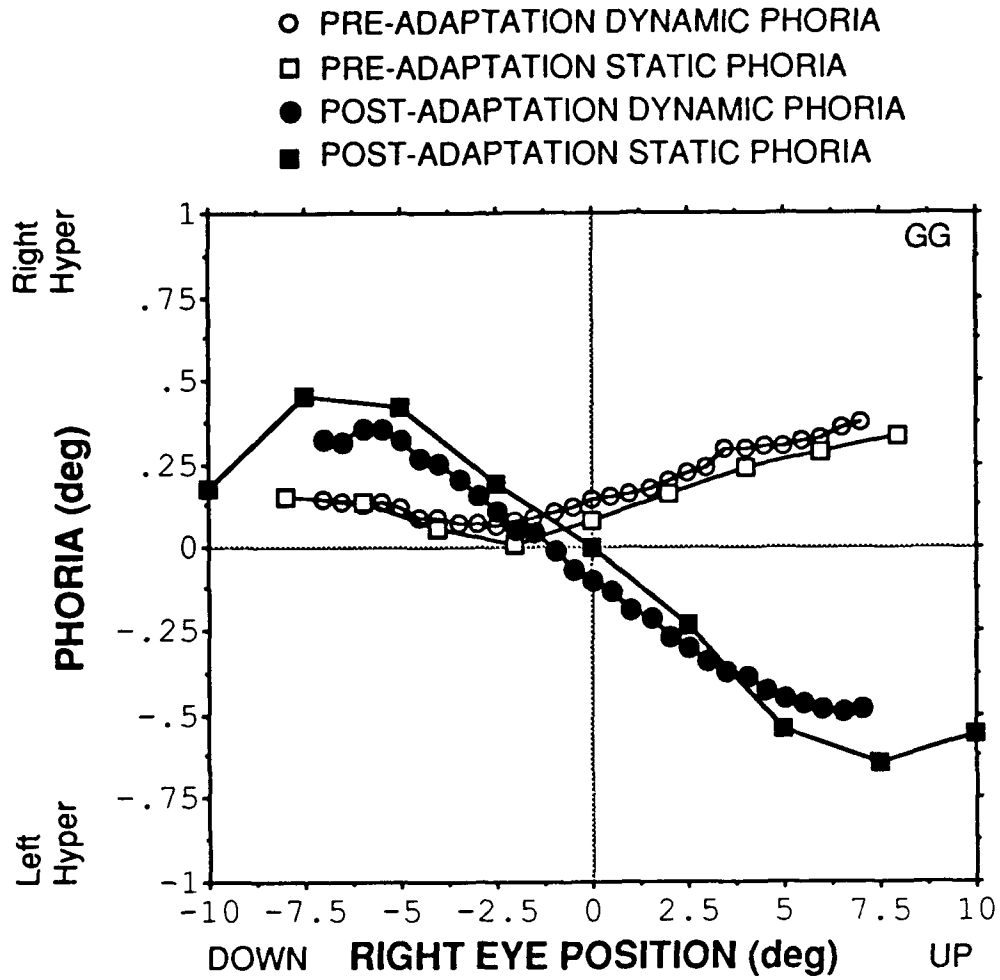
Fig 6c. Subject GG's pre- and post-adaptation dynamic and static phorias are plotted relative to right eye gaze position

Fig 7. Subject GG's pre- (top chart) and post-adaptation (bottom chart) dynamic and static phorias are plotted relative to right eye gaze position. Dynamic phorias are separated based on pursuit direction (upward versus downward). Static phorias are separated based on the direction of the intervening gaze-shifting saccade.
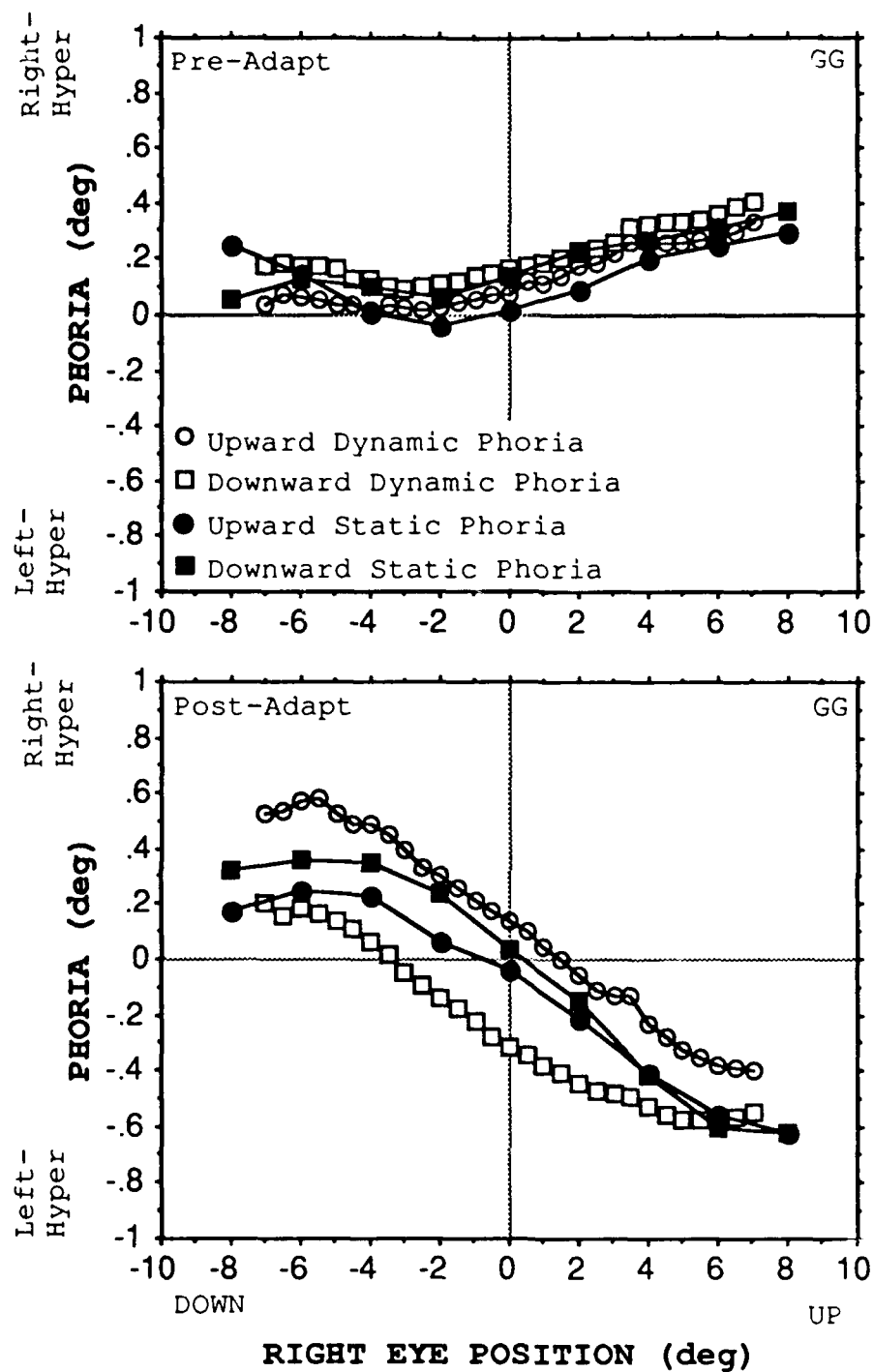
Fig 7.

Fig 8. One cycle of binocular eye traces (thin lines) from subject GG's pre- (top chart) and post-adaptation (bottom chart) pursuit trials. Phoria (R-L) is represented by a thick line. Nonconjugate pursuit adaptation is indicated by the shift from relative left-hyper phoria in the lower field of gaze during the pre-adaptation trial to relative right-hyper phoria in the lower field of gaze during the post-adaptation trial. A horizontal line was added to each chart to improve clarity by marking an arbitrary gaze position near the center of the field. In the pre-adaptation chart, phoria depends only on gaze position, and not pursuit direction. In the post-adaptation chart, phoria depends on gaze position, and pursuit direction.

Fig 8.

136
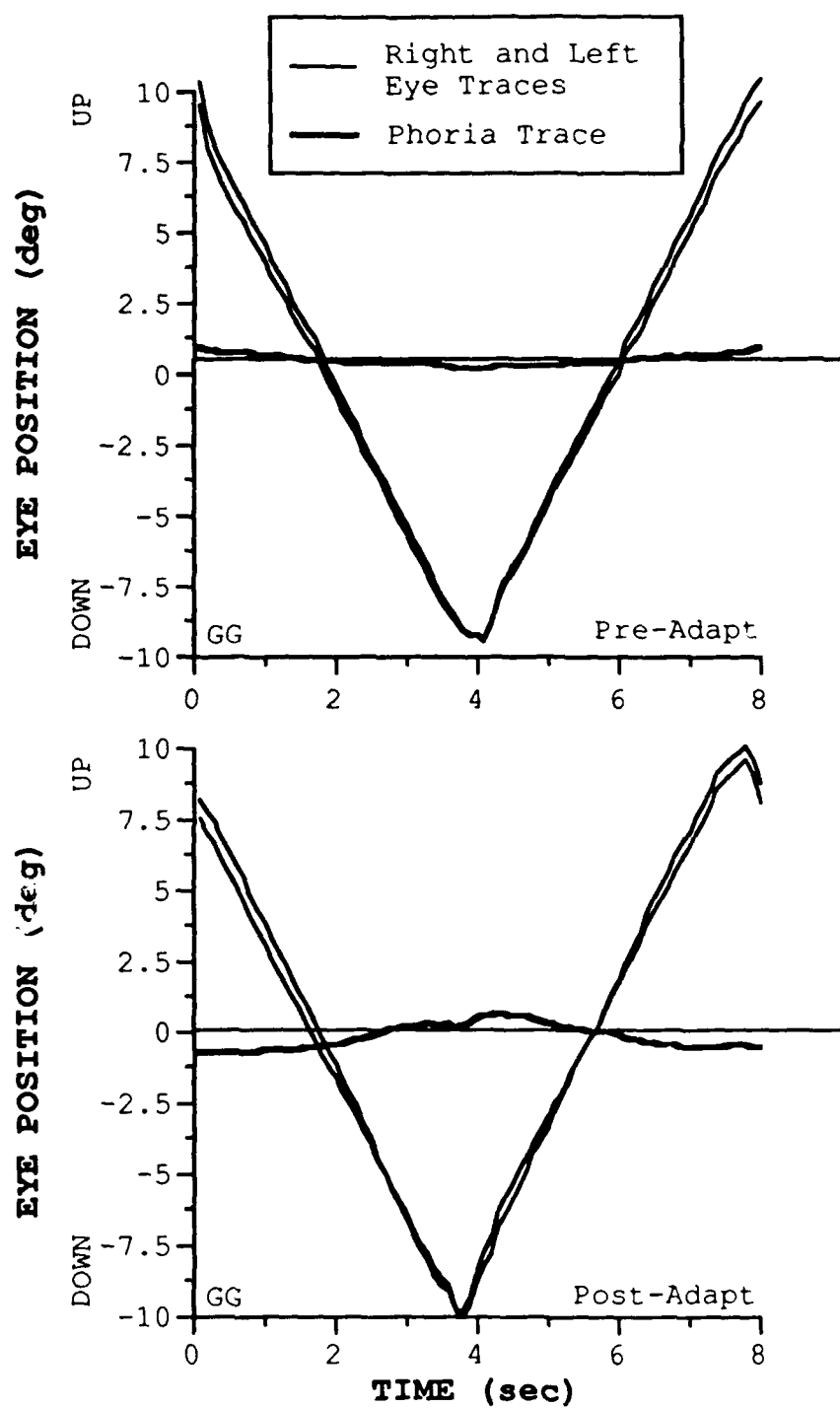
Fig 9. For each subject, the average change in pulse and late yoking ratios are plotted. Pre- and post-adaptation yoking ratios were grouped into one of six categories based on right eye saccade amplitude (see methods). Mean changes and standard deviations were calculated by differencing pre- and post-adaptation categorized data. Full adaptation (large open circles) is represented by a mean yoking ratio change of +0.1 for subject BL, and -0.1 for subjects DP and GG.
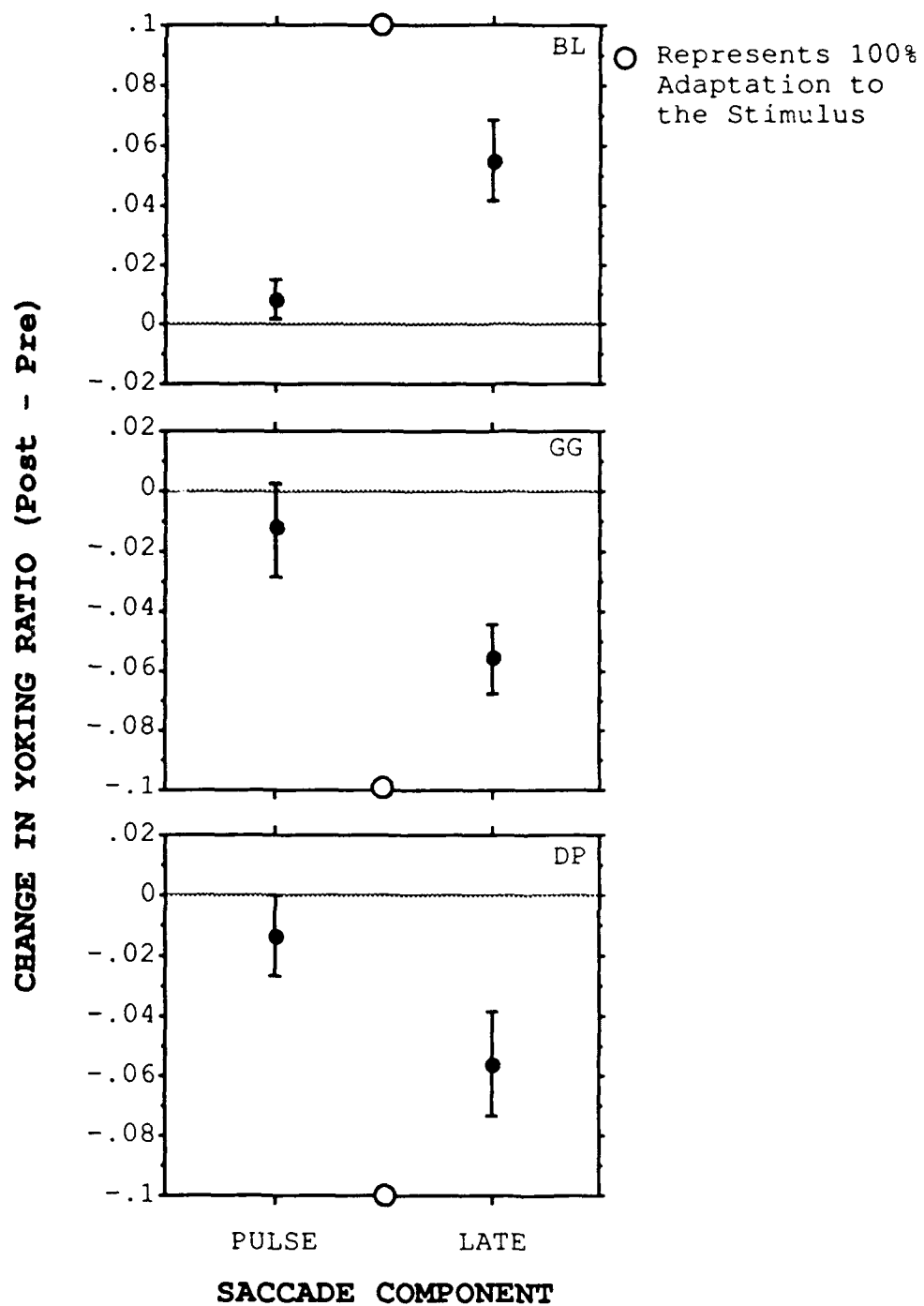
FIG 9.

Fig 10. Binocular eye traces (thin lines) from subject GG's pre- (top chart) and post-adaptation (bottom chart) <u>saccade trials</u>. Phoria (R-L) is represented by a thick line. A horizontal line was added to each chart to improve clarity by contrasting with post-saccadic phoria drift. Before adaptation, post-saccadic phoria drift was minimal. However after adaptation, a slow post-saccadic phoria drift developed that dependent on gaze position.
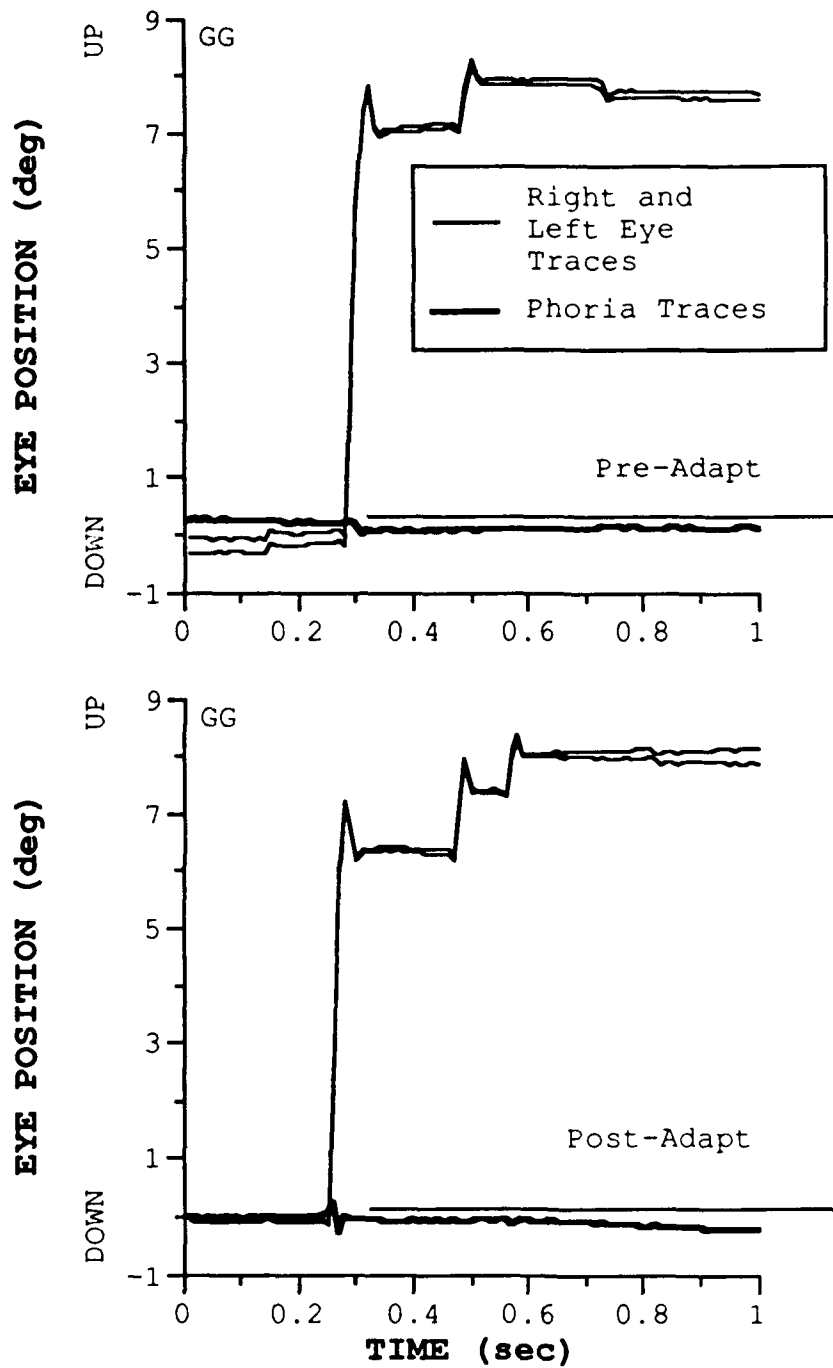
Fig 10.

140

CHAPTER 4

NONCONJUGATE VERTICAL PURSUIT AND VERICAL PHORIA ADAPTATION TO ASYMMETRICAL DISPARITIES

INTRODUCTION

Presumably, nonconjugate adaptation mechanisms assist compensation for age-related, pathological, and traumatic changes that effect the ocular motor system. Such age-related changes are unlikely to occur symmetrically and synchronously in both eyes. Therefore, active calibration of the ocular motor system is necessary to maintain accurate yoking of binocular eye movements and steady bifoveal fixation.

Nonconjugate adaptation of pursuit eye movements was induced in normals by either differential target motion (Chapters 2 and 3) or differential spectacle-mounted optical magnification (Horner et al (1988), Lemij (1990)) before the two eyes. With similar methods, gaze-specific phoria adaptation was induced in normals (chapter 3, Henson and Dharamshi (1982a,b), Sethi and Henson (1984), Zee and Levi (1989), Lemij (1990)). In chapter 3, vertical gaze-specific phorias measured during pursuit and steady fixation were remarkably similar, both before and after adaptation to stationary gaze-specific target disparities, indicating that vertical phoria adaptation and nonconjugate adaptation of vertical pursuit share a common mechanism(s).

In the above studies, the adapting target disparity varied proportional to (headcentric-) gaze position (i.e. gradient disparity). Appropriately, adaptive phoria changes were gradient-like. Unfortunately, these adaptation paradigms confound gaze-specific and gain-like adaptive nonconjugate mechanisms because both types of mechanisms would produce similar responses to gradient disparity.

In chapter 2, gaze-specific changes in binocular yoking during vertical pursuit were induced. However, the induced phoria changes were inappropriate because they did not match the adapting target disparities, and in one case the phoria change was paradoxical. With reference to nonconjugate mechanisms, an appropriate adaptation to a disparity stimulus which varied irregularly with gaze would be a stronger demonstration of gaze-specificity.

Gaze-specificity of nonconjugate vertical pursuit adaptation was investigated by adapting to a pursuit target which contained asymmetrical disparities. While the adapting target scrolled vertically, no disparity was present when the target was in the lower hemi-field of gaze; however, a 15% gradient disparity was incorporated when the target was in the upper hemi-field. Gaze-specific yoking changes during pursuit eye movements developed in all subjects. Furthermore, adaptive changes in gaze-specific dynamic (measured during pursuit) and static (measured during steady fixation) phorias were similar, suggesting that vertical

phoria and nonconjugate pursuit adaptation share a common mechanism(s).

METHODS

Subjects, equipment, procedures, and analyses were the same as those used in chapter 3 with the following exceptions:

1) The adaptation paradigm (described below) was changed.

2) Saccade data trials and analyses were omitted.

3) Pursuit yoking ratios were not calculated.

Adapting Stimulus

During the one hour adaptation period, the target smoothly scrolled vertically over the central 20 degrees at a speed of 5 deg/sec (triangular wave). While in the lower field, right and left eyes' targets scrolled at the same velocity. However, while in the upper field, the right eye's target scrolled 15% faster than the left eye's target (fig 1) for subjects BL and GG (10% faster for subject DP). Therefore, in the lower field there was no target disparity; however, in the upper field there was a 15% gradient disparity.

Subjects were instructed to maintain fixation on the center of the target's cross and, using moderate effort, to keep the targets fused. Subjects were also instructed to

close one or both eyes if they sat away from the eye tracker. During an adaptation period, accumulative time away from the task was less than 1 minute.

RESULTS

In the first minute of adaptation, two subjects reported brief diplopia when the target was in the extreme upper field position. Thereafter, no diplopia was reported.

Gaze-Specific Nonconjugate Adaptation of Vertical Pursuit

All subjects demonstrated greater nonconjugate pursuit adaptation in the upper field of gaze than the lower field. Figure 2 depicts pre- and post-adaptation eye traces (thin lines), with their associated phoria traces (thick lines). Before adaptation (top panel), the phoria trace was relatively flat, indicating the two eyes pursued at approximately the same velocity. After adaptation (bottom panel), the phoria trace remained flat in the lower field. However, phoria became increasingly right-hyper as gaze ascended in the upper field. This indicates left (occluded) and right (seeing) eyes pursued at the same velocity in the lower field; however, the right eye pursued at a higher velocity than the left eye in the upper field.

Role of Phoria Adaptation

For both the pre- and post-adaptation condition, little difference was found between gaze-specific static and dynamic phorias. Figure 3 compares the adaptive change in gaze-specific static and dynamic phorias. Adaptive changes in phorias were calculated by differencing pre- and post-adaptation phorias. Like the adapting stimulus, adaptive changes in static phoria between the upper and lower hemifield were unequal, indicating gaze-specific mechanisms. Unlike the adapting stimulus, the transition of adaptive changes in static phoria between the upper and lower hemifield was rounded. This indicates gaze-specific phoria adaptation is not localized to a specific gaze position, but there is a limited spread of adaptation to surrounding gaze positions. For example, subject BL's phoria change can be closely duplicated by convolving the adapting stimulus with a gaussian (normal) distribution with a 5 degree standard deviation. The gaussian distribution represents the graded spread of gaze-specific phoria adaptation. As in chapter 3, all subjects demonstrated similar changes in static and dynamic phorias, indicating vertical phoria adaptation underlaid the resulting nonconjugate pursuit adaptation.

The direction of pursuit travel (upward vs downward) had little effect on gaze-specific dynamic phorias. Similarly, the direction of the intervening saccade had little effect on gaze-specific static phorias. For each subject and

adaptation condition, table 1 shows the average difference in gaze-specific dynamic phorias due to the direction of pursuit travel, and the average difference in gaze-specific static phorias due to the direction of the gaze-shifting saccade. For both static and dynamic phorias, the typical average difference were less than .1 degrees.

SUBJECT	DYNAMIC		STATIC	
	Pre-Adapt	Post-Adapt	Pre-Adapt	Post-Adapt
BL	.03 (.05)	0.09 (.05)	0.00 (.05)	.16 (.06)
DP	.02 (.04)	0.00 (.04)	-.03 (.07)	-.03 (.08)
GG	-.11 (.03)	-.16 (.03)	-.03 (.05)	0.05 (0.09)

Table 1. For each subject and adaptation condition, the average difference (and standard deviation) between dynamic phorias during upward and downward pursuit eye movement was calculated from 29 gaze positions. Similarly, the average difference (and standard deviation) between static phorias separated by the direction of the intervening gaze-shifting saccade was calculated from 9 gaze positions. Positive values represent phorias measured during or after upward-directed eye movements being more right-hyper than phorias measured during or after downward-directed eye movements.

CONCLUSIONS

Evidence from this chapter and chapter 3 suggests vertical phoria adaptation has the following properties:

1) Gaze-specific, with a graded spread of adaptation to neighboring gaze positions.

2) Not sensitive to direction of gaze-shifting saccades.

3) Underlies nonconjugate adaptation of slow (pursuits), but not fast (pulse component of saccades), eye movements.

These properties are probably best suited to compensate for developmental and senile anatomical changes in the oculomotor plant. These age-related changes would include normal changes in the size of the ocular orbit, and in the size and distribution of the orbital contents (e.g. orbital fat and extraocular muscles). Such changes are unlikely to occur synchronously and symmetrically in the two eyes, and therefore, are likely to stress binocular alignment. It is not known whether normal anatomical changes effect binocular alignment over a limited or broad range of gaze positions.

In chapter 5 nonconjugate adaptation of vertical pursuit will be shown to have gaze- and direction-specific properties that are independent of static phoria adaptation. This suggests additional mechanisms, which appear to be specific to the pursuit system, underlie nonconjugate pursuit adaptation. Such mechanisms may compensate for normal neural attrition within the pursuit system, without disturbing the unaffected phoria system.

REFERENCES

Henson DB and Dharamshi BG (1982a), Binocular
oculomotor adaptation to induced incomitant
deviations, In Functional basis of ocular motility
disorders, Lennerstrand, Zee, and Keller (Eds.),
Pergamon Press: Oxford, pages 229 - 231

Henson DB and Dharamshi BG (1982b), Oculomotor
adaptation to induced heterophoria and anisometropia,
Invest. Ophthalmol. Vis. Sci. 22:234

Horner DG, Gleason G, and Schor CM (1988), The
recalibration of Hering's law for versional eye
movements in response to aniseikonia, Invest.
Ophthalmol. Vis. Sci. 29:136 (abstract 28)

Lemij HG (1990), Asymmetrical adaptation of human
saccades to anisometropic spectacles, Doctoral
Dissertation, Erasmus University of Rotterdam

Sethi (nee Dharamshi) B and Henson DB (1984), Adaptive
changes with prolonged effect of comitant and
noncomitant vergence disparities, Am. J. Optom.
Physiol. Opt. 61:506

Zee DS and Levi L (1989), Neurological aspects of
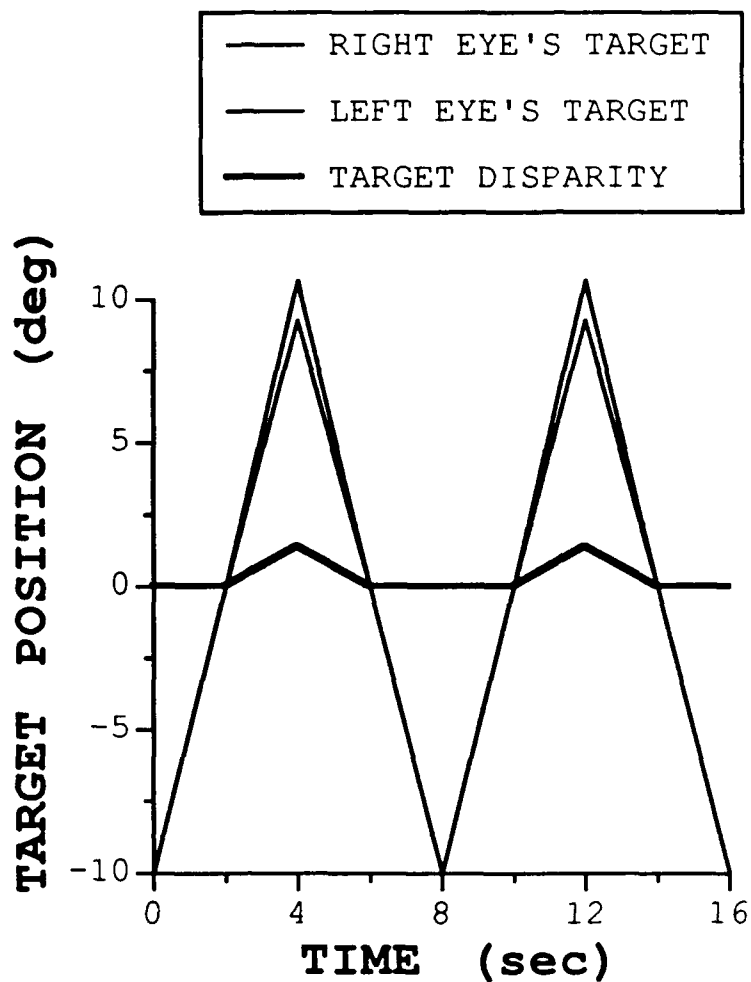vergence eye movements, Rev Neurol (Paris) 145:613

FIG 1. Two cycles of adapting target motion is depicted. Right and left eyes' targets (thin lines) move at the same velocity in the lower field, but in the upper field the velocity of the right eye's target was 15% faster. Target disparity (thick line) is the difference between right and left eye target positions. In the lower field there is no target disparity; however, in the upper field there is a 15% gradient target disparity.
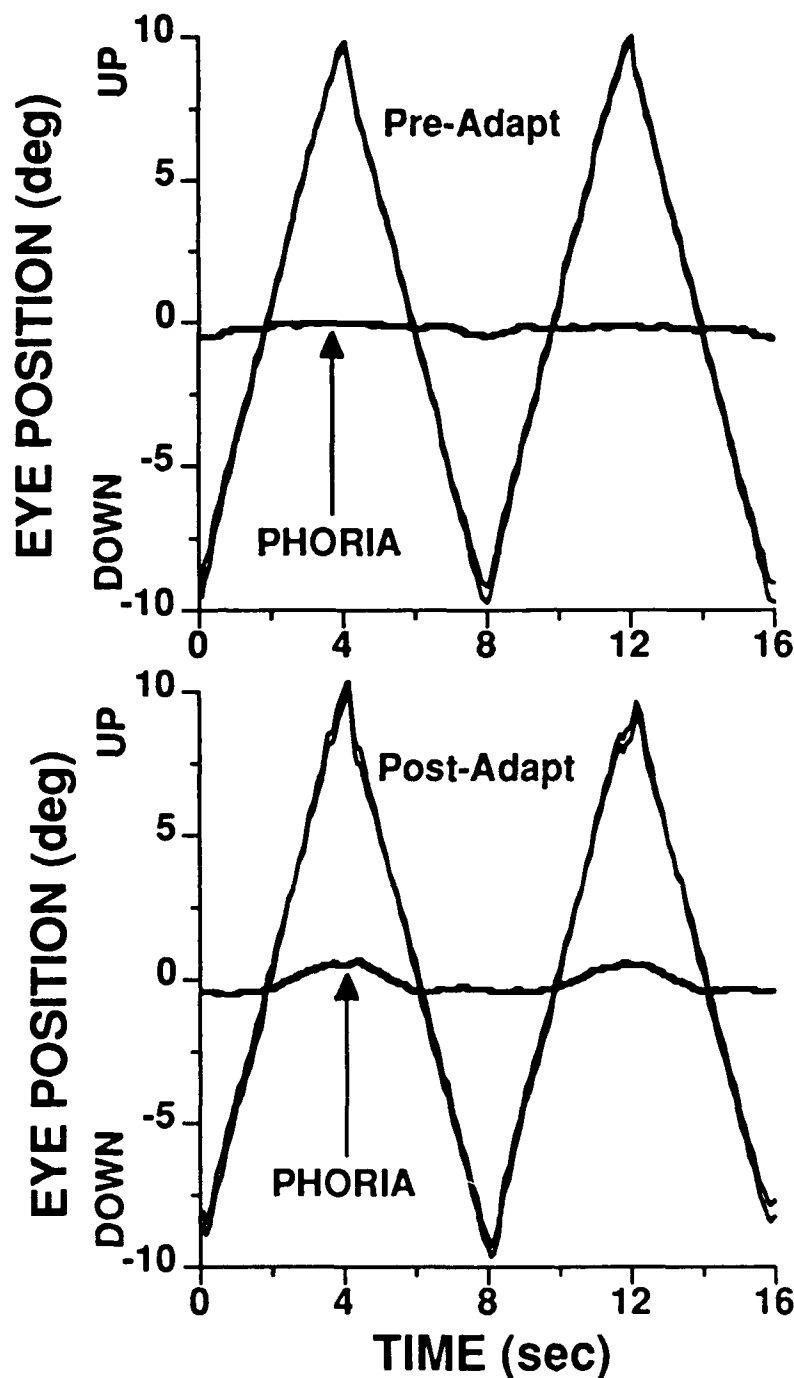
FIG 2. Pre- and post-adaptation eye traces (thin lines) with associated phoria traces (thick lines) are plotted. Left eye was occluded during both measurements. Before adaptation (top panel), a flat phoria trace indicates comparable right and left eye velocity. After adaptation (lower panel), the phoria trace remains flat when gaze is in the lower field. However, the phoria trace becomes increasingly right-hyper as gaze ascends in the upper field, indicating the right eye is moving faster than the left eye.

FIG 3. For each subject, adaptive changes in gaze-specific dynamic (circles) and static (squares) phorias are plotted relative to right eye gaze position. Adaptive changes were calculated by differencing pre- and post-adaptation gaze-specific phorias. Target disparity (thick line) is plotted for contrast.
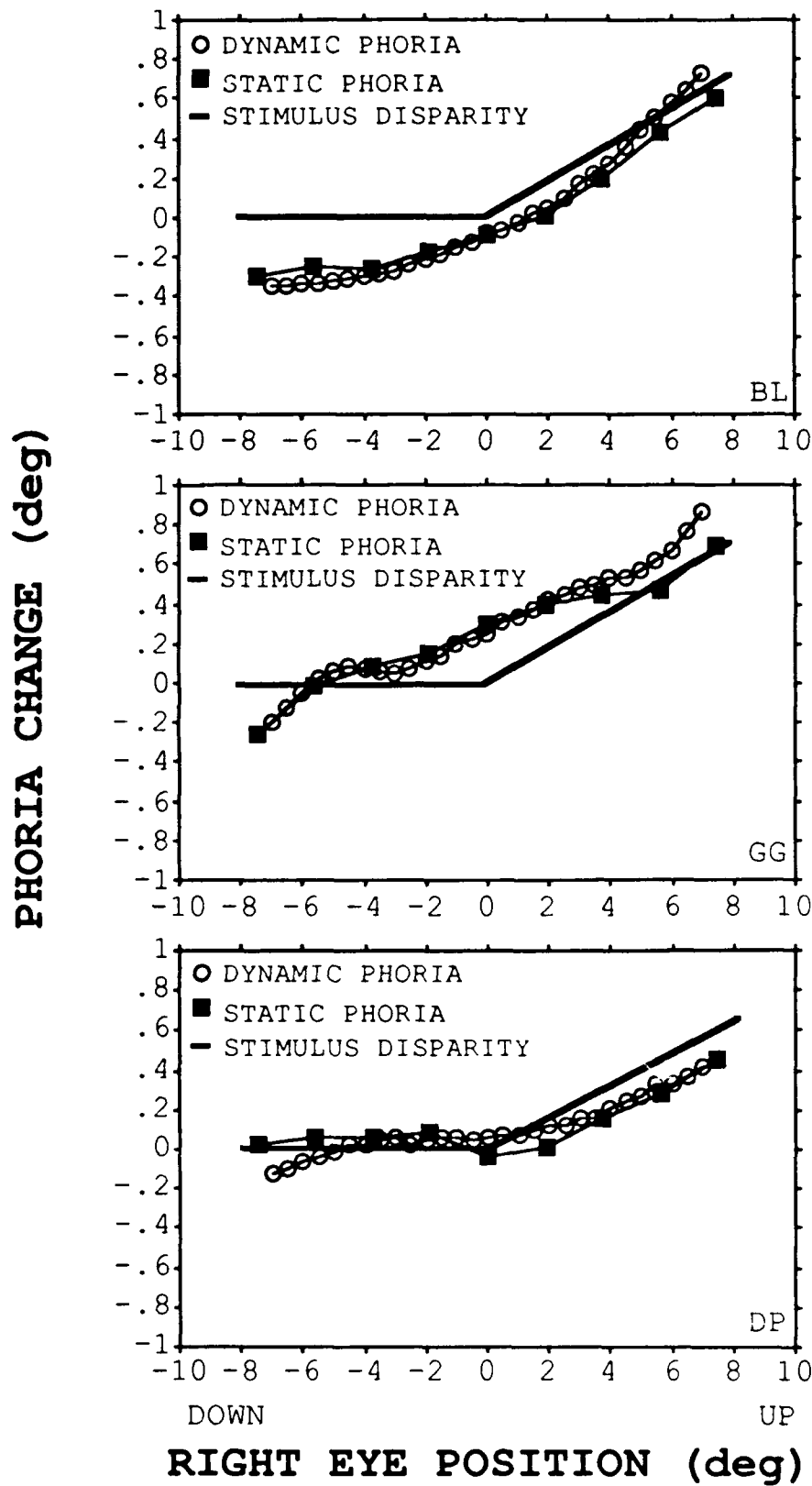
FIG 3.

CHAPTER 5

DIRECTION SPECIFICITY OF NONCONJUGATE ADAPTATION OF VERTICAL PURSUIT

INTRODUCTION

Experiments in the two previous chapters demonstrated that phoria adaptation plays an important role in nonconjugate adaptation of vertical pursuit eye movements. In both chapters, comparable adaptive changes in gaze-specific dynamic (measured during pursuit) and static (measured during steady fixation) phorias suggested the innervations which specify open-loop (monocular viewing) vertical vergence posture during steady fixation remain operative during relatively slow vertical pursuit eye movements. Within experimental conditions, static phorias did not appear to depend on the direction of the gaze-shifting saccade that immediately preceded the phoria measurement. In contrast, in chapter 3, two subjects exhibited a small uniform shift in dynamic phorias (.36 and .20 degrees), which depended on the direction of pursuit travel (upward versus downward). In the sense that the adapting stimulus did not have direction-specific disparities, these direction-sensitive responses are inappropriate. Nevertheless, these inappropriate responses hint at the existence of direction-specific nonconjugate pursuit mechanisms that can not be explained by phoria adaptation.

After inducing nonconjugate adaptation with spectacle-mounted plano-cylindrical lenses, Lemij (1990) demonstrated that nonconjugate pursuit adaptation was orientation selective. It did not transfer between vertical and horizontal meridians, nor did it transfer between two orthogonal oblique meridians. Direction-specificity of nonconjugate pursuit adaptation within a single meridian has not yet been studied.

Direction-specificity of nonconjugate pursuit adaptation along the vertical meridian was investigated here by exposing subjects to two adaptation paradigms on separate days. In the gaze-specific paradigm, target disparities depended only on target position. In the direction-specific paradigm, position-specific target disparities during upward target motion were antithetical to position-specific target disparities during downward target motion.
When there was no stimulus for direction-specific nonconjugate pursuit adaptation (gaze-specific paradigm), adaptive changes were not sensitive to pursuit direction, and gaze-specific dynamic and static phorias were similar. In contrast, when there was a stimulus for direction-specific nonconjugate pursuit adaptation (direction-specific paradigm), adaptive changes in dynamic phorias occurred selectively for pursuit direction (upward versus downward). Furthermore, gaze-specific phoria variations across the adapting field were different for dynamic and static measurements.

When the term "direction" is applied to dynamic phorias, it refers to the direction of the ongoing pursuit eye movement (upward versus downward) while dynamic phorias were measured. When the term "direction" is applied to static phorias, it refers to the direction of the gaze-shifting saccade (upward versus downward) that immediately preceded static phoria measurement.

EXPERIMENT 1: GAZE-SPECIFIC PARADIGM

METHODS

Subjects, equipment, procedures, and analyses were the same as those used in chapter 3, except saccade data trials and analyses were omitted.

Adapting Stimulus

During the one hour adaptation period, the target oscillated along the vertical meridian over the central 20 degrees at a speed of 5 deg/sec (.111 Hz clipped triangular wave) (fig 1). The target paused for 0.5 seconds at the extreme upper and lower positions (up or down 10 degrees). While the target was at either extreme position, there was zero target disparity. As the target scrolled either upwards or downwards towards the opposite extreme position, vertical target disparity increased until it reached a maximum of 1.25 degrees right-hyper at the straight ahead position. Then, as the target continued to move towards the opposite extreme

position, target disparity tapered to zero disparity. When present, target disparity was always right-hyper, and its amplitude depended only on target position.

RESULTS

Subjective Reports of Diplopia During Adaptation Period

Initially during the adaptation period, all subjects reported brief diplopia when the target was near the straight ahead position. After the first few stimulus cycles, diplopia was no longer reported.

Nonconjugate Pursuit Adaptation

After the adaptation period, all subjects demonstrated nonconjugate changes in binocular yoking during vertical pursuit eye movement. Adaptive changes (post – pre) in dynamic phorias were separated by pursuit direction and then plotted (open symbols), relative to right eye gaze position, in the top panels of figures 2a (subject BL) and 2b (subject GG). Subject DP's results were comparable to BL's. All subjects demonstrated a right-hyper shift in dynamic phorias that was not specific to pursuit direction. However, this shift was greater for central gaze positions than eccentric gaze positions, because (regardless of pursuit direction) the right eye moved relatively faster than the left eye in lower gaze positions and relatively slower in upper gaze positions.

Role of Gaze-Specific Static Phoria Adaptation

Adaptive changes in gaze-specific static phorias were separated by the direction of the preceding saccade, and then plotted (filled symbols) in the top panels of figures 2a (BL) and 2b (GG).

After adaptation, all subjects demonstrated a right-hyper static phoria shift that was greater for central gaze positions than eccentric gaze positions. Adaptive changes in gaze-specific dynamic and static phorias were similar.

Subject BL exhibited a generalized right-hyper phoria shift (fig 2a, top panel) which averaged 0.5 degrees for dynamic phorias and 0.4 degrees for static phorias. However, adaptive changes in phorias were greater (~0.3 degrees) for central gaze positions than eccentric gaze positions. Subject DP's results were comparable to BL's.

Subject GG exhibited a generalized right-hyper phoria shift (fig 2b, top panel) which averaged 0.35 degrees for dynamic phorias and 0.25 degrees for static phorias. Adaptive changes in phorias were greater (~0.45 degrees) for central gaze positions than eccentric gaze positions. While adaptive changes in dynamic and static phoria varied similarly across the adapting field of gaze, the maximum change in static phoria occurred two degrees lower in the adapting field than the maximum change in dynamic phoria.

Directional-Specificity of Adaptive Phoria Changes

Directional differences in dynamic phoria adaptation were quantified by differencing gaze-specific changes in dynamic phoria during upward and downward pursuit. Similarly, directional differences in static phoria adaptation were quantified by differencing gaze-specific changes in static phoria following upward and downward saccades. Directional differences in dynamic (open circles) and static (filled circles) are plotted in the bottom panels of figs 2a,b.

Adaptive changes in both dynamic and static phorias were equal in the two directions. For subjects BL and DP, directional differences in both dynamic and static phorias were not significantly different from zero ($P > .05$, within-subject 2 tail t-test). Similarly, for subject GG, directional differences in static phoria change (fig 2b, lower panel) were not significantly different from zero ($P > .05$, within-subject 2 tail t-test). However, directional differences in dynamic phoria change were significantly different from zero ($P < .001$, within-subject 2 tail t-test). The average directional difference was only 0.1 degrees. This difference, although statistically significant, is probably not reliable. In within-subject t-tests, the assumption of independent measurements is violated, resulting in decreased variability. This leads to an increased likelihood of a type I statistical error (reject null hypothesis when it is true).

EXPERIMENT 2: DIRECTION-SPECIFIC PARADIGM

METHODS

Subjects, equipment, procedures, and analyses were the same as those used in chapter 3, except saccade data trials and analyses were omitted. For each subject, the experimental sessions for experiments 1 and 2 were separated by at least two weeks.

Adapting Stimulus

During the one hour adaptation period, the target oscillated along the vertical meridian over the central 20 degrees at a speed of 5 deg/sec (.111 Hz clipped triangular wave) (fig 3). During the stimulus cycle, the target paused for 0.5 seconds, without disparity, at the upper and lower extreme positions (up and down 10 degrees). As the target moved upwards from the lower extreme position, target disparity increased until it reached a maximum of 1.25 degrees right-hyper at the straight ahead position. As the target continued to move towards the upper extreme position, target disparity tapered to zero disparity. Subsequently, as the target moved downwards, target disparity increased until it reached a maximum of 1.25 degrees left-hyper at the straight ahead position. As the target continued to move towards the extreme lower position, target disparity tapered to zero disparity. The target cycle then repeated.

Therefore, the amplitude and direction (right- versus left-hyper) of target disparity depended on target position and the direction (upward versus downward) of target motion. Vertical disparity was produced for both upward and downward movements by advancing the position of the target before the right eye ahead of the target before the left eye.

RESULTS

Gaze-specific Subjective Reports of Diplopia During Adaptation Period

Initially during the adaptation period, all subjects reported brief diplopia while the target was near the straight ahead position. After the first few stimulus cycles, subjects BL and DP reported diplopia only when the target was near the straight ahead (maximum disparity) position and target motion was upward (right-hyper disparity). Similarly, after the first few stimulus cycles, subject GG reported diplopia only when the target was near the straight ahead position and target motion was downward (left-hyper disparity).

For each subject, diplopia diminished throughout the adaptation period, however, the time course of this reduction was idiosyncratic. After 15 minutes of adaptation, subject GG no longer reported diplopia. However, the target disparity could be sensed as "eye strain" when the target was near the straight ahead position. At the end of the adaptation period, target disparities were no longer sensed

in this fashion. For subject BL, diplopia subsided after 25

minutes of adaptation, but target disparities could be sensed

as "eye strain". At the end of the adaptation period,

subject BL could still, although diminished, sense target

disparity during upward target motion. Throughout the

adaptation period, subject DP intermittently reported

diplopia.

Nonconjugate Pursuit Adaptation

Following the adaptation period, all subjects demonstrated

nonconjugate changes in binocular yoking during vertical

pursuit eye movement. Figure 4 plots subject GG's eye

position traces during pre- and post-adaptation pursuit

trials (left eye was occluded). Before adaptation (top

panel), variations in dynamic phoria (thick trace) are

relatively small and gaze-specific. These small variations

denote that the two eyes were moving at nearly the same

velocity. To illustrate gaze-specificity, a vertical

(dotted) line was added to the top panel such that it

intersected a trough in the eye position traces. Immediately

to left of the vertical line, pursuit eye movements are

directed downward. Immediately to the right of the vertical

line, pursuit eye movements are directed upwards. Similar to

the eye position traces, the phoria trace is even-symmetric

about the vertical line, indicating that pre-adaptation

dynamic phoria depended on gaze position, but not pursuit

direction.

After adaptation (fig 4, lower panel), variations in dynamic phoria (thick trace) were larger. Therefore, the two eyes were moving at differential velocities, indicating that nonconjugate pursuit adaptation had occurred. During the pursuit cycle, regardless of pursuit direction, dynamic phoria became increasingly right-hyper when gaze was in the lower field and increasingly left-hyper when gaze was in the upper field (compare phoria trace between points b and c and between points c and d in lower panel of fig 4). Consequently, during upward pursuit, the right eye was relatively faster (than the left eye) in the lower field of gaze, but slower in the upper field. During downward pursuit, the right eye was relatively slower in the lower field, but faster in the upper field. Regardless of pursuit direction, the right eye positionally led the left eye. Both, direction- and gaze-specific nonconjugate adaptation mechanisms are needed to reconcile these observations of binocular yoking plasticity.

To illustrate direction- and gaze-specificity in post-adaptation dynamic phorias, four arrows (a,b,c, and d) were placed in the lower panel of figure 4, such that their tips were at the same height as the peaks of the phoria trace (a and c). Since all of the arrow tips are at the same height, they represent a single gaze position. At this specified gaze position, phorias during upward pursuit (a and c) were equal and phorias during downward pursuit (b and d) were equal, suggesting for a particular pursuit direction the

dynamic phoria amplitude depended on gaze position. However, phorias during upward and downward pursuit (a and b) were unequal and opposite in sign (right- versus left-hyper), suggesting that at a given gaze position, dynamic phoria amplitude depended on the direction of pursuit travel.

Role of Gaze-Specific Phoria Adaptation

In prior experiments (gaze-specific paradigm, and chapters 3 and 4), adaptive changes in gaze-specific dynamic and static phorias were closely matched, and both showed little or no direction specificity. These observations suggest a common adaptation mechanism(s) underlies vertical static phoria adaptation and nonconjugate pursuit adaptation.

In this experiment (direction-specific paradigm), adaptive changes in gaze-specific dynamic and static phorias were different. Similar to figure 2, direction-specific adaptive changes (post - pre) in dynamic (open symbols) and static (filled symbols) phorias are plotted separately for each subject in the top panels of figures 5a,b,c. Gradient-like adaptive changes in static phorias were observed in all subjects, such that adaptive changes in static phorias became progressively more right-hyper (or less left-hyper) as gaze descended to lower field positions and progressively more left-hyper (or less right-hyper) as gaze ascended. In contrast, adaptive changes in dynamic phorias were greater for central gaze positions than higher and lower eccentric gaze-positions. Furthermore, directional differences were

observed for adaptive changes in dynamic phorias, but not in adaptive changes static phorias. Directional differences are discussed more fully below.

The above observations that adaptive changes in dynamic and static phoria differ in terms of gaze position and direction of motion indicates that separate mechanisms underlie vertical static phoria adaptation and nonconjugate pursuit adaptation. These observations and those from previous experiments indicate multiple mechanisms underlie nonconjugate adaptation of vertical pursuit. Some of these mechanisms are shared with vertical phoria adaptation, and some are not.

Directional-Specificity of Adaptive Phoria Changes

Directional differences in dynamic phoria adaptation (open circles in the bottom panels of figs 5a,b,c) were quantified by subtracting adaptive changes in gaze-specific dynamic phoria during downward pursuit from adaptive changes during upward pursuit (open squares and circles, respectively, in the top panels). Similarly, directional differences in static phoria adaptation (filled circles in bottom panels) were quantified by differencing gaze-specific changes in static phoria following upward- and downward-directed saccades (filled circles and squares, respectively, in the top panels).

For all subjects, adaptive changes in dynamic phorias were sensitive to pursuit direction. During upward pursuit,

adaptive changes in dynamic phorias were relatively more right-hyper than during downward pursuit. This directional difference in dynamic phoria adaptation is depicted in figure 5 by the vertical separation of open circles and squares in the top panels and by the vertical elevation of the open circles above zero in the bottom panels. For each subject (BL, GG, and DP), the average (standard deviation) adaptive change in dynamic phorias during upward pursuit was 0.55 (0.12), 0.82 (0.19), and 0.46 (0.11) degrees more right-hyper than during downward pursuit. Separate within-subject t-tests indicate these differences were significantly different than zero (For all subjects, $T > 23$, $P < .0001$).

It was considered that these direction-specific differences in adaptation might be approximated by the left (occluded) eye lagging temporally behind the right (seeing) eye during pursuit data trials by 110; 164; and 92 msec for subjects BL; GG; and DP, respectively. However, this was not the case, since the two eyes always reversed direction synchronously during the pursuit data trials (measurement resolution of 10 msec).

In contrast, directional differences in static phoria adaptation averaged less than .1 degrees for each subject. Separate within-subject t-tests indicate these differences were not significantly different from zero (For all subjects, $T < 1.7$, $P > .05$). Directional differences in static phoria adaptation is depicted in figure 5 by the vertical separation of filled circles and squares in the top panels and by the

vertical separation of filled circles from zero in the bottom panels.

Gaze-Specificity of Direction-Specific Mechanisms

Aside from offset differences (discussed above), directional differences in nonconjugate pursuit adaptation were gaze-specific. In the top panels of figure 5, the open circles, representing adaptive changes in gaze-specific dynamic phoria during upward pursuit, have a dome-shaped pattern for subjects BL (fig 5a) and GG (fig 5b). These dome-shaped patterns imply, for upward pursuit, right-hyper dynamic phoria shifts were greater for central gaze positions than eccentric gaze positions. Subject DP (fig 5c) demonstrated little adaptive change in dynamic phoria during upward pursuit. The open squares, representing adaptive changes in gaze-specific dynamic phoria during downward pursuit, have a bowl-shaped pattern for all subjects (fig 5a,b,c). These bowl-shaped patterns imply, for downward pursuit, left-hyper dynamic phoria shifts were greater for central gaze positions than eccentric gaze positions. These dome- and bowl-shaped patterns emulate the shape of the adapting target's direction- and position-specific disparities, and therefore, they represent an appropriate gaze-specific response to the adapting stimulus. The dissimilarity of the adaptive change patterns for upward and downward pursuit indicates that the mechanisms that underlie

these direction-specific responses are, to some degree, independent of each other.

CONCLUSIONS

Multiple Mechanisms Underlie Nonconjugate Adaptation of Vertical Pursuit

In chapter 3, subjects were exposed to stationary gaze-specific vertical disparities. Although during the adaptation period, pursuit eye movements were not stimulated, these stationary disparities were highly effective in inducing nonconjugate pursuits during monocular viewing (and gaze-specific static phoria adaptation.) When analyzed as gaze-specific dynamic phorias, these nonconjugate changes were accounted for by concurrent changes in gaze-specific static phoria.

In chapter 4, subjects were exposed to a pursuit stimulus that stimulated equal eye movements in the lower field and faster right eye movements (than the left eye) in the upper field. This nonconjugate pursuit stimulus was effective in inducing gaze-specific phoria adaptation (and nonconjugate pursuit adaptation). And again, adaptive changes in gaze-specific dynamic and static phorias were similar. Together, these two studies indicate that static vertical phoria adaptation and nonconjugate pursuit adaptation shared a common mechanism(s).

The significant finding of this study is that more than one mechanism underlies nonconjugate adaptation of vertical

pursuit. In the first part of this study (gaze-specific paradigm), subjects adapted to a pursuit stimulus that incorporated target disparities, whose amplitudes depended only on target position. As with the aforementioned experiments, which also contained purely position-specific target disparities, adaptive changes in dynamic phorias were gaze-specific and similar to adaptive changes in static phoria. These results, once again, support the idea of a common mechanism(s) underlying vertical static phoria adaptation and nonconjugate pursuit adaptation. In the second part of this study (direction-specific paradigm), subjects adapted to a pursuit stimulus that incorporated target disparities, whose amplitudes depended on both, position and direction of target motion. Unlike previous studies, subsequent adaptive changes in gaze-specific dynamic and static phorias were dissimilar. Furthermore, adaptive changes in dynamic pursuit, but not static phorias, were sensitive to direction of target motion (discussed below). These differences in gaze- and direction-specificity indicate separate mechanisms also underlie vertical phoria adaptation and nonconjugate pursuit adaptation.

Two categories of mechanisms underlie nonconjugate adaptation of vertical pursuit. One category, 'phoria mechanisms', is shared with vertical static phoria adaptation. The other category, 'non-phoria mechanisms', is not shared with vertical phoria adaptation. Separate non-phoria mechanisms exists for upward and downward pursuit.

Whether each of these mechanisms represent rudimentary processes is not known. All, or some, of these mechanisms may be composites of more basic processes.

Nonconjugate Mechanism: Phoria Mechanism

The phoria mechanism is gaze-specific, and has been shown to respond appropriately, although not completely, within one hour to a variety of gaze-specific adapting stimuli: gradient disparity over the entire adapting field (chapter 3), zero disparity in one hemifield and gradient disparity in the other hemifield (chapter 4), and converse gradient disparities in opposite hemifields (gaze-specific paradigm.) Since a gain-based mechanism would only respond appropriately to a full-field gradient disparity, the phoria mechanism is clearly not gain-based.

The phoria mechanism is stimulated by multiple gaze-specific disparities and is able to respond to these disparities during steady fixation (chapter 3) and vertical pursuit eye movements (gaze-specific paradigm and chapter 4).

The phoria mechanism does not appear to be sensitive to direction. In static phoria data trials (chapter 3 methods), gaze was shifted either progressively downward or upward by small saccades (2 to 2.5 degrees) between phoria measurements. In all studies to date (chapters 3, 4, and 5), the direction of the gaze-shifting saccades made little difference on gaze-specific phoria amplitude.

In these same studies, the greatest phoria variability was consistently found at the extreme gaze positions of phoria measurement. These extreme positions were always approached from the same direction by a centrifugal saccade; however, the amplitude of the saccade was either large (8 or 10 degrees) or small (2 to 2.5 degrees). This increased variance suggests that static phoria measurements are partially determined by the amplitude of the preceding saccade. Therefore, gaze-specific static phorias may be determined, to some extent, by how the eyes got to the gaze position. The effects of saccade direction and amplitude on subsequent gaze-specific static phorias needs to be studied.

Nonconjugate Mechanism: Non-Phoria Mechanisms

Separate non-phoria mechanisms exists for upward and downward pursuit, and each is gaze-specific. In the direction-specific paradigm, adaptive changes in dynamic phorias were relatively more right-hyper for upward pursuit than for downward pursuit. In addition, these direction-specific adaptive changes were greater for central gaze positions than eccentric gaze positions, indicating non-phoria mechanisms are gaze-specific. Relative to pursuit direction, gaze-specific adaptive changes in dynamic phorias were unique, indicating that the separate non-phoria mechanisms for upward and downward pursuit are, to some extent, independent of each other.

The adequate stimulus for non-phoria mechanisms is unknown. Unlike previous experiments (gaze-specific paradigm, and chapters 3 and 4), the direction-specific paradigm induced direction-specific nonconjugate pursuit yoking changes in all subjects. The most obvious difference between the adapting stimuli in the direction-specific paradigm and the prior studies, is that two distinct sets of gaze-specific disparities were used in the direction-specific paradigm. Each set was associated with a particular pursuit direction. Therefore, an adequate stimulus for non-phoria mechanisms appears to be a differential set of gaze-specific target disparities for upward and downward pursuit.

Assuming (direction-specific) non-phoria mechanisms require simultaneous processing of disparity and pursuit direction information, it is not known whether direction information must be processed during pursuit eye movements. A way to test this question is to adapt subjects to a similar target disparity pattern used in the direction-specific paradigm except that, instead of superimposing gaze- and direction-specific target disparities on a smoothly oscillating target, discrete stationary target disparities would be sequentially presented (similar to the adapting paradigm in chapter 3).

Interaction of Phoria and Non-Phoria Mechanisms

This study's most puzzling result is that, in response to the direction-specific paradigm's adapting stimulus, all

subjects demonstrated gradient-like adaptive changes in static phorias. This gradient response, by itself, cannot be reconciled as an appropriate response because it does not mimic either of the adapting target's two direction-specific disparity patterns (fig 3), nor some weighted average of the two patterns. In contrast, all subjects demonstrated appropriate gaze-specific adaptive changes in static phorias in the gaze-specific paradigm (experiment 1). The adapting target's disparity pattern during upward target motion was the same in the gaze-specific and direction-specific paradigms. Therefore, phoria mechanisms, indicated by static phoria changes, are capable of responding to at least one of the two direction-specific disparity patterns presented in the direction-specific paradigm, yet they responded inappropriately. In contrast, adaptive changes in dynamic phorias were appropriate in both studies. Why phoria mechanisms responded inappropriately and non-phoria mechanisms responded appropriately is unclear.

One possibility is that nonconjugate adaptation of vertical pursuit is driven by either phoria mechanisms or non-phoria mechanisms, but not both (XOR (exclusive or) Hypothesis). Within the XOR Hypothesis, adaptive changes in static phorias reflect phoria mechanisms, and adaptive changes in dynamic phorias reflect either phoria or non-phoria mechanisms. Hypothetically, when target disparities are purely gaze-specific, phoria mechanisms intercede. However, if target disparities vary with pursuit direction,

then non-phoria mechanisms intercede. In this latter case, the phoria mechanisms, being purely gaze-specific, may be confused by the duality of disparities presented at each gaze-position, and respond (inappropriately) by returning to some idiosyncratic bias.

A second possibility is that nonconjugate adaptation of vertical pursuit is simultaneously driven by phoria and non-phoria mechanisms (Additive Hypothesis). Within the Adaptive Hypothesis, adaptive changes in static phorias reflect phoria mechanisms, and adaptive changes in dynamic phorias reflect a composite of phoria and non-phoria mechanisms. Presumably, phoria mechanisms have a lower threshold than non-phoria mechanisms. Therefore, purely gaze-specific target disparities are primarily compensated for by phoria mechanisms. In contrast, phoria mechanisms can not compensate for gaze-specific target disparities that vary with pursuit direction, leaving non-phoria mechanisms to play the major role in nonconjugate pursuit adaptation.

To see the contribution of non-phoria mechanisms, adaptive changes in gaze-specific static phorias (representing phoria mechanisms) were subtracted from adaptive changes in gaze-specific dynamic phorias (representing phoria and non-phoria mechanisms). Because static and dynamic phorias were measured at different gaze positions, each subject's adaptive changes in gaze-specific static phorias were estimated with a single third-order polynomial function. The polynomial

coefficients were calculated using a least squares method and are listed separately for each subject in Table 1.

SUBJECTS	x^3	x^2	X	OFFSET
BL	$8.03\ x10^{-4}$	$-1.88\ x10^{-3}$	$-8.30\ x10^{-2}$	-0.111
GG	$2.93\ x10^{-4}$	$-1.90\ x10^{-3}$	$-5.52\ x10^{-2}$	0.209
DP	$7.55\ x10^{-4}$	$2.04\ x10^{-3}$	$-6.24\ x10^{-2}$	-0.248

TABLE 1 A third-order polynomial function was used to model adaptive changes in static phorias (direction-specific paradigm), The polynomial's coefficients are listed separately for each subject. The coefficients were derived by a least squares method.

For each subject, the contribution to adaptive changes in dynamic phorias made by upward(circles) and downward (squares) non-phoria mechanisms are plotted separately in figure 6. Two parallel lines were arbitrarily placed in each panel to help illustrate slope and gaze-specific differences between contributions by upward and downward non-pnoria mechanisms.

Casual inspection of the three panels (subjects) in figure 6 reveals a interesting finding: non-phoria mechanisms responded similarly for all subjects. In contrast, all three subjects demonstrated different patterns of adaptive change in dynamic phorias (open symbols in top panels of figs 5a,b,c). For subject BL (fig 5a), the greatest change in dynamic phoria for upward pursuit was in the lower field and

for downward pursuit, the greatest change occurred in the upper field. For subject GG (fig 5b), adaptive change in dynamic phorias for upward and downward pursuit were symmetrical with each other. For subject DP (fig 5c), adaptive change in dynamic phorias occurred for downward pursuit, but not upward pursuit.

After assuming the Additive Hypothesis and removing the effects of phoria mechanisms (static phorias) from dynamic phorias, only the effects due to non-phoria mechanisms remain. Non-phoria mechanisms responded similarly in all three subjects (fig 5a,b,c). First, adaptive changes due to non-phoria mechanisms for upward pursuit were more right-hyper than those for downward pursuit, indicating separate direction-specific mechanisms. Second, greater gaze-specific changes occurred for downward pursuit than for upward pursuit, indicating these two direction-specific mechanisms are, to some extent, independent of each other. Third, both direction-specific mechanisms produced adaptive changes in the upper field that are more right-hyper than adaptive changes in the lower field. Furthermore, when the adaptive changes in the lower extreme field is compared to those in the upper extreme field, the overall increase in right-hyper is similar for upward and downward pursuit. (Use parallel lines to aid comparisons in figure 6.) This similarity suggests the presence of an underlying gain mechanism that is common to both direction-specific non-phoria mechanisms. Therefore, (upward and downward) non-

phoria mechanisms may be composites of a mutually shared gain mechanism and separate gaze-specific mechanisms.

The gradient-like adaptive changes in static phorias may serve to compensate for inappropriate changes produced by the non-phoria gain mechanism. Perhaps, an adequate stimulus for the non-phoria gain mechanism is the relative position of each eye's target. In the direction-specific paradigm's adaptation period, the right eye's target always positionally led the left eye's, thus (theoretically) stimulating non-phoria gain mechanism.

REFERENCES

Lemij HG (1990), Asymmetrical adaptation of human saccades to anisometropic spectacles, Doctoral Dissertation, Erasmus University of Rotterdam
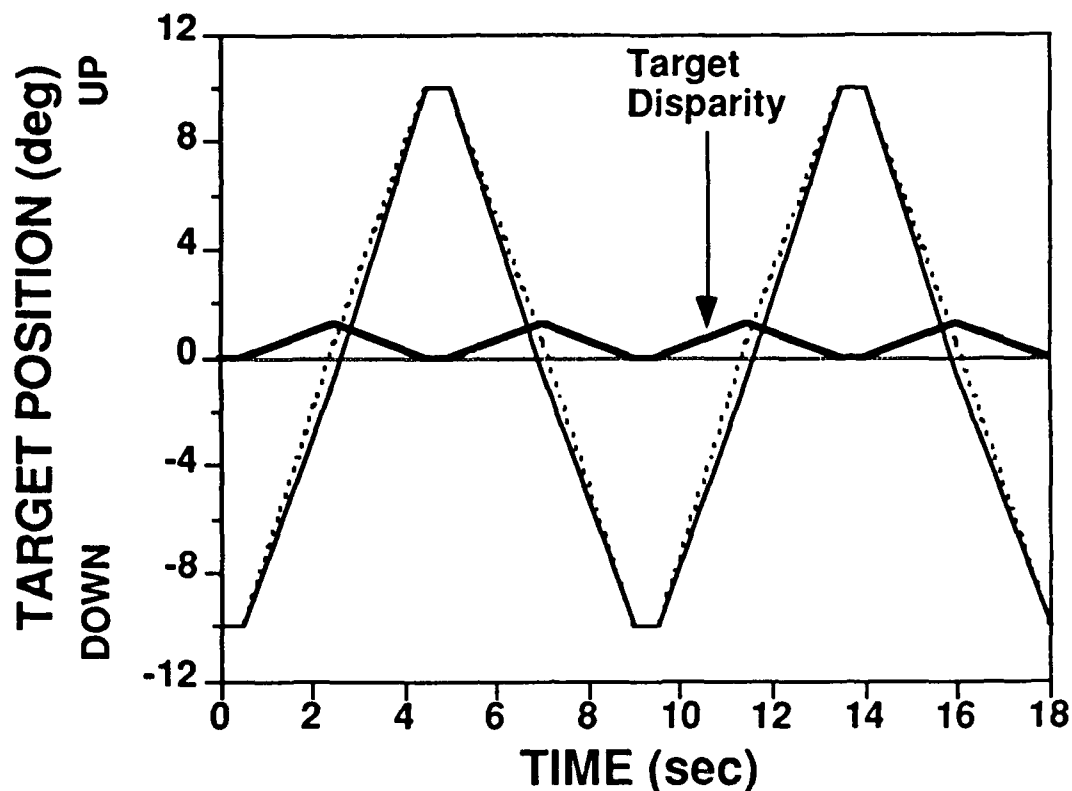
Fig 1. In the _Gaze-specific Paradigm_, right (dotted line) and left (thin line) eyes' targets oscillated along the vertical meridian over the central 20 degrees at an average speed of 5 deg/sec. The targets paused for 0.5 seconds without disparity at the upper and lower extreme positions (up or down 10 degrees). As the targets moved towards the opposite extreme position, target disparity (thick line) increased until it reached a maximum of 1.25 degrees right-hyper at the straight ahead position. Then, as the targets continued to move towards the opposite extreme position, target disparity tapered to zero disparity. Target disparity is equal to the vertical difference between the positions of the right and left eyes' targets (R - L).

Fig 2. _Gaze-specific Paradigm_ Data are plotted separately for subjects BL (fig 2a) and GG (fig 2b).

(Top panel) Gaze-specific adaptive changes in dynamic (open symbols) and static (filled symbols) phorias are separated by direction and plotted relative to right eye gaze position. For dynamic phorias, direction refers to pursuit direction (upward versus downward). For static phorias, direction refers to the direction of the gaze-shifting saccade that immediately preceded the phoria measurement.

(Bottom panel) Directional differences in adaptive phoria change are plotted relative to right eye gaze position. Directional differences in dynamic phoria adaptation (open circles) were quantified by differencing gaze-specific changes in dynamic phoria during upward- and downward-directed pursuit. Similarly, directional differences in static phoria adaptation (filled circles) were quantified by differencing gaze-specific changes in static phoria following upward- and downward-directed saccades.
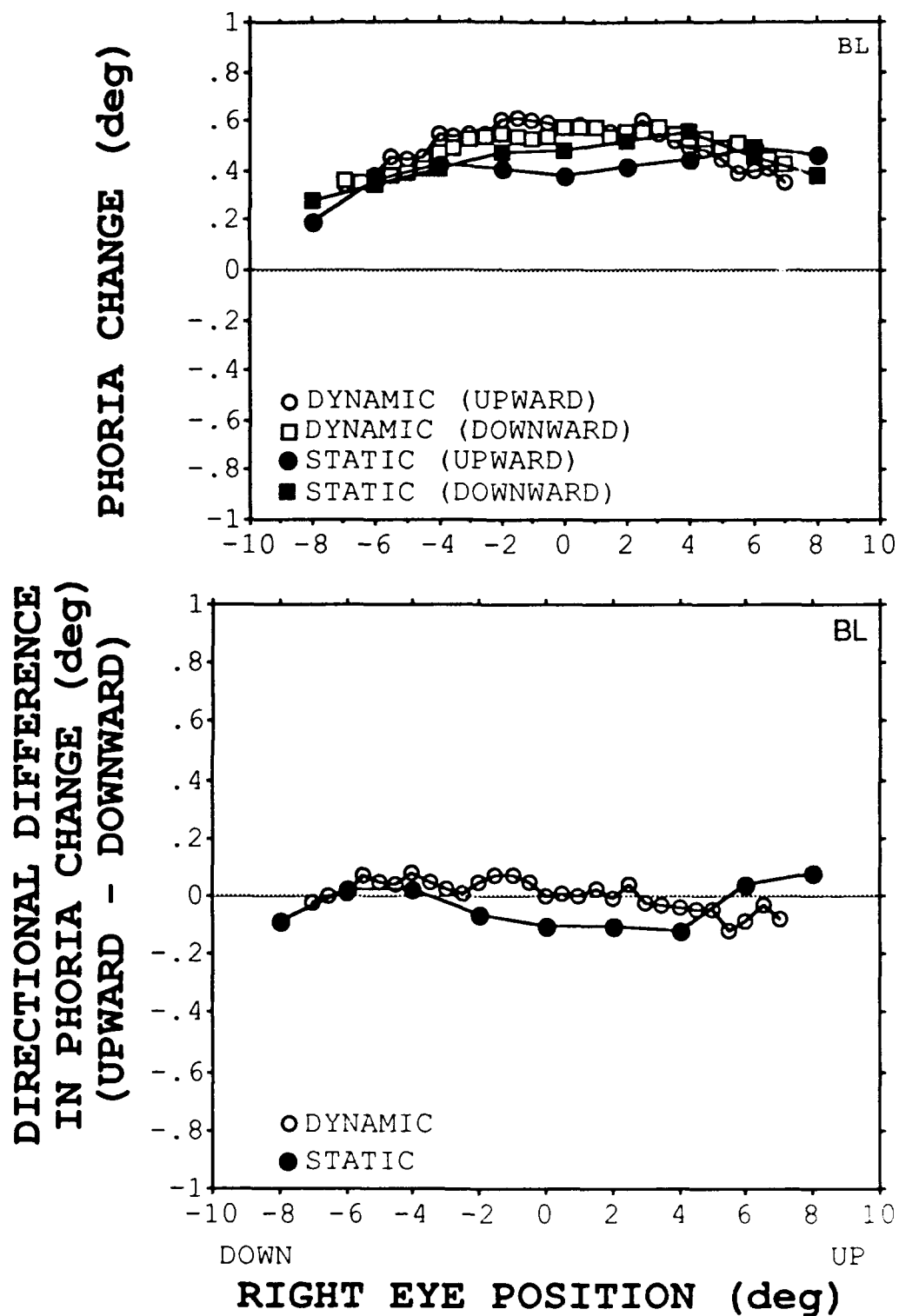
Fig 2a. Gaze-specific Paradigm - Subject BL
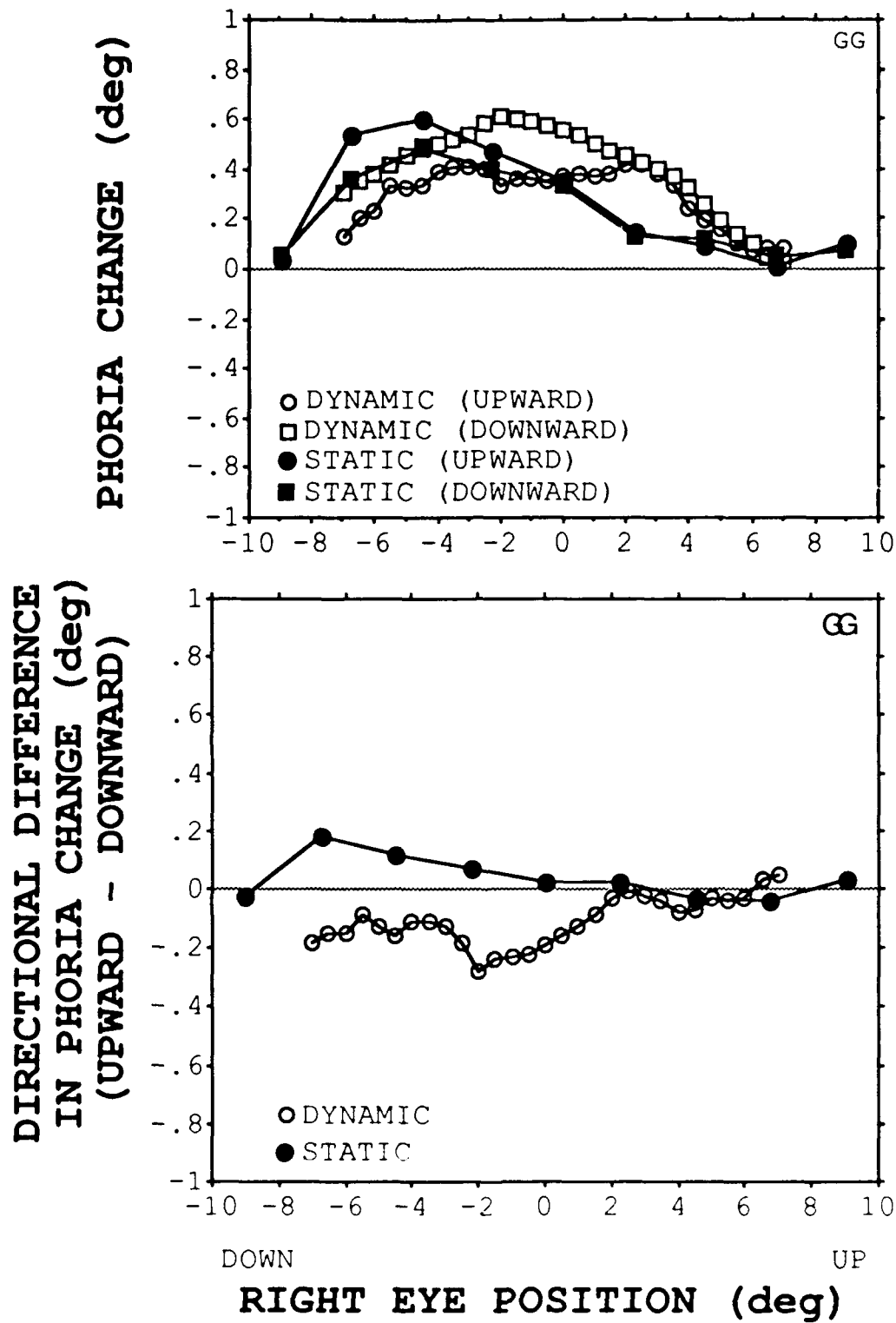
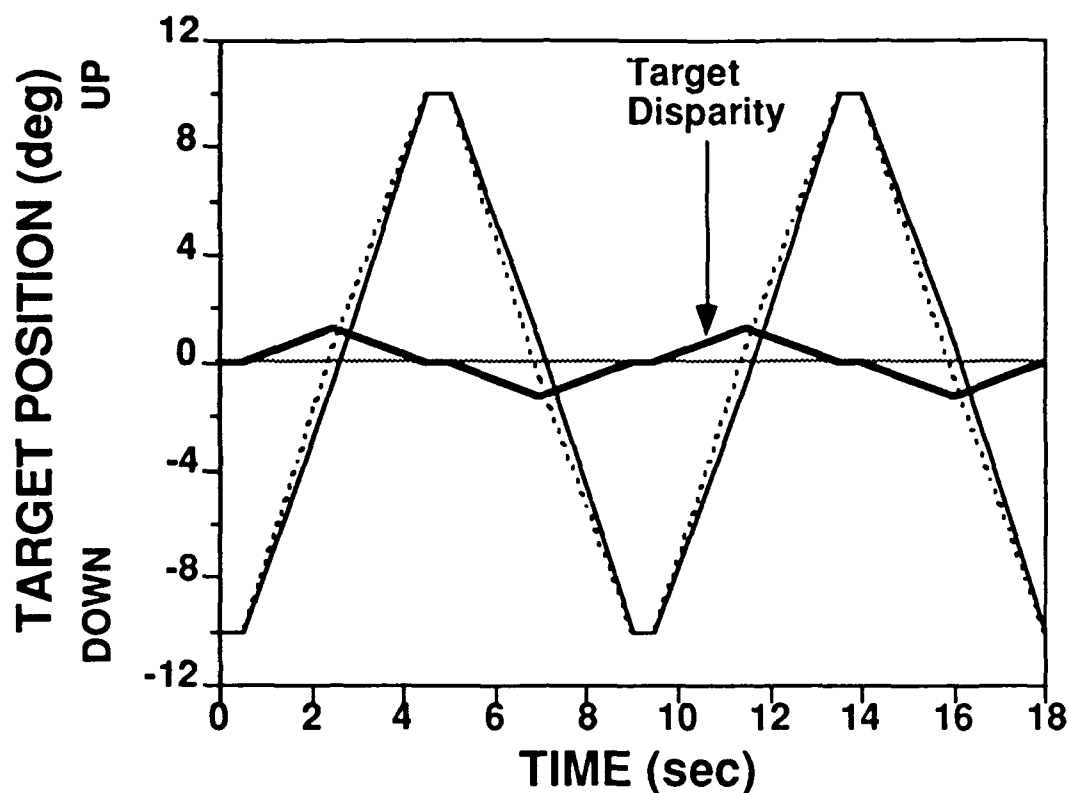**Fig 2b.** Gaze-specific Paradigm – Subject GG

Fig 3. In the <u>Direction-specific Paradigm</u>, right (dotted line) and left (thin line) eyes' targets oscillated along the vertical meridian over the central 20 degrees at an average speed of 5 deg/sec. The targets paused for 0.5 seconds, without disparity, at the upper and lower extreme positions (up or down 10 degrees). As the targets moved towards the opposite extreme position, target disparity (thick line) increased until it reached a maximum at the straight ahead position. Then, as the targets continued to move towards the opposite extreme position, target disparity tapered to zero disparity. During upward target motion the maximum disparity was 1.25 degrees <u>right-hyper</u>. During downward target motion the maximum disparity was 1.25 degrees <u>left-hyper</u>. Target disparity is equal to the vertical difference between the positions of the right and left eyes' targets (R - L).
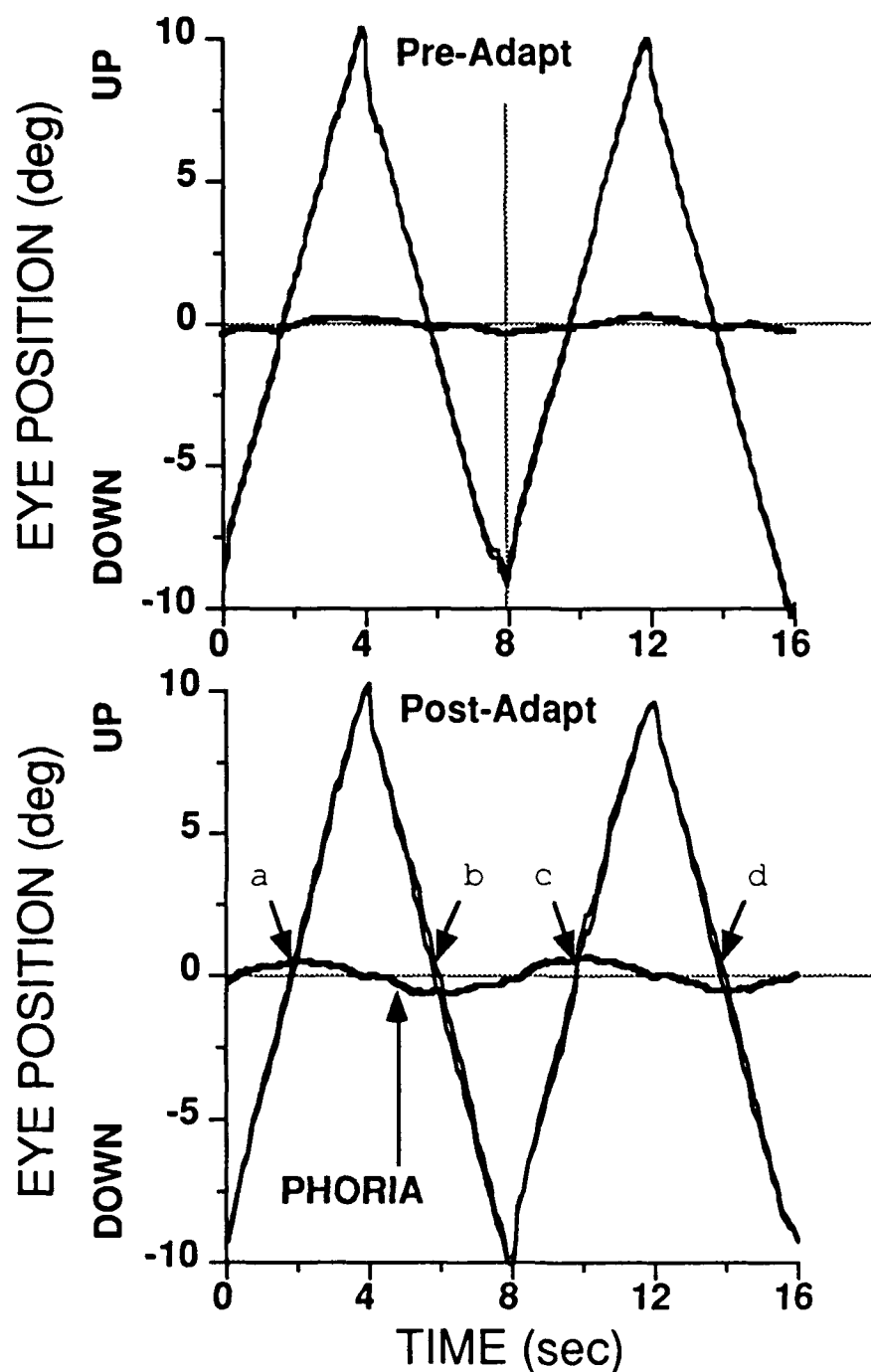
Fig 4. Subject GG's eye position traces (thin lines) are plotted during pre- (top panel) and post- (bottom panel) adaptation pursuit trials (left eye occluded). The phoria trace (thick line) is the difference between right and left eye position (R - L). Four arrows, whose tips indicate a specific gaze position, were added to the lower panel to increase appreciation of direction-specific changes in phoria. (see text for details).

Fig 5. <u>Direction-specific Paradigm</u> Data are plotted separately for subjects BL (fig 5a), GG (fig 5b), and DP (fig 5c).

(Top panel) Gaze-specific adaptive changes in dynamic (open symbols) and static (filled symbols) phorias are separated by direction and plotted relative to right eye gaze position. For dynamic phorias, direction refers to pursuit direction (upward versus downward). For static phorias, direction refers to the direction of the preceding gaze-shifting saccade.

(Bottom panel) Directional differences in adaptive phoria change are plotted relative to right eye gaze position. Directional differences in dynamic phoria adaptation (open circles) were quantified by differencing gaze-specific changes in dynamic phoria during upward- and downward-directed pursuit. Similarly, directional differences in static phoria adaptation (filled circles) were quantified by differencing gaze-specific changes in static phoria following upward- and downward-directed saccades.
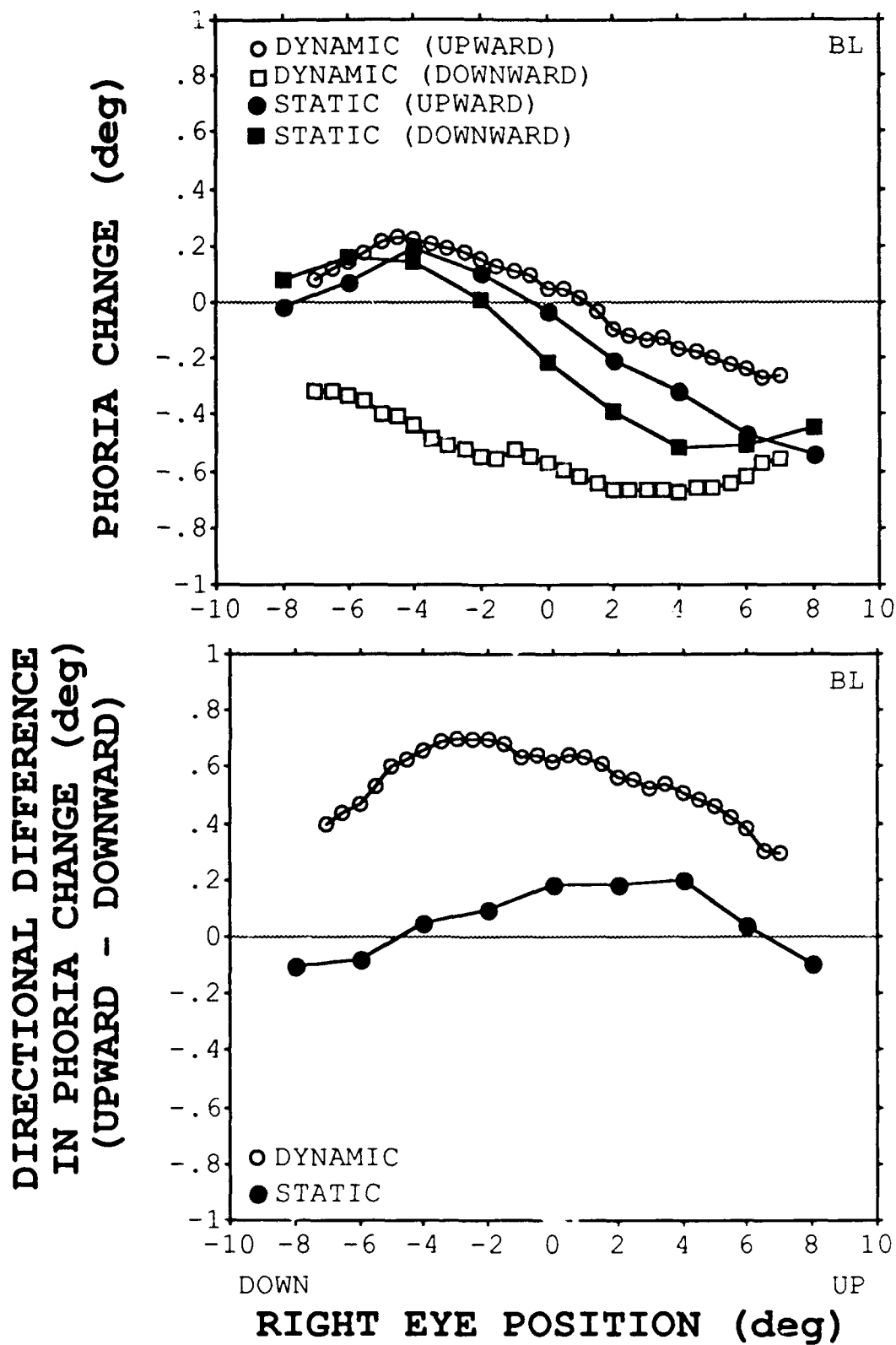
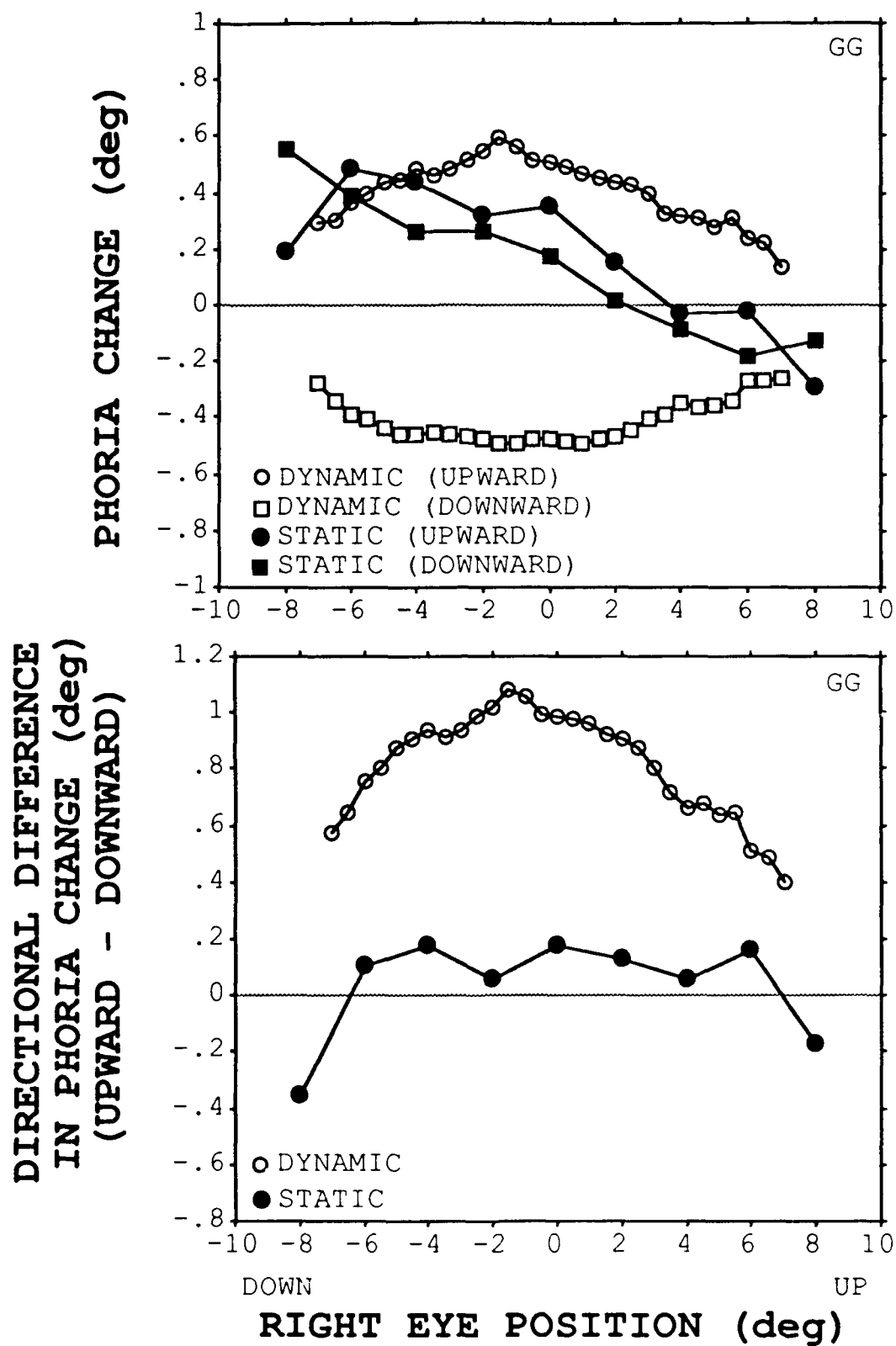**Fig 5a.** Direction-specific Paradigm - Subject BL

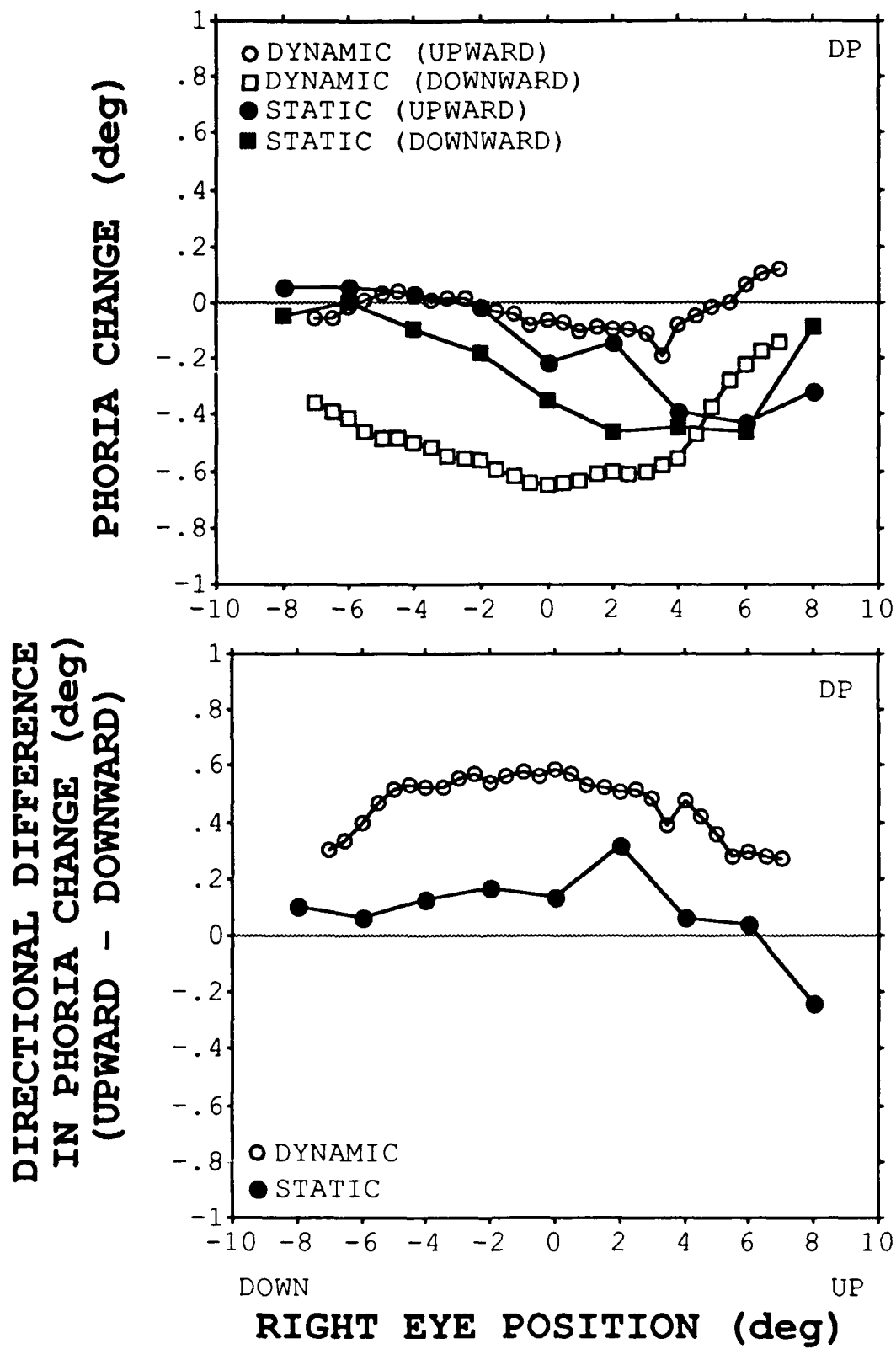**Fig 5b.** Direction-specific Paradigm - Subject GG

Fig 5c. Direction-specific Paradigm - Subject DP

Fig 6. For each subject, adaptive changes due to non-phoria mechanisms are plotted separately for upward (circles) and downward (squares) pursuit. Adaptive changes due to non-phoria mechanisms are calculated by subtracting adaptive changes in gaze-specific static phorias from adaptive changes in gaze-specific dynamic phorias (Additive Hypothesis was assumed; see text for details). Two parallel lines are added to each panel to better illustrate gaze-specific changes.
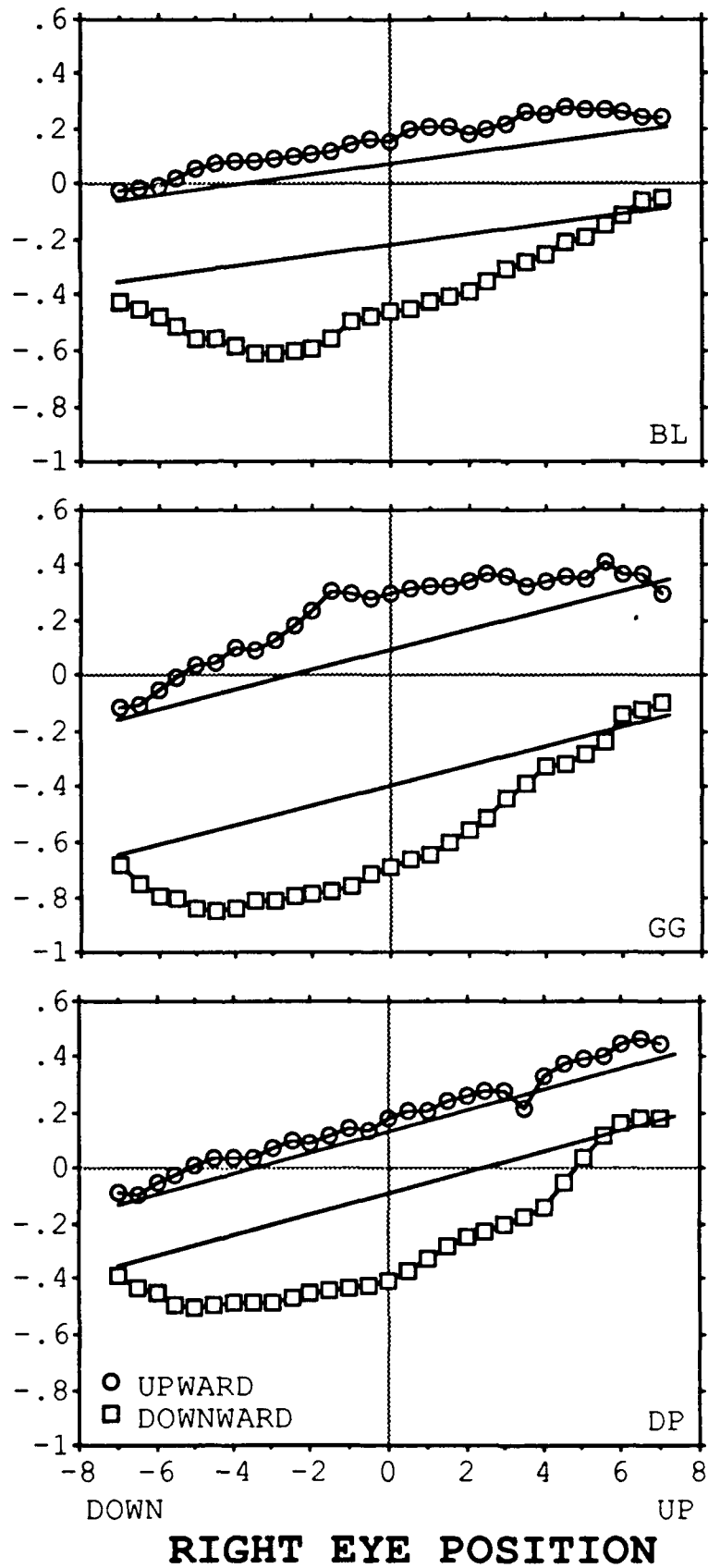
Fig 6.

CHAPTER 6

SPATIAL ASPECTS OF VERTICAL PHORIA ADAPTATION

INTRODUCTION

Normally, the visual axis of an occluded eye remains
within a few degrees of a distant stationary target, that is
visually fixated by the fellow seeing eye. Phoria is the
resulting open-loop (monocular viewing) vergence posture, and
is measured as the occluded eye's angular error of fixation.
By convention, phoria is divided into horizontal and vertical
vector components. In this paper, the term 'phoria' is used
in the traditional sense; in previous chapters, 'phoria' was
termed 'static phoria'.

Horizontal (Hirsch, Alpern, and Schultz (1948), Scobee and
Green (1948)) and vertical (Scobee and Bennet (1950)) phorias
are stable throughout life, presumably due to an adaptive
process. Classically, phoria adaptation has been
demonstrated by placing a weak ophthalmic prism before one
eye while binocularly fixating a distant stationary object.
Placing a prism before one eye creates a single uniform
binocular disparity in all gaze positions, causing the
measured phoria to initially change by an amount equal to the
prism power. However, within a few minutes with the prism
still in place, the measured phoria reduces towards the pre-
prism value, indicating a change in the relative open-loop
alignment of the two eyes (phoria).

Phoria adaptation can vary with (orbitocentric) gaze position. Anisometropic spectacles produce differential optical magnification before the two eyes, thereby producing binocular disparities with amplitudes that vary proportional to gaze position (gradient disparity). Long time anisometropic spectacle wearers have gaze-specific phorias (measured through the spectacles) that are less than would be predicted from optical considerations (Oohira et al (1991),(Ellerbroch and Fry (1942), Ellerbroch (1948), Allen(1974), Oohira et al (1991)). This discrepancy suggests phoria adaptation varies with gaze position proportionally to prismatic gradients caused by magnification. Henson and Dharamshi (1982 a,b) demonstrated gaze-specific phoria adaptation in normal subjects after placing them in a normal work environment for four hours with an optical magnifier before one eye.

Henson and Dharamshi (1982 a,b) reported that when gaze was restricted to a single position while adapting to a vertical binocular disparity (prism), the resulting phoria adaptation was maximum at the gaze position of adaptation. However, there was a graded spread of adaptation to neighboring gaze positions along both the horizontal and vertical meridian. Along the horizontal meridian, the half-height of adaptation was approximately 2 degrees from the gaze position of adaptation (Henson and Dharamshi (1982 a).

Sethi (nee Dharamshi) and Henson (1985) provided additional evidence supporting the concept of graded spread

of phoria adaptation from gaze positions of adaptation.
Subjects were exposed to a gradient disparity (spectacle-
mounted optical magnification before one eye), however,
binocular experience was restricted to gaze positions within
the central 37 degrees. After two hours of adaptation,
phoria adaptation increased with eccentricity (similar to the
disparity stimulus) for those gaze positions that were
binocularly stimulated during the adaptation period.
However, there was a graded (decreasing with further
eccentricity) spread of phoria adaptation into gaze positions
that were not binocularly stimulated during the adaptation
period.

In another study, Sethi and Henson (1984) demonstrated
that vertical phoria adaptation to uniform disparity (prism)
is faster than adaptation to gradient disparity (spectacle-
mounted differential optical magnification). This finding
was illustrated by an example of a subject exhibiting
complete phoria adaptation to (1.1 degrees) vertical prism in
less than 0.5 hours, however, phoria adaptation to (~4%)
vertical gradient disparity was incomplete after 17 hours.
Differences in adaptation rates were explained as a
consequence of the spread of adaptation to neighboring gaze
positions. When binocular disparity is equal for all gaze
positions (prism), spread of adaptation from stimulated gaze
positions assists adaptation at neighboring gaze positions.
In contrast, when binocular disparity varies with gaze
position (e.g. gradient disparity), neighboring gaze

positions, each being stimulated by different amounts of binocular disparity, interfere with each other.

Although never explicitly stated, Henson and Sethi (nee Dharamshi) appear to propose a single mechanism model of phoria adaptation (for review see Sethi (1986)). In this model, gaze-specific phoria adaptation is stimulated by corresponding gaze-specific binocular disparities. However, there is a graded spread of adaptation from stimulated gaze positions to neighboring gaze positions. An <u>adaptive field</u> was defined as the area of gaze positions that are influenced by phoria adaptation at a particular gaze position. A single phoria mechanism responds to both uniform (prism) and non-uniform disparities. In the case of non-uniform binocular disparity (binocular disparity varies with gaze position), the spread of adaptation limits not only the spatial resolution of adaptation, but also limits the speed of adaptation. In this paper, <u>space</u> (spatial) <u>refers to orbital orientation</u> of the seeing eye during phoria measurement.

The vertical spatial spread of vertical phoria adaptation from a single stimulated gaze position has not yet been fully quantified. Also, it is not known whether neighboring adaptive fields interact linearly when they are differentially stimulated. This study examines these two unknowns. In the first experiment (<u>one-point study</u>) of this two-part study, the spread of vertical phoria adaptation from a single stimulated gaze position was examined. The resulting spatial spread of adaptation was more broadly tuned

than what was reported by Henson and Dharamshi (1982b). In the second experiment (two-point study), the spatial interaction of two differentially stimulated adaptive fields was examined. When neighboring adaptive fields are simulated differentially, they interact with each other nonlinearly.

EXPERIMENT 1: ONE-POINT STUDY

METHODS

Subjects

Four subjects participated in this study. Subjects GG and BL were habitually uncorrected myopes with refractive errors less than 0.5 diopters. Subjects CS and DP were two-diopter isotropic myopes. Subject CS normally wore spectacles, however, DP normally wore soft contact lenses. All subjects had stereopsis thresholds of at least 40" arc. Subject GG, the author, was 37 years old. Respectively, subjects BL, DP and CS were 46, 24, and 48 years old; each had an overview knowledge of the study.

Equipment

Binocular vertical eye positions were measured with a SRI dual-Purkinje eye tracker (Crane and Steele (1978)). Voltage analogues, representing independent right and left eye positions, were amplified and then, digitized. Equipment resolution was on the order of a few minutes of arc. Digital resolution exceeded equipment resolution. An EGA graphic

monitor displayed vertical binocular eye position and vergence traces immediately following each trial for on-line inspection by the experimenter. Trials were saved to a hard disk for later off-line analysis.

Target motion was simulated by rotation of vertical-deflecting mirror galvanometers (Crane and Clark (1978)). Unequal target motion before each eye was induced by independent control of mirror galvanometers before each eye. The SRI dual-Purkinje eye tracker's viewing optics allows a 24 degree diameter field of view.

An AT clone computer was used for data acquisition and storage, on-line data display, and control of left and right vertical-deflecting mirror galvanometers. A bite bar and head rest were used to minimize head movement during data trials and adaptation periods

Visual Stimulus

The target (fig 1) consisted of a bright uniformly lit background with an opaque cross, circle, and diamond concentrically superimposed on it. Background illumination was dim (.5 cd/m^2), such that the ambient features of the laboratory were barely visible. Target distance was 160 centimeters.

Because horizontal vergence posture may effect vertical phoria measurements (Verhoeff (1939), Ellerbrock (1948)), horizontal vergence posture was controlled, while leaving vertical vergence posture open-loop, by placing a set of two

vertically-oriented lines within the SRI's viewing optics before each eye (fig 1). These horizontal-fusion locks extended over the entire vertical extent of the visible field.

During data trials, the left eye was prevented from seeing the target by placing a translucent occluder within the SRI's viewing optics, distal to the horizontal-fusion locks. The horizontal-fusion locks were backlighted by the bright stimulus target and therefore, remained visible to both eyes.

Procedures

Pre-Experiment Procedures

Before the start of each experiment, the eye tracker viewing optics were adjusted so that, for each eye, the images of the target and horizontal-fusion locks were set conjugate with optical infinity. For subjects CS and DP, both two-diopter isometropic myopes, a -2.00 D lens was placed before each eye within the SRI viewing optics, conjugate with the normal spectacle plane. Then, the images of the horizontal-fusion lines were placed conjugate with the target images.

Before each experiment, subject's horizontal and vertical phorias were neutralized. (See chapter 3 for details.) Subject's pupils were dilated with one drop of 0.5% tropicamide hydrochloride (Ellis (1977)) in each eye to assist measuring eccentric eye positions by preventing vignetting of the fourth Purkinje image.

Calibration

Each eye was calibrated separately each time a subject entered the eye tracker for data trials. During calibration, the uninvolved eye was occluded. Three hundred milliseconds of digitized (100 Hz) analogue voltages were taken at nine positions, 2.5 degrees apart, spanning the central twenty degrees along the vertical meridian. Gaze positions (degrees) and digitized analogue voltages were fit to a third-order polynomial. The calibration curve was then applied to the calibration data and the results were plotted on an EGA monitor in both graphical and numerical format. The calibration was acceptable if, at each calibration step, the calculated eye position was within 0.1 degrees of the predicted eye position. If the calibration was rejected the procedure was repeated. After a calibration was accepted for each eye the two sets of four polynomial constants were stored to a file to transform data during later off-line analysis. Calibration files were only applied to trials that immediately followed their generation.

Data Trials

Before and after a six minute adaptation period (discussed below), two data trials where conducted. In each trial, the target stepped to one of nine positions in a twenty-one step sequence that spanned the central sixteen degrees along the vertical meridian. The target position sequence is

graphically depicted in figure 2. While the subject monocularly fixated the stationary target at each stimulus position, the experimenter monitored voltages, related to each eye's gaze position, on an oscilloscope and pressed a key when both voltage traces where steady to sample binocular eye positions at 100 Hz for 300 msec. The target then stepped to the next position. The period between target steps was 1.5 to 3 seconds long. A calibration and two static phoria trials took approximately 4 minutes.

After each trial, vertical binocular eye position traces were plotted on an EGA monitor for inspection by the experimenter. The experimenter repeated the trial if severe mechanical artifacts were present (e.g. lost lock on the fourth Purkinje image). Otherwise, the trial was saved to a hard disk for later off-line analysis.

Because subjects were monocularly viewing during data trials (left eye occluded), pre- and post-adaptation changes in ocular motor yoking behavior are attributed to neural re-programming, rather than fusional vergence.

Adapting Stimulus

The lone adapting stimulus was a 1.25 degree right-hyper disparity located 9 degrees in the upper field along the vertical meridian. Because of the relative small measurement range (20 degrees) of the SRI eye tracker, 9 degrees up was chosen as the adapting gaze position in order to maximize the range in which the spread of adaptation could be measured.

During the six-minute adaptation period, subjects were
instructed to maintain fixation on the center of the target's
cross and, using moderate effort, to keep the targets fused.

Data Analysis

Phoria data were analyzed strictly by computer algorithm.
Initially pre- and post-adaptation data were processed
separately. Vertical phorias were calculated as the vertical
difference between right and left eye gaze position (R-L),
and were separated by right eye gaze position. Gaze-specific
phorias from both trials were averaged. Finally, adaptive
changes in gaze-specific phorias were quantified by
differencing pre- and post-adaptation phorias (post-pre).

RESULTS

In the top panel of figure 3, adaptive changes in gaze-
specific phorias are plotted separately for each of the four
subjects. Gaze-specific adaptive changes in phoria were
averaged across subjects and plotted (bold Xs). The large
filled circle near the top right corner of the upper panel
represents the adapting stimulus of 1.25 right-hyper
disparity located 9 degrees above the straight ahead. All
subjects demonstrated a right-hyper shift in phoria.

The spread of adaptation from the adapting gaze position
(9 degrees up) to lower gaze positions was mainly
idiosyncratic. For each subject, the adaptive phoria change
occurring at the adapting gaze position (nine degrees up) was

subtracted from the adaptive phoria change occurring at other gaze positions and then plotted in the lower panel of figure 3. Subject BL (filled squares) demonstrated a flat response. Except for the lowest gaze-position measured, subject CS (open circles) also demonstrated a flat response. However, subject GG (filled circles) demonstrated greater (up to 0.3 degrees) adaptation away from the adaptation gaze position. And in contrast, subject DP demonstrated a reduction of adaptation away from the adaptation gaze position (up to 0.6 degrees). Therefore, only subject DP, behaved as Henson and Dharamshi's (1982b) subjects. The flat, near-zero trace of the averaged data (bold Xs) indicates the averaged adaptive phoria change was not gaze-specific. Therefore, Henson and Dharamshi's hypothesis of a single spatially-tuned phoria adaptation mechanism is not supported by these data.

EXPERIMENT 2: TWO-POINT STUDY

METHODS

Subjects, equipment, general procedures, and initial data analyses were the same as those used in experiment 1 with the following exceptions:

1) Subject DP did not participate.

2) During phoria data trials, the same 21 step sequence (fig 2) was used as in experiment 1 except that

phorias were measured at 2 degree increments in gaze over the central 16 degrees.

Adapting Stimulus

During the 40 minute adaptation period, each 10.5 seconds two vertical disparities were alternately presented. These two gaze-specific disparities were equal in amplitude, but opposite in sign, and their relative location was symmetrical about the straight-ahead along the vertical meridian. The right-hyper disparity was always presented in the upper hemi-field and the left-hyper disparity was always presented in the lower hemi-field.

Each subject sat in 18 different experimental sessions. Amplitude and separation of the two stimulating disparities were unique to each session. Table 1 lists _total_ (peak-to-peak) _stimulus disparity_ amplitudes for each of the 18 conditions. Each experimental condition was determined by the spatial separation of the two adapting disparities (6, 12, and 18 degrees) and by the linear disparity gradient created by the two disparities (4.17% to 25%). For example, in the case of the largest disparity used (lower right corner of table 1), the two adapting disparities were spaced 18 degrees apart and the total stimulus disparity was 4.50 degrees. Therefore, a 2.25 right-hyper disparity was located at 9 degrees up and a 2.25 left-hyper disparity was located at 9 degrees down. This condition created a 25.0% _stimulus disparity gradient_ (4.5/18 = 0.25). For each subject, two to

three experimental sessions were spaced over the course of a
week. The adapting conditions used for a particular session
were pseudo-randomly determined.

STIMULUS DISPARITY GRADIENT	STIMULUS SEPARATION		
	6 deg	12 deg	18 deg
4.17 %	0.25	0.50	0.75
8.33 %	0.50	1.00	1.50
12.50 %	0.75	1.50	2.25
16.67 %	1.00	2.00	3.00
20.83 %	1.25	2.50	3.75
25.00 %	1.50	3.00	4.50

TABLE 1. Total (peak-to-peak) differences (deg) in stimulus
disparities are categorized by the two adapting disparities'
spatial separation and their resulting disparity gradient.

During the adaptation period, subjects binocularly viewed
a disparate target at a particular gaze position for ten
seconds. Then, the left eye's target was blanked (by extreme
rotation of the left vertical-deflecting mirror
galvanometer), followed by the right eye's target stepping to
the fellow adapting position. Five hundred milliseconds
later, the left eye's target would be be presented at its new
position, creating the new disparity. Then, the cycle would
repeat. Gaze-shifting saccades were stimulated monocularly
to prevent nonconjugate adaptation of the saccadic pulse
(chapters 2 and 3).

Subjects were instructed to maintain fixation on the
center of the target's cross and, using moderate effort, to
keep the targets fused. Subjects were also instructed to

close one or both eyes if they sat away from the eye tracker. During an individual's adaptation period, accumulative time away from the task was less than 1 minute.

RESULTS

Subjective Reports During the Adaptation Period

All subjects could sensorially fuse (when possible) the disparate targets faster after a shift in fixation (and disparity) at the end of the adaptation period, as compared to the beginning. Subjects reported that fusion of the disparate targets was easier (faster, less effort) when the stimulus disparities were smaller and/or more widely separated. However, the amount of adaptation manifested could not be reliably predicted from these subjective reports, especially for narrow stimulus separations. In these cases, subjects usually felt they were fully adapted at the end of the adaptation period because they saw no, or brief, diplopia. However, the measured phoria change was usually relatively small.

During the adaptation period, all subjects reported they could not sense the stimulus disparity when the total stimulus disparity was less than 0.5 degrees. For the largest stimulus disparity (4.5 degrees), subject GG could only fuse the lower target (within the ten second exposure interval) at the end of the adaptation period, but could fuse both targets (within the ten second interval) at the end of the adaptation period for all other experimental conditions.

Subjects BL and CS could not fuse either target when the total stimulus disparity was greater than 3 degrees, but could fuse both targets at the end of the adaptation period for all other experimental conditions.

Adaptive Change in Gaze-Specific Phorias as a Function of Stimulus Separation

For each experimental condition, all subjects demonstrated adaptive change in gaze-specific phorias, including when the stimulus disparity was too small to be perceptually detected and when the stimulus disparity was too large to be fused.

As in experiment 1, adaptive changes were calculated by differenceing pre- and post-adaptation gaze-specific phorias. As an example, figure 4 plots one subject's adaptive change in phorias for three experimental conditions: stimulus separation was varied (6, 12, or 18 degrees) while total stimulus disparity was held constant (2 degrees). (Two of these parameters are different than what is used in this study, however, these data were obtained under the same experimental protocol used in this study and are typical of this study's data.)

Adaptive changes in gaze-specific phoria for all three subjects was manifest as an approximate linear interpolation between the two stimulated gaze positions. Figure 4 illustrates this interpolation for one subject as a linear gradient change over the central 12 degrees for each plotted line. For larger stimulus separations the response peaked at

adapted gaze positions, and declined at larger separations.

For small stimulus separations (6 degrees), there was a

limited extrapolation of the gradient response beyond the

adapted gaze positions that was evident for all subjects. In

figure 4 (circles), the gradient shift in phoria adaptation

can be seen to extend beyond the central 6 degrees.

When stimulus separation was 6 degrees and stimulus

disparity was less than 0.75 degrees, the change in phoria

was not always gradient-like. For example, adaptive phoria

changes may have occurred in one hemi-field, but not the

other.

Effectivity of Vertical Phoria Adaptation

As a method of data reduction, only the response gradient,

i.e. the linear rate of phoria change occurring over the

central 12 degrees, was considered in subsequent analyses.

The response gradient was calculated by dividing the response

amplitude (the difference in adaptive changes in phoria that

occurred at up and down 6 degrees) by the 12-degree

separation (fig 5). This method of analysis is justified

because in nearly all cases the adaptive change in phoria

manifested as gradient-like over the central 12 degrees

(discussed above). Stimulus gradient was defined as the

linear rate of disparity change induced by the adapting

stimulus, and is calculated by dividing the total stimulus

amplitude by the stimulus separation (fig 5).   Effectivity

(of vertical phoria adaptation) was defined as the ratio of

response gradient to stimulus gradient. Effectivity is

analogous to a system's gain (ratio of output to input).

STIMULUS DISPARITY GRADIENT	STIMULUS SEPARATION (deg)		
	6	12	18
4.17%	BL .22 CS .25 GG .22	BL .42 CS .40 GG .35	BL .45 CS .55 GG .45
8.33%	BL .53 CS .22 GG .37	BL .40 CS .83 GG .60	BL .85 CS .46 GG .82
12.50%	BL .49 CS .53 GG .45	BL .95 CS .80 GG .47	BL .67 CS .66 GG 1.30
16.67%	BL .87 CS .65 GG .43	BL .60 CS .81 GG .97	BL .83 CS 1.08 GG 1.06
20.83%	BL .98 CS .49 GG .54	BL 1.00 CS .88 GG .80	BL 1.09 CS .92 GG .73
25.00%	BL .85 CS .55 GG .47	BL .75 CS .99 GG .70	BL .93 CS .86 GG .85

TABLE 2. Response Amplitudes for each subject and experimental condition. Response amplitudes were calculated by subtracting the adaptive change (post - pre) in phoria that occurred at 6 degrees down from the adaptive change that occurred at 6 degrees up.

For each subject and experimental condition, response

amplitudes are listed in table 2.   In order to reduce the

effect of day-to-day variation, data from all subjects were

averaged together (within each square of table 2) in

subsequent analyses.

For each stimulus separations, response gradients are

plotted against total stimulus disparity (fig 6, top panel).

With increasing total stimulus disparity, response gradients

increase up to a point, that is peculiar to each stimulus

separation, and then decline. Interestingly, while response

gradient and total stimulus disparity are increasing

together, data from all three separations fall close to a

common curve. When the same response gradients are plotted

against stimulus gradient (fig 6, bottom panel), all three

curves peak at a stimulus gradient of approximately 18%,

indicating that stimulus gradient is a meaningful parameter.

For each stimulus separation, effectivity is plotted

against stimulus gradient in figure 7. Effectivity decreases

linearly ($r^2 > 0.95$ in each case) with stimulus gradient,

indicating that as the stimulus gradient increases, vertical

phoria adaptation mechanisms respond less effectively. This

linear relationship is described by the following equation:

$$E = I - (S * D) \tag{1}$$

where E, I, S, and D represents effectivity, y-intercept,

slope, and stimulus disparity gradient, respectively. By

definition, effectivity is equal to the ratio of response

gradient to stimulus gradient.

$$E = \frac{R}{D} \tag{2}$$

R represents the response gradient. Combining the above two

equations results in the following equation:

$$\frac{R}{D} = I - (S * D) \qquad\qquad (3)$$

Finally by multiplying both sides of equation 3 by D, the equation that defines the response gradient curves seen in figure 6 (bottom panel).

$$R = (\underline{I * D}) - (\underline{S * D^2}) \qquad\qquad (4)$$

Both equations 1 and 4 are made up of two components (emphasized by underlining). The first component depends on I and is related to the spatial spread of adaptation. The second component depends on S and is related to the gradient decline of effectivity relative to the stimulus gradient. The significance of these two components is discussed more fully below.

DISCUSSION

Observations Consistent with the Spatial-Spread Model

Henson and Sethi (1982a) proposed that phoria adaptation spreads over limited adaptive fields (discussed above). Because neighboring adaptive fields overlap each other, when phoria adaptation is differentially stimulated at multiple gaze positions, phoria adaptation at a particular gaze position is equal to the weighted sum of output from all

adaptive fields involved at that particular gaze position (Sethi (1986)).

This spatial-spread model of phoria adaptation can be simulated by representing a gaze-specific disparity as a delta function whose area is equal to the stimulus disparity amplitude, and by representing the adaptive field's spatial spread function as a Gaussian function with a peak height of one. The adaptive change in gaze-specific phoria can be derived by convolving scaled delta functions (gaze-specific disparities) with the Gaussian (spread) function.

In this manner, two (two-point study) experimental conditions were simulated by the spatial spread model, and their results are illustrated in figure 8. Total stimulus disparity was 1.5 degrees and stimulus separation was either 6 degrees (top panel) or 18 degrees (bottom panel). The size and location of the stimulus disparities are represented by two filled circles in each panel. A Gaussian function with a sigma (σ) of 10 degrees was used because it resulted in the closest simulation of the data in figure 4. These simulations contain two features that agree with the results of this study (compare to fig 4). First, there is an approximate linear interpolation of phoria change between the two stimulated gaze positions. Second, for narrow stimulus separations, there is a limited extrapolation of the gradient-like phoria change beyond the stimulated gaze positions.

Observations Not Consistent with the Spatial-Spread Model

The spatial-spread model can not explain other aspects of the data. Using the spatial-spread model ($\sigma = 10$ degrees), each (two-point study) experimental condition was simulated, and the resulting effectivities (top panel) and response gradients (bottom panel) were plotted relative to stimulus gradient in figure 9. The spatial-spread model predicts that effectivity varies as a function of stimulus separation, but not as a function of stimulus gradient.

Effectivity varies as a function of stimulus separation due to the graded spread of adaptation. When two antagonistically stimulated adaptive fields are close to each other, they mutually cancels each other. This mutual cancellation results in a diminished response amplitude, therefore a diminished response gradient, and finally, diminished effectivity. Because the spread of adaptation is graded, as stimulus separation increases, mutual cancellation decreases, resulting in larger response amplitudes, and ultimately larger effectivities.

The spatial-spread model also predicts that effectivity is independent of stimulus gradient. This can is best explained with an example. For a given stimulus separation, the total stimulus disparity must be doubled to produce a doubling of the stimulus gradient. The convolution model of spatial spread predicts that doubling the input, simply doubles the output (scaling). Accordingly, this results in a doubling of the response amplitude at all gaze positions, and in a

doubling of the response gradient. Since, both stimulus and response gradients were doubled, their ratio (effectivity) remains unchanged. The effect of spatial spread of phoria adaptation on effectivity is described by the y-intercept (I) in equation 1.

Counter to these predictions (fig 9, top panel) there is a linear decline of effectivity, relative to stimulus gradient, that is seen in the data (fig 7). This linear decline is represented in the slope (S) of equation 1. It is unlikely the decline of effectivity seen in the data (fig 7) was due to saturation of fusional mechanisms which are thought to drive phoria adaptation (Schor (1979)), because even when total stimulus disparity was relatively small (less than 2 degrees) and sensory fusion was relatively easy, a decline of effectivity was still observed.

The bottom panel in figure 9 plots predicted response gradients of the spatial-spread model relative to stimulus gradient. The spatial-spread model predicts a positive linear relationship between response gradient and stimulus gradient, that is described by the first component of equation 4 (R = (I * D)). For a given Gaussian σ, the slope in the bottom panel of figure 9 is equal to the y-intercept (I) of the effectivity plot and is determined by stimulus separation.

In figure 10 (top panel), for a stimulus separation of 18 degrees, differences between response gradients predicted by the spatial-spread model (σ = 10 degrees) are graphically

contrasted with a smooth curve that closely resembles the experimental data in figure 6 (triangles in bottom panel). According to the spatial-spread model, the response gradient increases linearly with the stimulus gradient (slope = I). In reality, as the stimulus gradient increases, the response gradient increases at a decelerating rate and eventually rolls-off at a stimulus disparity gradient of ~18%. The difference between predicted and experimental measures of response gradients are depicted by the gray areas in figure 10. The amplitude of the response gradient lag (gray area) is proportional to the stimulus gradient squared and is described by the second component of equation 4 (response gradient lag = $S * D^2$).

The simulated data in the top panel of figure 10 are replotted in the bottom panel as response effectivity to illustrate the linear reduction of effectivity predicted by equation 1. The effectivity lag (gray area) is proportional to the stimulus gradient and is described by the second component of equation 1 (effectivity lag = $S * D$).

Spatial-Spread and Gradient-Limited Model

A model was constructed that incorporated the spatial-spread model, but added another parameter to account for the linear decrease in effectivity associated with stimulus gradient. Parameters used in this model were determined through a series of steps.

The first step determined the standard deviation (σ) of a
single Gaussian function, which was assumed to represent the
graded spread of adaptation within all adaptive fields.
There was a small range of sigmas that could approximate the
results. The sigma that best predicted the 18-degree
separation data was arbitrarily chosen because its y-
intercept in figure 7 was approximately 1. Applying the
spatial-spread model, it was determined that a Gaussian
function with a standard deviation of 9.25 degrees (peak
height = 1) produced an effectivity equal to 1.02 (i.e. the
effectivity y-intercept for 18-degree separation data in
figure 7).

As illustrated in the top panel of figure 9, a reduction
of the y-intercept is predicted with decreasing target
separation. The experimental measures of y-intercept in
figure 7 verifies this prediction. However, the reduction of
the y-intercept predicted by a single Gaussian function (fig
9, top panel) was greater for small target separations than
for empirically determined y-intercepts (fig 7).
Accordingly, in the second step, the maximum height of the
Gaussian function was modulated independently for each
stimulus separation, such that resulting effectivity plots
would yield the same y-intercepts as the experimental data
(fig 7). Gaussian function heights were set to 2.95, 1.44
and 1.00 for stimulus separations of 6, 12, and 18 degree,
respectively. Increasing the Gaussian function's height is
akin to exerting greater effort of motor fusion in response

to closely-spaced disparate targets, which theoretically
would result in a greater phoria adaptation response (Schor
(1979)).

Finally, an _effectivity scaling factor_ was calculated. In
the current (mathematical) model, the resulting effectivity
was first calculated using the spatial-spread model. Then,
response amplitude (and therefore, response gradient and
effectivity) was reduced at all gaze positions proportional
to stimulus gradient (D) by the following scaling function
(G):

$$G = 1 - (K * D) \tag{5}$$

where K represents the effectivity scaling factor. Since the
effectivity plot's y-intercept (I) represents the maximum
effectivity obtainable with a given Gaussian function (and
stimulus separation), the following equation can be deduced:

$$E = I * (1 - (K * D)) \tag{6}$$

which can be expanded to:

$$E = I - ((\underline{I * K}) * D) \tag{7}$$

and contrasted with equation 1:

$$E = I - (\underline{S} * D) \tag{1}$$

After removing similar terms from equations 7 an 1, the following equation remains:

$$S = I * K \tag{8}$$

Solving for K, results in:

$$K = S / I \tag{9}$$

The effectivity scaling factor (K) is equal to the ratio of the slope and y-intercept of the effectivity regression lines in figures 7 and 11. Table 3 lists the effectivity scaling factor for each stimulus separation. The average effectivity scaling factor was 2.78.

STIMULUS SEPARATION	6 deg	12 deg	18 deg
SLOPE	-1.07	-2.32	-3.09
INTERCEPT	0.48	0.82	1.02
SCALING FACTOR	2.23	2.83	3.30

TABLE 3. Slope and intercept of regression lines in figure 7 are listed separately for each stimulus separation. Effectivity scaling factors, calculated as the ratio of slope to intercept, are also listed.

A spatial-spread gradient-limited model of vertical phoria adaptation was devised with the following parameters. The spatial spread of adaptation was described by a single 9.25-degree Gaussian function, effectivity was decreased

proportional to the stimulus gradient by a factor of (1 -
(2.78 * Stimulus Gradient)), and finally, the amplitude of
t Gaussian was given separate parameters for each stimulus
separation (3.30, 1.44 and 1.00 for the 6, 12, and 18 degree
separations.) Figures 11 and 12 illustrates the models'
predictions for effectivities and response gradients.
Figures 11 and 12 should be contrasted with figures 6 and 7
(actual data). Although the predicted data makes a
reasonable match with the actual data, the low number of
subjects involved in this study precludes making serious
quantitative predictions. This study's main conclusion is
that the vertical spatial spread of adaptation is
insufficient to fully describe vertical gaze-specific phoria
adaptation. A linear decline of effectivity with increasing
gradient disparity is also required.

The spatial-spread gradient-limit model predicts an upper
disparity gradient limit, above which vertical phoria
adaptation mechanisms do not respond. In figure 12, all
three lines converge to zero effectivity (x-intercept) at a
stimulus disparity gradient of 0.36. Therefore, local
vertical phoria mechanisms can not respond to two disparities
if their relative difference in amplitude is greater than 1/3
of their separation. The upper gradient disparity limit is
equal to the reciprocal of the effectivity scaling factor (K)
$\left(\frac{1}{K} = \frac{1}{2.78} = 0.36\right)$.

Implications For Noncomitant Strabismus

Zee et al (1984) suggested a method to evaluate and monitor strabismic patients using the Lancaster red-green test. During the Lancaster red-green test, binocular vision is dissociated by placing a green filter before one eye and a red filter before the other eye. Then in a darken room, the experimenter shines a green light on a screen. The patient fixates the green light on the screen, which only the eye with the green filter in front is able to see. The patient then attempts to point a hand-held red light, seen only by the fellow eye, at the green light on the screen. However, assuming normal retinal correspondence, the patient will point the red light in the direction the fovea of the eye with the red filter in front is pointing. Using this technique, the degree of strabismus, or phoria, can be measured at different gaze elevations. By graphing the position of one eye relative to the other, attributes of strabismus, or phoria, can be determined. For example, if the deviation is concomitant, then the slope of the plot equals one. However, if the deviation is non-concomitant, then the slope will not equal one. The data from this study suggests that, for _vertical_ deviations, if the slope is less than 0.64 (1 - 0.36), or greater than 1.36, then gaze-specific vertical phoria adaptation can not occur.

Persistence of Phoria Adaptation

Each subject sat for 18 experimental sessions at a rate of 2 - 3 sessions per week. In the beginning of the study, all subjects exhibited pre-adaptation phorias of uniform amplitude over all measured gaze positions. However, after approximately two weeks, all subjects started to exhibit pre-adaptation phorias that were more right-hyper in the upper field of gaze and more left-hyper in the lower of gaze, similar to the adapting stimuli. In another week, this pre-adaptation phoria bias became larger. For example, one subject (GG) became 0.7 degrees more right-hyper at 6 degrees up relative to 6 degrees down (a phoria gradient of approximately 6%).

On non-experiment days, two subjects began "de-adapting" by adapting to a stimulus disparity gradient, whose sign was opposite to that used in experimental sessions. (The parameters of the de-adapting stimulus were 12-degree stimulus separation, 2-degree total stimulus disparity, and 10 minutes duration). In 2-3 days, these subjects lost their pre-adaptation phoria bias. The third subject (GG) did not "de-adapt", but submitted to phoria measurements twice a week, without subsequent adaptation. His phoria bias ebbed back to normal over a 2.5 week period. Why 1.5-2 hours of phoria adaptation per week was not compensated by phoria adaptation to normal binocular disparities during the remainder of the week is not known. Perhaps phoria is

determined by antagonistic mechanisms, and a strengthening of
one mechanism due to practice results in a competitive
imbalance between the two opposing mechanisms.

Adaptation Without Fusion

A puzzling aspect of this investigation is that adaptive
changes in gaze-specific phoria occurred in response to large
disparities that could not be completely fused. Sethi and
North (1987) reported two of four subjects who could not fuse
3.4 degrees of vertical prism within a 3.5 minute period,
still demonstrated phoria adaptation.

Phoria adaptation is thought to be driven by motor fusion.
During adaptation with the largest disparity in the two-point
study, all three subjects reported that there was a small
decrease in diplopic separation during the 10-second exposure
periods. During this most-difficult adaptation period,
object eye position recordings were taken on one subject
(GG). Subject GG made substained, but incomplete vertical
fusional movements when the target was in the lower field
(left-hyper disparity) of ~0.75 degrees. However, when the
target was in the upper field (right-hyper disparity),
subject GG's vertical vergence posture merely returned to its
pre-adaptation phoria value.

Similar horizontal disparity vergence movements were
observed in response to nonfusible disparate targets of
dissimilar shape, or with compound vertical disparity
(Westheimer and Mitchell (1969), Mitchell (1970)). The three

subjective observations and one objective recording suggest
small incomplete motor fusional responses occurred, and were
apparently adequate to stimulate a small amount of gaze-
specific phoria adaptation.

Global and Local Verical Phoria Mechanisms

Henson and Dharamshi (1982 a,b) proposed a single spatial-
spread mechanism for vertical phoria adaptation that
responded to both uniformly and nonuniformly distributed
disparity. Such a model requires a graded spread of
adaptation from stimulated gaze positions. Henson and
Dharamshi's (1982a,b) original study reported that when
vertical prism adaptation was limited to a single gaze
position, the resulting phoria adaptation was maximum at the
stimulated gaze position and there was a graded spread of
adaptation to neighboring gaze positions along both the
horizontal and vertical meridian. In experiment 1, this
study observed that the vertical spread of phoria adaptation
from a single stimulated gaze position was idiosyncratic, and
on average, its spread does not appear to be spatially tuned
over a 20 degree range.

Also, other observations from previous chapters in this
dissertation, do not support a single-mechanism model of
vertical phoria adaptation. In three experiments, presented
in chapters 2 and 3, subjects adapted to 10 gradient
disparities that were presented, depending on the experiment,
primarily during either saccade, pursuit, or steady fixation

eye movements. In all cases, subjects reported, within a few minutes of the start of the adaptation period, that diplopia suddenly abated in one "easy" hemi-field with a concurrent increase in diplopic separation in the opposite "difficult" hemi-field. For each subject, the easy hemi-field depended on the disparity stimulus (right- versus left-hyper) and not the hemi-field itself (upper versus lower). Resolution of diplopia in the difficult hemi-field took considerably longer (0.5 to 2 hours depending on subject and experiment). The most eccentric gaze position (largest disparity) in the "difficult" hemi-field was the last position to be fused. These observations are not consistent with Henson and Dharamshi's proposed series of overlapping (orbitocentric) gaze-specific adaptive fields. First, it is unlikely that multiple independent adaptive fields would all have the same phoria bias, which is needed to generate the observed initial rapid broadly-tuned phoria shift. Second, because adaptive fields have a graded spread, the most extreme position in the "difficult" hemi-field would not be expected to be the last position fused since it is furthermost from the dominant adaptive fields.

These observations are more easily reconciled by separate global and local vertical phoria adaptation mechanisms. The global mechanism has a rapid onset and its effect generalizes over all orbitocentric gaze positions. The local phoria mechanism has a slower onset, consists of gaze-specific adaptive fields within which there is a graded spread of

adaptation, and its ability to respond is limited by the stimulus disparity gradient.

The orientation of each eye in its orbit is determined by a balance of forces exerted by roughly-opposing extraocular muscles. When an extraocular muscle of one eye is compromised by neuro-muscular paresis, the balance of forces that determine eye position is disturbed in all gaze positions, not just in the gaze positions where the paretic muscle is the agonist (on-direction). Therefore, binocular balance is disturbed in all gaze positions. However, the resulting binocular imbalance is not equal in all gaze positions (noncomitant). The binocular imbalance is greatest in the paretic muscle's on-direction and least in the paretic muscle's off-direction. For example, if the left superior rectus acquired a minor paresis, in up-gaze a right-hyper strabismus may manifest. However, in down-gaze a smaller right-hyper strabismus, or right-hyper phoria, may manifest.

The purpose of the global phoria mechanism is to rapidly compensate for the average shift in right-hyper deviation, thereby rapidly restoring at least part of the field to single binocular vision (e.g. lower hemifield in this example). This mechanism will minimize the most extreme deviation by nulling the average vergence error of the non-comitant deviation. The consequence of the global mechanism is to reduce the absolute size of the gaze-specific disparity stimulus for which the local mechanisms must respond to. This rapid response occurs in minutes and is followed by the

slower local phoria mechanism that makes gaze-specific adjustments to compensate for the remaining noncomitant binocular deviations which by definition vary across the orbital field. This local process is likely to be responsible for the sparse clinical reports of the "spread of comitance" in which the ocular deviation becomes more uniform across the orbital field (Zee and Optican (1985)). The degree of adaptation to this non-uniform deviation is limited by both the spatial resolution limit and gradient limit of the local adaptation mechanism. Most noncomitant deviations exceed the limits of these two components and are not corrected by the local mechanism, even after the overall deviation has been reduced by the global process.

The small limits of disparity to which the local vertical phoria mechanism responds, suggests that it mainly functions to compensate for gradual developmental and senile changes in the oculomotor system (i.e. size of the orbit, distribution and proportion of intraorbital contents, normal neuro-muscular attrition). These changes are likely to be gradual in onset and specific to a region of gaze positions. In addition, the local mechanism compensates for normal developmental growth factors such as widening of the interpupillary distance (IPD) which introduces vertical disparities in eccentric targets viewed above and below the horizon or visual plane. At near distances within arm's reach, these disparities are quite large (Tyler 1983) and require preprogrammed vergence movements of the eyes for

fusion. Because the IPD increases gradually with age, there is ample time for the local mechanism to adapt to these developmental changes and maintain single binocular vision in all directions of gaze.

REFERENCES

Allen DC (1974), Vertical prism adaptation in anisometropes, Am. J. Optom. Physiol. Opt. 51:252

Crane H and Clark M (1978), Three dimensional visual stimulus deflector, Applied Optics 17:706

Crane H and Steele C (1978), Accurate three dimensional eye tracker, Applied Optics 17:691

Ellerbrock V and Fry GA (1942), Effects induced by anisometropic corrections, Am. J. Optom. and Arch. Am. Acad. Optom. 19:444

Ellerbrock VJ (1948), Further study of effects induced by anisometropic corrections, Am. J. Optom. and Arch. Am. Acad. Optom. 25:430

Ellis PP (1977), Ocular therapeutics and pharmacology, 5th Edition, Mosby Company:Saint Louis

Henson DB and Dharamshi BG (1982a), Oculomotor adaptation to induced heterophoria and anisometropia, Invest. Ophthalmol. Vis. Sci. 22:234

Henson DB and Dharamshi BG (1982b), Binocular oculomotor adaptation to induced incomitant deviations, In Functional basis of ocular motility disorders, Lennerstrand, Zee, and Keller (Eds.), Pergamon Press: Oxford, pages 229 - 231

Hirsch MJ, Alpern M, and Shultz HL (1948), The variation of phoria with age, Am. J. Optom. and Arch. Am. Acad. Optom. 25:535

Mitchell DE (1970), Properties of stimuli eliciting vergence eye movements and stereopsis, Vision Res. 10:145

Oohira H, Zee DS, and Guyton DL (1991a), Disconjugate adaptation to long-standing, large-amplitude spectacle-corrected anisometropia, Invest. Ophthalmol. Vis. Sci. 32:1693

Schor CM (1979), The relationship between fusional vergence eye movements and fixation disparity, Vision Res. 19:1359

Scobee RG and Bennet EA (1950), Hyperphoria, a statistical study, Arch. Ophthalmol. 43:458

Scobee RG and Green EL (1948), Relationships of laterial heteophoria, Am, J. Ophth. 31:427

Sethi B (1986), Vergence adaptation: a review, Doc. Ophthal. 63:247

Sethi (nee Dharamshi) B and Henson DB (1984), Adaptive changes with prolonged effect of comitant and noncomitant vergence disparities, Am. J. Optom. Physiol. Opt. 61:506

Sethi (nee Dharamshi) B and Henson DB (1985), Vergence-adaptive change with a prism-induced noncomitant disparity, Am. J. Optom. Physiol. Opt. 62:203

Sethi (nee Dharamshi) B and North RV (1987), Vergence adaptive changes with varying magnitudes of prism-induced disparities and fusional amplitudes, Am. J. Optom. Physiol. Opt. 64:263

Tyler, CW (1983), Sensory Processing of Binocular Disparity, In Vergence eye movements: basic & clinical aspects, Schor and Ciuffreda (Eds.), Butterworths: Boston, pages 199-295

Verhoeff FH (1939), Hyperphoria tests based on a new principle, Arch. Ophthalmol. 22:743

Westheimer G and Mitchell DE (1969), The sensory stimulus to disjunctive eye movements, Vision Res. 9:749

Zee DS and Optican LM (1985), Studies of adaptation in human oculomotor disorders. Chapter 11 in Adaptive mechanisms in gaze control, Berthoz A and Melville Jones G (Eds.), Elsevier: Amsterdam, Elsevier: Amsterdam, pages 165-176

Zee DS, Chu FC, Optican LM, Carl JR, and Reingold D (1984), Graphic analysis of paralytic strabismus with the Lancaster red-green test, Am. J. Ophthalmol. 97:587
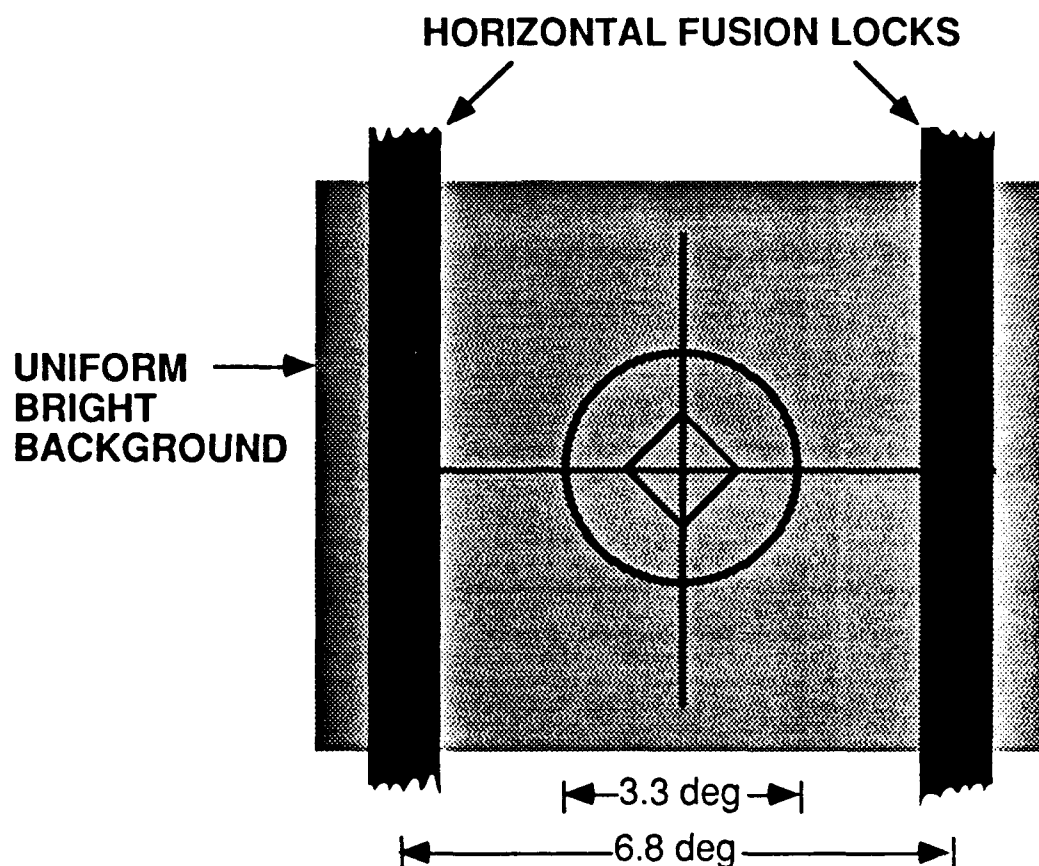
FIG 1. The tracking target, scaled 33% here, was superimposed on a 25 x 19 cm bright background. The horizontal-fusion locks were contained within the right and left eye channels of the SRI visual optics. The horizontal fusion locks extended the entire height of the visible field (24 degrees), and were always visible to both eyes. During trials, while the left eye was prevented from seeing the tracking target, the horizontal-fusion locks controlled horizontal vergence posture, but vertical vergence posture remained open-loop. Viewing distance was 160 cm.
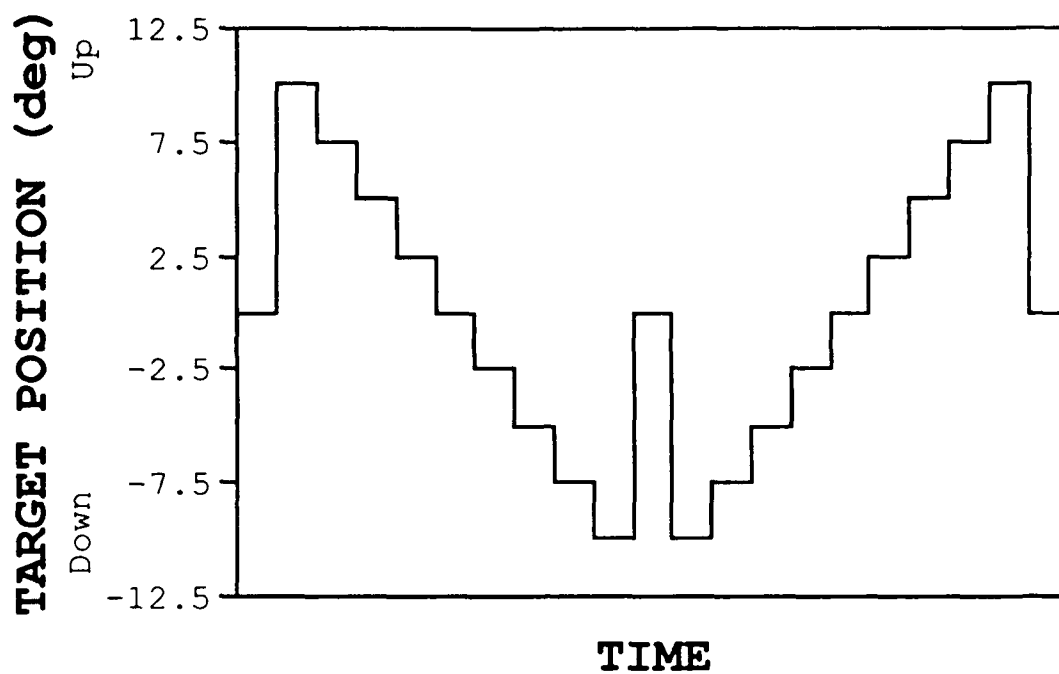
FIG 2. Schematic depicts sequence of target positions used during static phoria trials. The time intervals between target steps were determined by the experimenter (see text for details), and were not equally spaced as shown in this figure.

FIG 3.

(Top panel) Adaptive changes (post - pre) in gaze-specific phorias are plotted separately for each subject. The large filled circle near the upper right corner, represents the adapting stimulus disparity. The average gaze-specific adaptive change is represented by bold **X**s. Positive numbers on the axis of abscissa represent the upper field of gaze and negative numbers represent the lower field.

(Bottom panel) The difference between gaze-specific adaptive change in phoria occurring at the stimulated gaze position (9 degrees up) and other gaze positions are plotted relative to right gaze position. Positive numbers on the axis of abscissa represent the upper field of gaze and negative numbers represent the lower field.
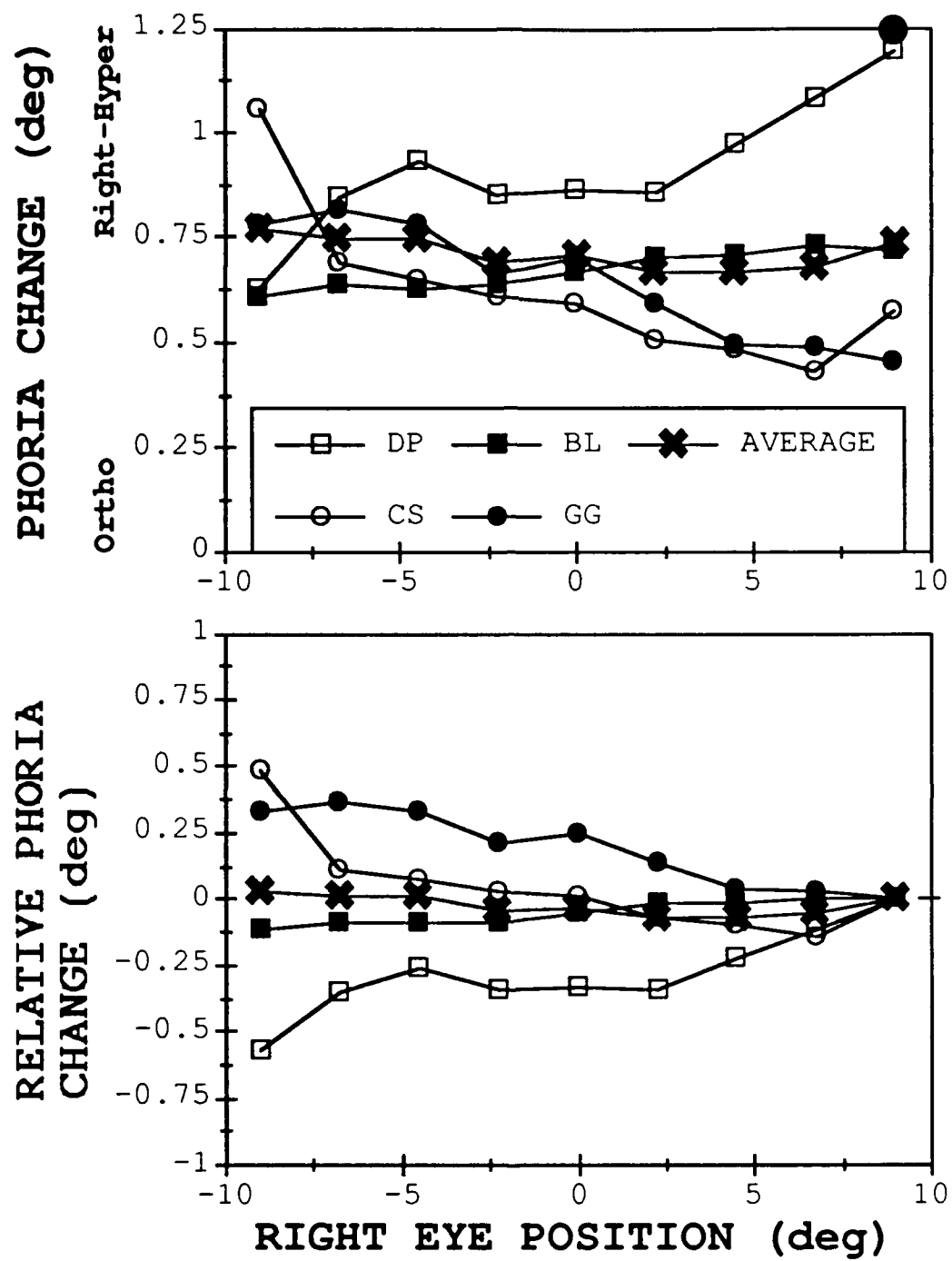
FIG 3.
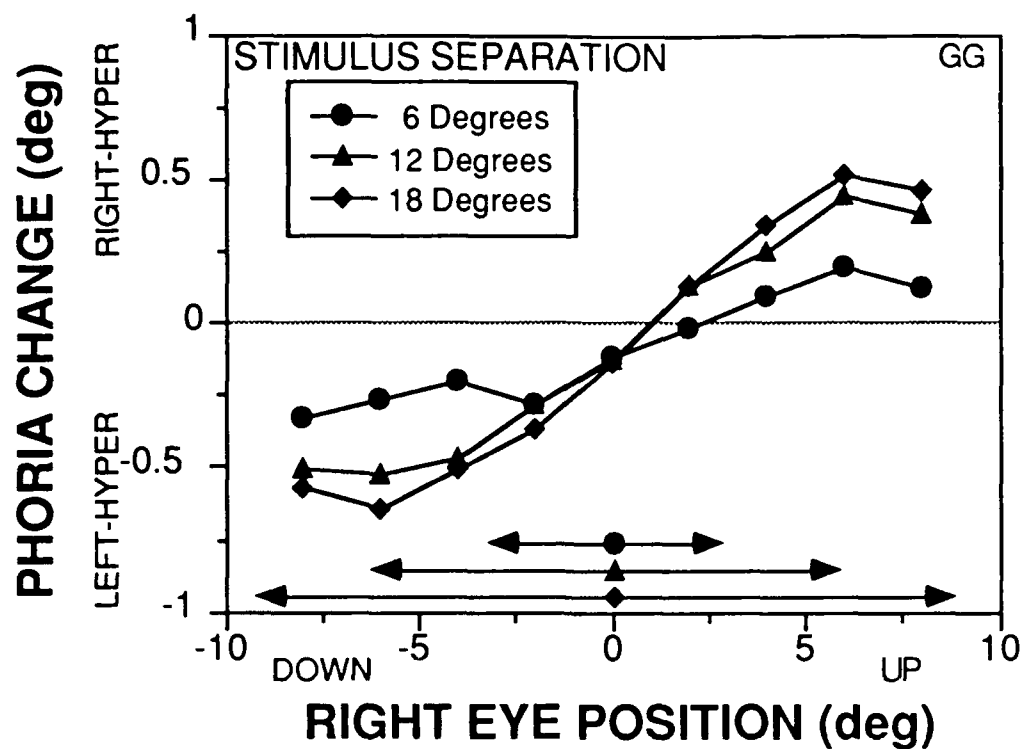
FIG 4. Adaptive changes (post - pre) in gaze-specific phorias are plotted, relative to right eye gaze position, for three experimental conditions: total stimulus disparity was 2 degrees, and stimulus separation was either 6, 12, or 18 degrees. Arrow tips illustrate stimulus location for each of the three stimulus separations.
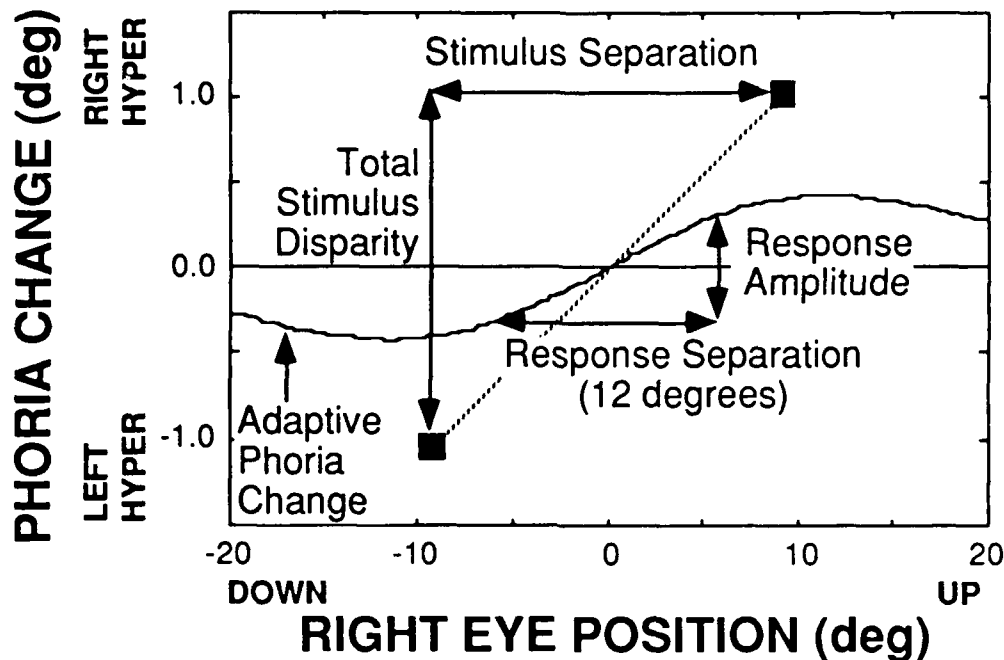
FIG. 5. Terms are illustrated to enhance understanding.

Location and strength of the adapting stimuli are represented by two large squares. Stimulus separation is equal to the squares' horizontal separation. Total stimulus disparity is equal to the squares' vertical separation. The stimulus (disparity) gradient is represented by the slope of a (dotted) line connecting the two squares.

The sine wave-like line represents the phoria adaptation response (post-pre). Response separation is defined as (the central) 12 degrees. Response amplitude is equal to the difference in phoria response that occurs at up and down 6 degrees. The response gradient is represented by the assumed linear slope between the phoria response that occurs at up and down 6 degrees.

Phoria adaptation effectivity is equal to the ratio of response gradient to stimulus gradient.
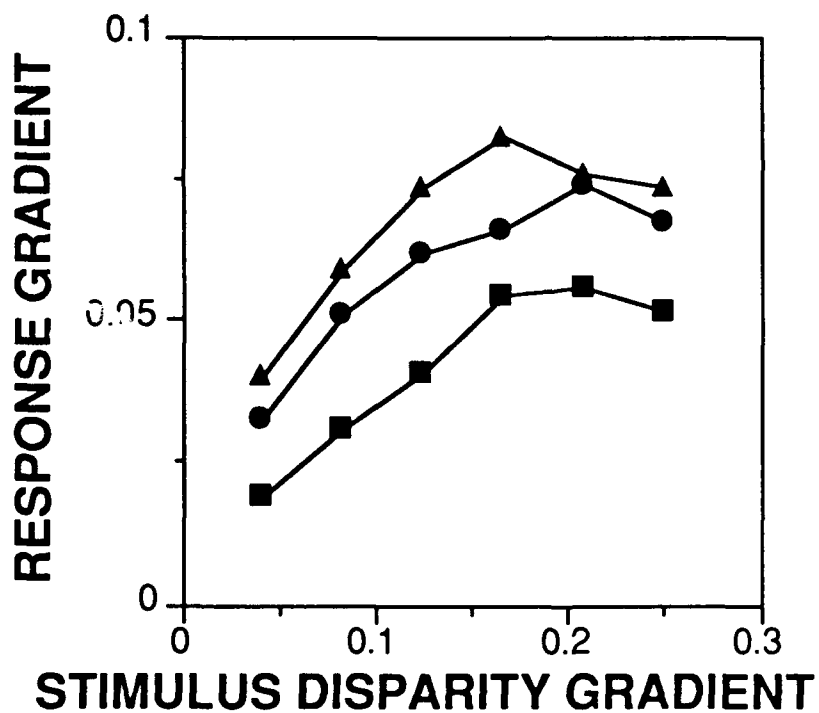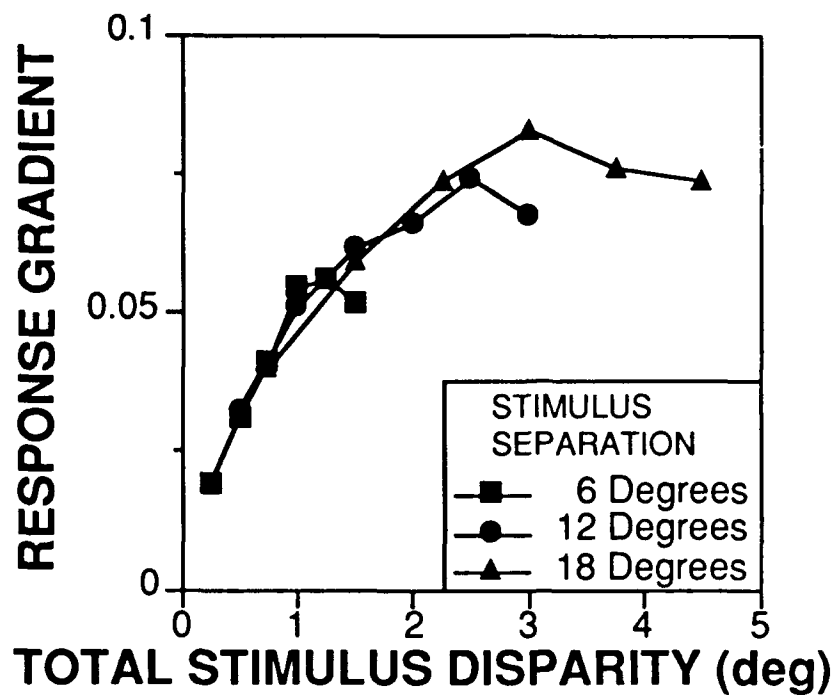
FIG. 6. For each stimulus separation, response gradients
are plotted, relative to total stimulus disparity *(Top Panel)*
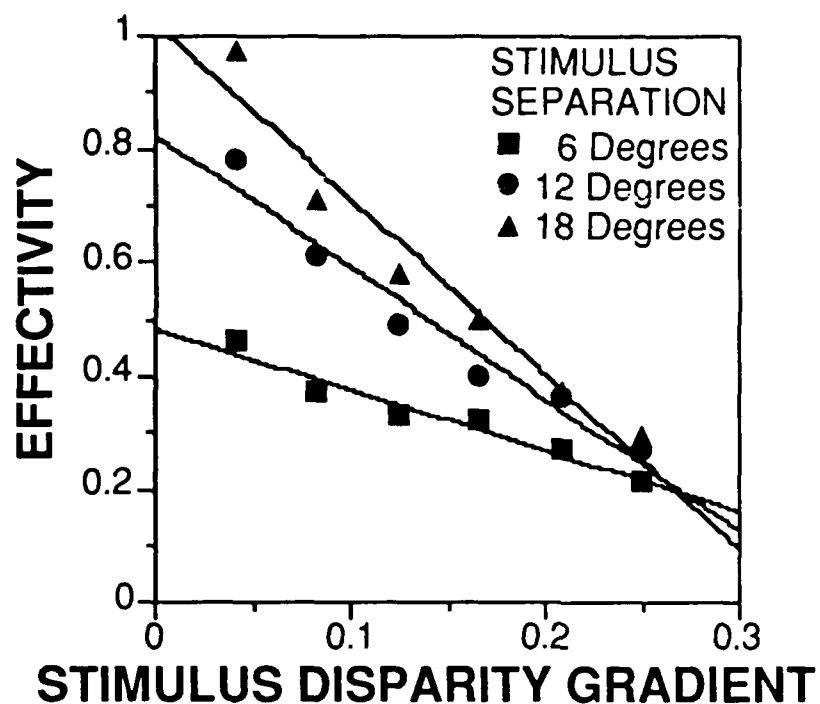and stimulus gradient *(Bottom Panel)*.

FIG. 7. For each stimulus separation, phoria adaptation effectivity is plotted against stimulus gradient, and fitted with a linear regression line. Regression line attributes are listed below.

STIMULUS SEPARATION	Y-INTERCEPT	SLOPE	r^2
6	0.48	-1.07	.95
12	0.82	-2.32	.96
18	1.02	-3.09	.95
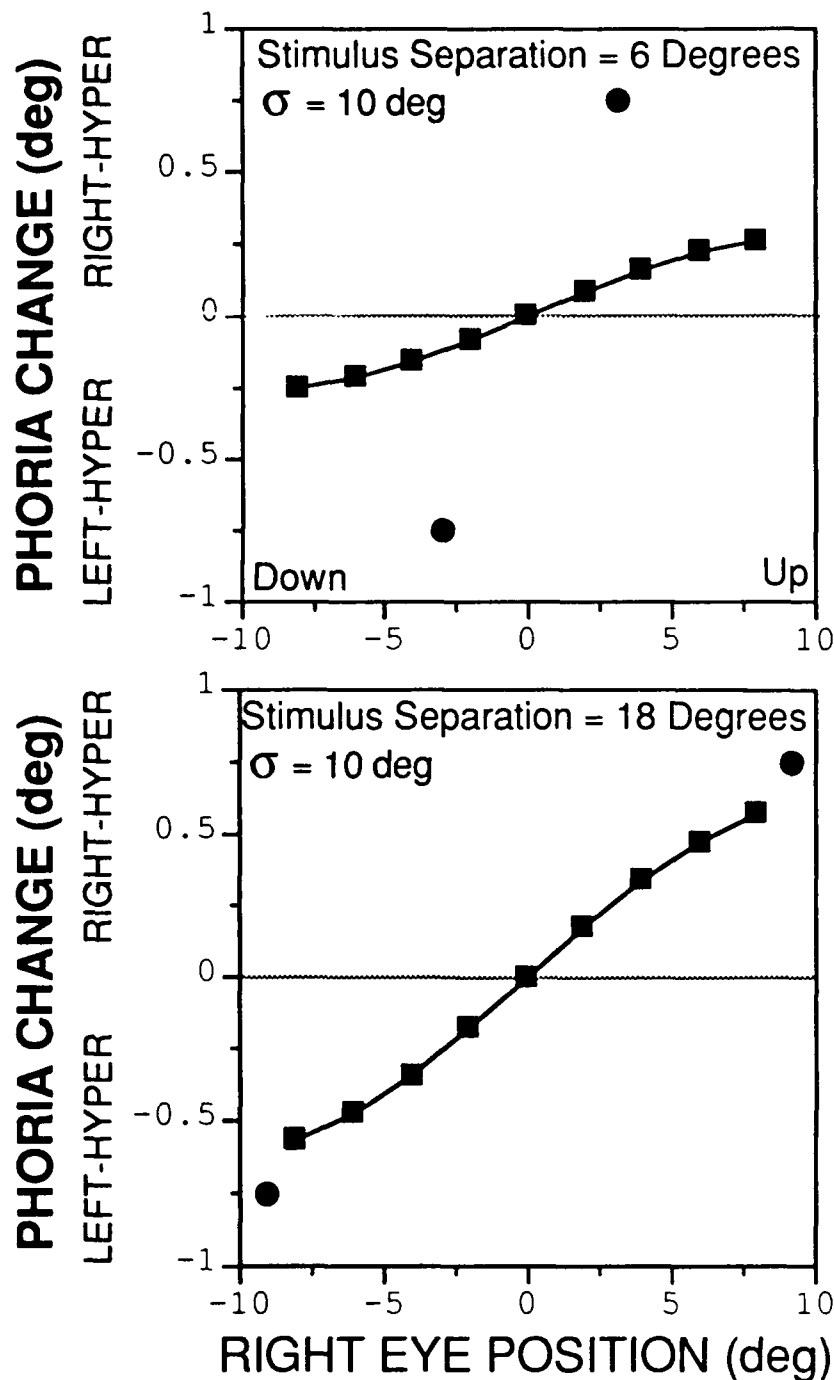
FIG. 8. Gaze-specific adaptive changes in vertical phoria are predicted with the Spatial-Spread Model. The graded spread of adaptation within an adaptive field was assumed to be a Gaussian function with a standard deviation (sigma) of 10 degrees. The total stimulus disparity was 1.5 degrees. Stimulus separation was either 6 *(top panel)* or 18 *(bottom panel)* degrees. The size and location of the stimulus disparities are represented by two filled circles in each panel.
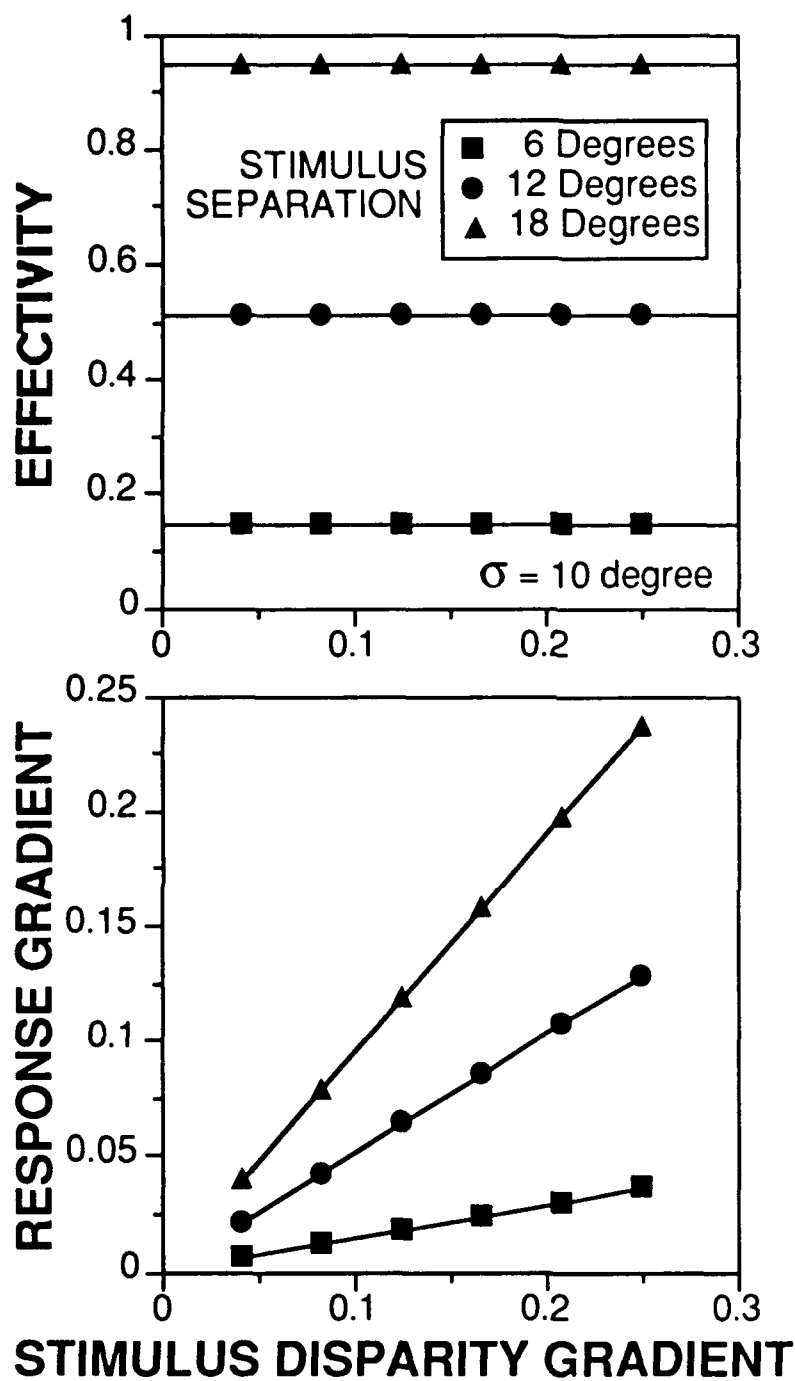
FIG. 9 Results from simulation by spatial-spread model (see text for details). Phoria adaptation effectivity (top panel) and response gradient (bottom panel) are plotted relative to stimulus gradient.

FIG. 10. Response gradient (top panel) and effectivity (bottom panel) are plotted against stimulus gradient in order to contrast predictions made by the spatial-spread model with experimental data (stimulus separation of 18 degrees).

(Top panel) The spatial-spread model predicts a positive linear relationship between response and stimulus gradients (upper straight edge of shaded area). In reality, the response gradient lags behind the stimulus gradient at an accelerating rate (lower edge of shaded area). The shaded area portrays the discrepancy between data predicted by the spatial-spread model and a smooth curve that closely approximates the actual data.

(Bottom panel) The spatial-spread model predicts response and stimulus gradients are independent of each other (flat upper edge of shaded area). In reality, the response gradient declines linearly with stimulus gradient (lower edge of shaded area). The shaded area portrays the discrepancy between data predicted by the spatial-spread model and a linear regression line that approximates the actual data.
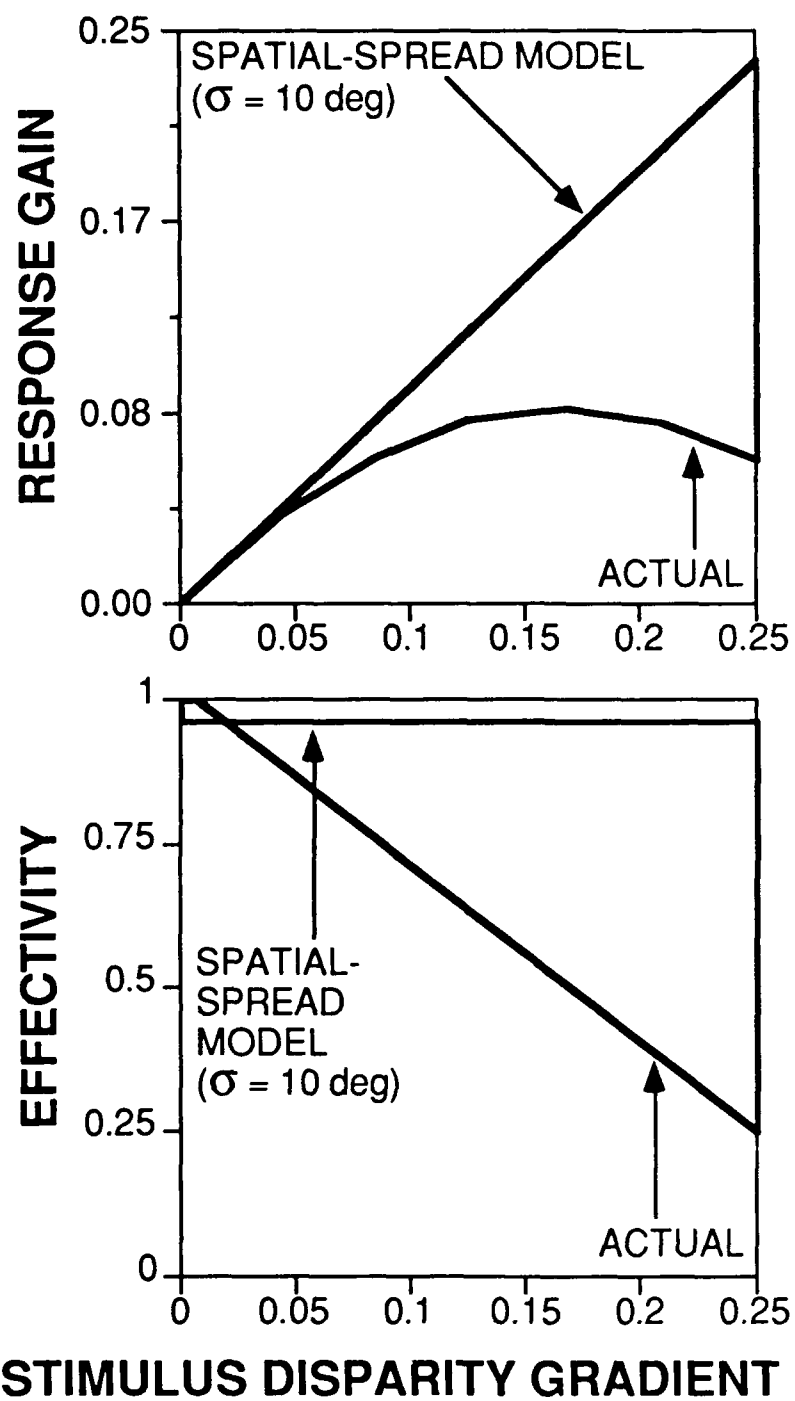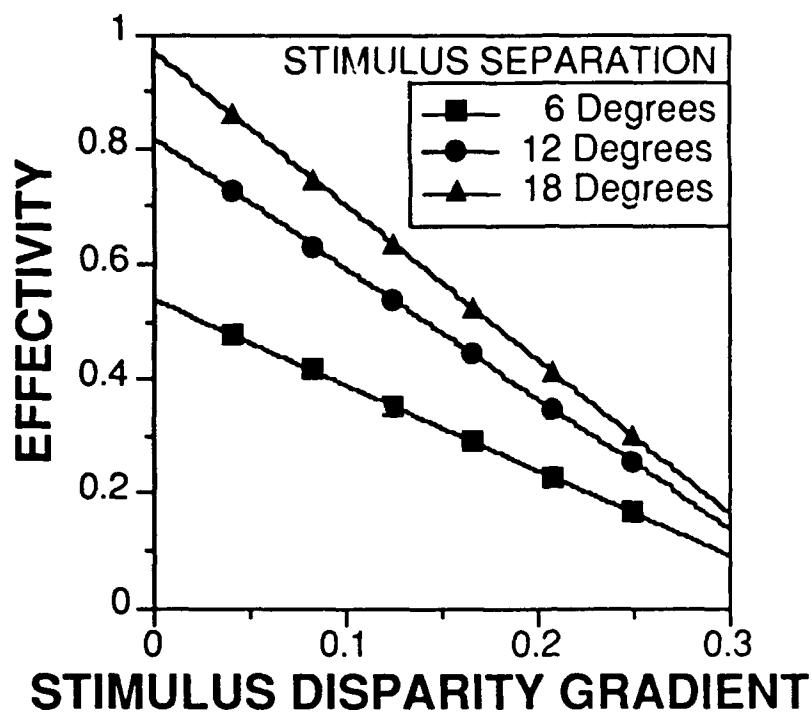
FIG. 10.

FIG. 11. Spatial-spread gradient-limited model simulation (Contrast with figure 7). See text for details.

For each stimulus separation, phoria adaptation effectivity is plotted against stimulus gradient, and fitted with a linear regression line. Regression line attributes are listed below.

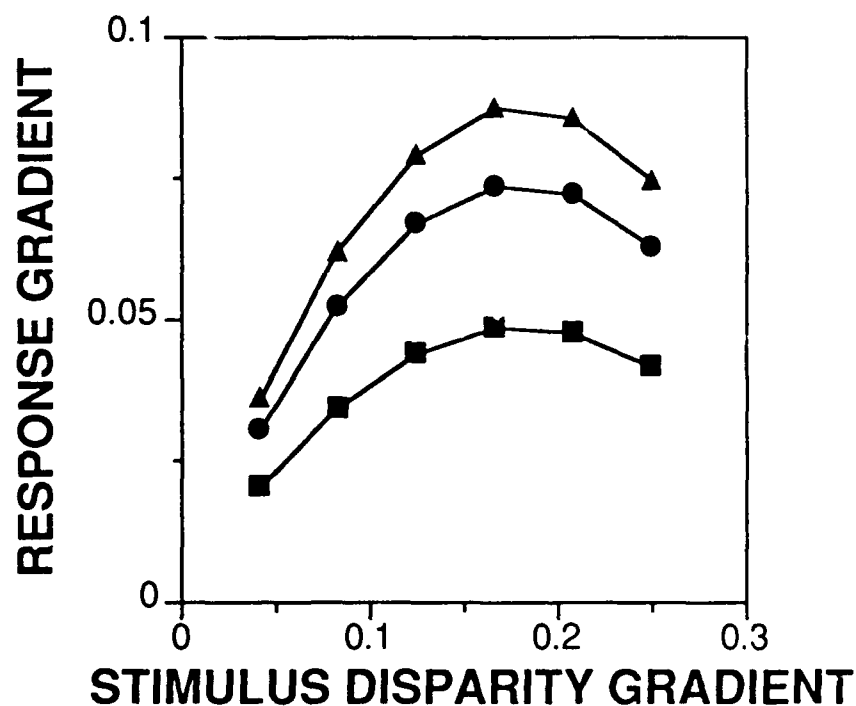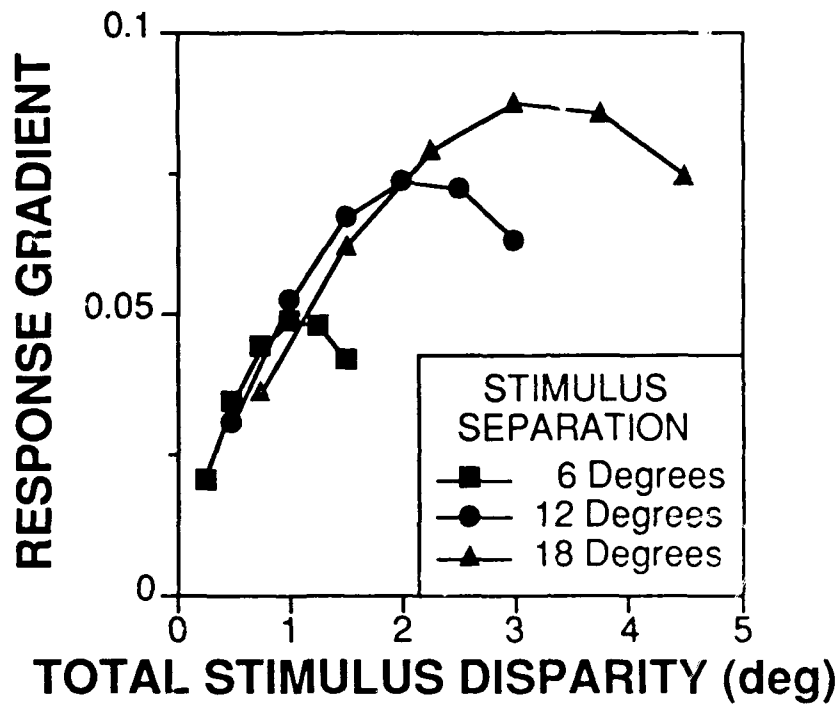| STIMULUS SEPARATION	Y-INTERCEPT	SLOPE	r^2
6	0.54	-1.49	1.00
12	0.82	-2.27	1.00
18	0.97	-2.69	1.00

FIG. 12. Spatial-spread gradient-limited model simulation (Contrast with figure 6). See text for details.

For each stimulus separation, response gradients are plotted, relative to total stimulus disparity *(Top Panel)* and stimulus gradient *(Bottom Panel)*.